Rodrigue Tanguy

Remote sensing analysis of recent coastal change and its controlling factors in Darnley Bay (Amundsen Gulf, Canada)

UNIVERSIDADE DO ALGARVE

FACULDADE DE CIÊNCIAS E TECNOLOGIA

2021

Rodrigue Tanguy

Remote sensing analysis of recent coastal change and its controlling factors in Darnley Bay (Amundsen, Canada)

Master in Marine and Coastal Systems

Mestrado em Sistemas Marinhos e Costeiros

Work performed under the supervision of:

Gonçalo Vieira, Institute of Geography and Spatial Planning, University of Lisbon

Gonçalo Prates, University of Algarve

UNIVERSIDADE DO ALGARVE

FACULDADE DE CIÊNCIAS E TECNOLOGIA

2021

Remote sensing analysis of recent coastal change and its controlling factors in Darnley Bay (Amundsen Gulf, Canada)

Declaração de autoria de trabalho

Declaro ser o(a) autor(a) deste trabalho, que é original e inédito. Autores e trabalhos consultados estão devidamente citados no texto e constam da listagem de referências incluída.

Declaration of authorship of work

I declare to be the author of this work, which is original and unpublished. Authors and works consulted are duly cited in the text and are included in the list of references.

Faro, September 30th, 2021

Copyright

Acknowledgments

First of all, I would like to thank my supervisors Gonçalo Vieira and Gonçalo Prates for giving me the opportunity to write my thesis combining the expertise of both and for their support throughout the whole process. Thanks to Dustin Whalen who was the founder of this project, and provided major data and information. Without him, this project would not be possible. Despite the unusual times, they always took the time to respond to emails and meet virtually when I had questions. I am also very grateful for their encouragement and help presenting an early stage of my results at the ASSW2021 online conference to gather some additional experience. A special thanks to the other master students of IGOT involved in the Nunataryuk project with which we shared experiences and solved the issues encountered during the work process. A special thanks to my girlfriend Holly, who supported me along the project and who corrected my sentences. I dedicated this work to my sister Clara, who is a great geographer, she always believed in me. Thanks to all my friends and family for their support.

This work is part of the Nunataryuk funded under the European Union's Horizon 2020 Research and Innovation Programme under grant agreement no. 773421, and with co-funding by the Climate Change Preparedness in the North (CCPN) program.

Abstract

As the Arctic warms, permafrost coasts are experiencing higher rates of erosion, threatening coastal communities and infrastructure, and altering sediment and nutrient budgets. However, some areas are still neglected by research. The mouth of the Gulf of Amundsen is home to Darnley Bay, while the coast of the ecologically important Cape Parry to Paulatuk area included in the Anguniaqvia Niqiqyuam Marine Protected Area has been still little studied. This area is home to Arctic char, cod, beluga whales, ringed and bearded seals, polar bears and sea birds. It is also an important area for the Inuvialuit who have an intrinsic attachment to their land ensuring the survival of their culture and food source.

Settled in Paulatuk, Inuvialuit are witnessing the warming of their territory and the degradation of the permafrost. This study aims to establish the geomorphological characterization of the Paulatuk coast and peninsula and to quantify coastal changes over 55 years, using a new very high resolution survey based on CNES Pleiades imagery from August 2020, as well as historical aerial imagery from 1965. Key areas, such as Paulatuk, were also surveyed using unmanned aerial vehicles in 2019.

The results indicate a small average erosion rate of -0.1 m/year of the surveyed coastlines from 1965 to 2020. At a regional scale, there is a disparity in erosion rates depending on the type of substrate. Erosion rates are significantly different in function of the type of coastal material. Unconsolidated areas show erosion rates of up to -3 m/year while consolidated express stability. These values are relatively low compared to other sites on the Beaufort Sea Coast (e.g. Qikiqtaryuk/Herschel Island, Yukon coast, Mackenzie delta), which are more susceptible to erosion due to soil composition, ground ice content, cliff height and exposure to swells. The very high resolution geomorphological mapping provide important spatial information to the coastal community. Paulatuk is showing signs of degrading permafrost landscape with subsidence zones and potential thaw ponds drainage. A preliminary assessment suggest that infrastructure construction influences permafrost degradation and that future soil thawing process could become a threat for the community. This study, based on unprecedented very high resolution data contributes to the general characterization and identification of erosion rates of the Arctic coasts.

Keywords: Coastal dynamics, Permafrost, Darnley Bay, Paulatuk, Remote sensing.

Resumo

Com o progressivo aquecimento do Ártico, as costas com permafrost estão progressivamente a sofrer taxas de erosão mais elevadas, ameaçando as comunidades e infraestruturas costeiras, alterando os balanços de sedimentos e nutrientes, e influenciando o ciclo do carbono. No entanto, amplas regiões ainda têm uma dinâmica ainda pouco conhecida. Este é o caso do Golfo de Amundsen, onde se integra Darnley Bay, bem como a costa da importante área ecológica entre o Cabo Parry e Paulatuk, incluída na Área Protegida Marinha Anguniaqvia Niqiqyuam. Esta área é um importante habitat do *Arctic char*, bacalhau, belugas, focas aneladas e de barbas, ursos polares e de várias aves marinhas. É também uma área importante para os Inuvialuit que mantêm uma ligação intrínseca à sua terra, garantindo a sobrevivência da sua cultura e fonte alimentar natural.

Estabelecidos em Paulatuk, os Inuvialuit são testemunhas do aquecimento do seu território e da degradação do permafrost. Este estudo visa estabelecer a caracterização geomorfológica da costa entre o Cabo Parry e Paulatuk e quantificar as principais modificações da linha de costa num período de 55 anos. Utiliza-se, para isso, um novo levantamento de muito alta resolução baseado nas imagens do satélite CNES Pleiades de Agosto de 2020, bem como fotos aéreas de 1965. Áreas-chave, como Paulatuk, foram levantadas utilizando veículos aéreos não tripulados em 2019.

Os resultados indicam uma taxa média de erosão da linha de costa de -0,1 m/ano entre 1965 e 2020. À escala regional, esta taxa é variável, dependendo principalmente do tipo de substrato costeiro. As áreas não consolidadas apresentam taxas de erosão de até -3 m/ano, enquanto que valores muito próximos de 0 m/ano, caracterizam as costas talhadas em substrato consolidado. Estes valores são relativamente baixos em comparação com outros setores da costa do Mar de Beaufort (por ex.: Qikiqtaryuk/Herschel Island, Yukon, delta do Rio Mackenzie), que são mais susceptíveis à erosão devido à composição do solo, teor de gelo no solo, altura das arribas e exposição à ondulação. A cartografia geomorfológica de muito alta resolução realizada forneceu informações espaciais importantes para a comunidade costeira de Paulatuk. A Peninínsula de Paulatuk mostra sinais de degradação do permafrost, com zonas de subsidência e aumento da extensão dos lagos termocársicos. Uma avaliação preliminar sugere que a construção de infra-estruturas está a influenciar a degradação do permafrost e que o futuro processo de descongelamento do solo poderá tornar-se uma ameaça para a comunidade. Este estudo, apoiado em dados de deteção remota com muita alta resolução, é um contributo para

consolidar a caracterização da costa de Darnley Bay e para a identificação das taxas de erosão costeira no Árctico.

Palavras-chave: Dinâmica costeira, Permafrost, Darnley Bay, Paulatuk, Detecção remota

Summary

List of figures

List of Tables

1. Introduction

1.1 Motivation

In the context of global warming, the role of high latitude regions in future climate projections is crucial for the planet. Polar regions are fragile environments, sensitive to the impact of human activity and to climate change (Godard & André, 2013, French, 2018). The richness in natural resources such as fisheries, energy and freshwater, of the Arctic, its location on new potential international maritime trade routes and geostrategic importance rises significantly its economic and strategical interest.

Rapid climate change in the periglacial regions, especially in the Arctic is modifying the thermal balance and permafrost landscapes where degradation by thermokarst and thermal erosion processes occur (Godin, 2015). The loss of material cohesion by thawing of ice-wedges is exacerbating coastal erosion. The Beaufort Sea Coast, in northern Canada, westwards of Amundsen Bay, where this study focusses, is presenting rapid coastal erosion rates, reaching up to 20 m/yr. in some sectors (Solomon, 2005; Obu et al., 2017), threatening coastal communities and infrastructures (Arctic Report Card, 2020). Moreover, the large amount of carbon and mercury stored in permafrost soils can be released into coastal waters and the atmosphere (Wegner et al., 2015), inducing a greenhouse effect increase, and potentially impacting aquatic resources and human health. Monitoring coastal changes and understanding the response of the shoreline to environmental forcing such as relative sea level (RSL), storminess and duration of open water season, are necessary to develop coastal management strategies useful for local Inuit communities.

The lack of studies on recent coastal erosion in the Amundsen Gulf area makes Darnley Bay and the hamlet of Paulatuk especially interesting sites, where remote sensing may be used as a tool to characterise recent changes of this permafrost coastline. Ultra high resolution data provided from 2019 UAV surveys by the University of Lisbon and Geological Survey of Canada, coupled with specially acquired very high-resolution satellite imagery (CNES Pleiades, August 2020) were used to establish a geomorphological characterisation of the complex landscape of the region. Moreover, the erosion rate of the coastline were assessed by a diachronic analysis over 55 years using other archived remote sensing datasets.

1.2 Objectives

The overall objective of this dissertation is to assess coastal changes in a poorly studied area, which is Darnley bay, using remotely sensed data from 1965 to 2020. The specific aims of this study are:

1) A geomorphological characterisation of the coast at a regional and local scale.
2) Quantifying coastal changes as a function of the type of coast within Darnley Bay
3) Investigating the evolution of permafrost degradation in the hamlet of Paulatuk.
4) Identifying the factors leading to those changes.

2. State of the art

2.1 Effect of climate change on Arctic periglacial environments.

In the 5th report about climate change, the Intergovernmental Panel on Climate Change assessed the projected impact of an increase in global average temperature of 1.5 °C above pre-industrial levels (1850-1900). The current trend is an increasing global temperature at 0.2 °C per decade (IPCC, 2018). As shown in the report on the Ocean and Cryosphere in a Changing Climate (SROCC, 2019), air surface temperature of the Arctic have doubled over the two last decades having an effect on biological resources, ice-extent, oceanic and coastal systems, and permafrost regions (Figure 1).

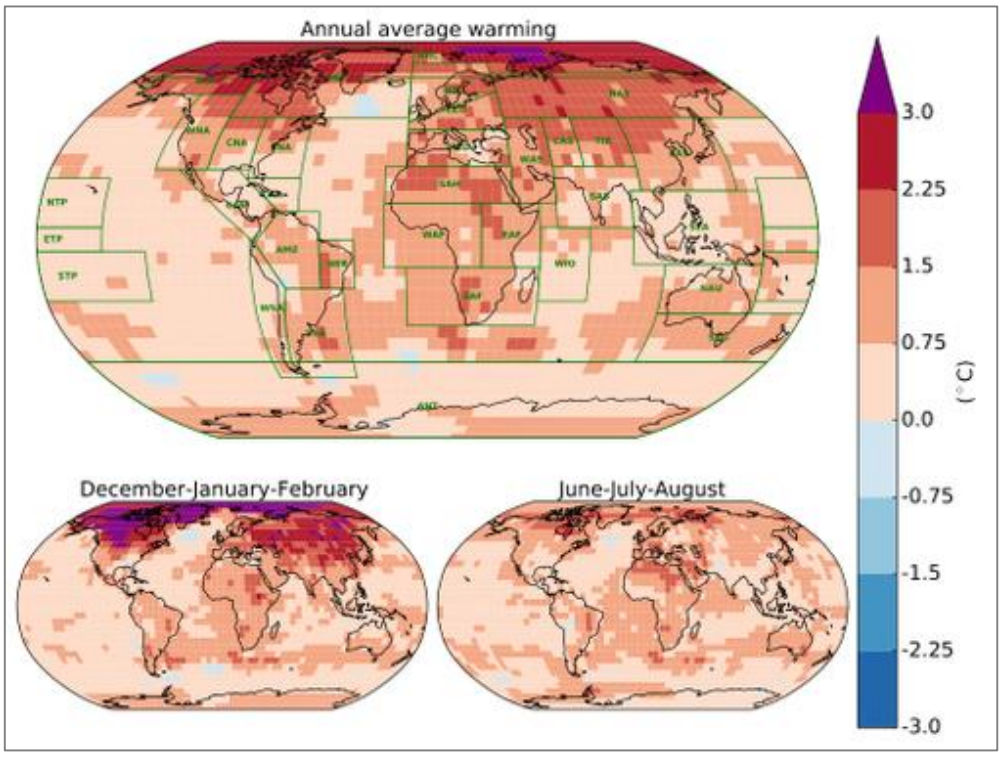

Figure 1. Regional annual average air temperature warming between 2006 and 2015, relative to 1850- 1900. Source: IPCC 2018

The warming of the Arctic is modifying the hydrological cycle and leading to the decline of sea-ice, grounded ice and glaciers and small ice caps extent. This ice mass budget loss coupled with the thermal expansion of the oceans is affecting sea level rise (SLR). Global SLR is accelerating and rose by 3.6 mm during the period 2006-2015. The SLR scenarios for the next century show an increase up to 16 mm/yr. and about 70 % of the coastlines to experience SLR effects (IPCC, 2019). Those effects will have considerable impacts on permafrost landscapes, Indigenous communities, infrastructures and industry. However, in the past, Arctic regions

already experienced sea level variations. The knowledge of isotastic movements is crucial to understand the modern Arctic shorelines and their vulnerability to sea-level rise. Isotastic movements occur in regions that were glaciated during the Pleistocene, such as in northern America and northern Europe. As ice-sheets retreated during the Holocene deglaciation, the earth's crust rebounded and sea level rose. The combination of the glacio-isotastic rebound with the simultaneous marine transgression explains the equilibrium of the high latitudes modern shoreline. In some area, the post-glacial rebound is faster than the eustatic sea level rise, creating raised shorelines such as in the Hudson Bay or in Scandinavia (Wiley et al., 2020).

Permafrost is a contraction for “permanently frozen ground” and is defined as “ground that remains at or below 0°C for a least two consecutive years”. It reflects a “thermodynamic balance of ground surface temperature, which is controlled by air temperature and the geothermal gradient” (Pollard, 2018). Permafrost of the Arctic has been intensively studied in recent years in reason to its sensitivity to global warming, impacts on the global carbon budget, for potential resource exploitation and, more recently, owing to the high rates of coastal retreat. Permafrost landscapes cover ¼ of northern hemisphere land mass and represent 50% of Russia and Canada (Figure 2). Studies have shown that the increase of land-surface temperatures accelerate permafrost degradation by thawing and erosion processes. This warming promotes thermokarst processes, active layer thickening and gas hydrates and methane release. The IPCC scenarios indicate a decrease by 20 to 35 % of the northern hemisphere permafrost mainly due to the thawing of discontinuous permafrost (IPCC, 2019). The increase of air surface temperature, the snow cover variability and increasing wild fires are the factors driving terrestrial permafrost degradation.

Coastal permafrost represents 34 % of Earth’s coasts and is particularly vulnerable to coastal erosion. In the Arctic the average coastal erosion rate is 0.5 m/yr. (Obu et al., 2017), but these rates are heterogeneous and dependent of various factors. The spatial and temporal variability of permafrost coastal erosion can be explained by large scale factors. In the Arctic, erosion is limited to the ice-free season which last from June to August, varying in function of the region. During this period, waves generated by storms associated to thawing process are eroding the coasts and degrading the ground surface. The highest erosion rates are associated to unconsolidated permafrost while consolidated permafrost remains much stable (Lantuit et al. 2012). The factors explaining the spatial variability erosion rates are depending on sedimentary composition, ground-ice content, cliff height and orientation. The temporal variability of erosion is explained by ice-free season length variation, storminess and wave height, relative

sea-level rise and precipitations (Harper, 1990; Hequette & Barnes, 1990; Couture & Pollard, 2000; Solomon, 2005; Galley et al., 2008; Lantuit et al., 2012; Obu et al., 2017; Lim et al, 2020).

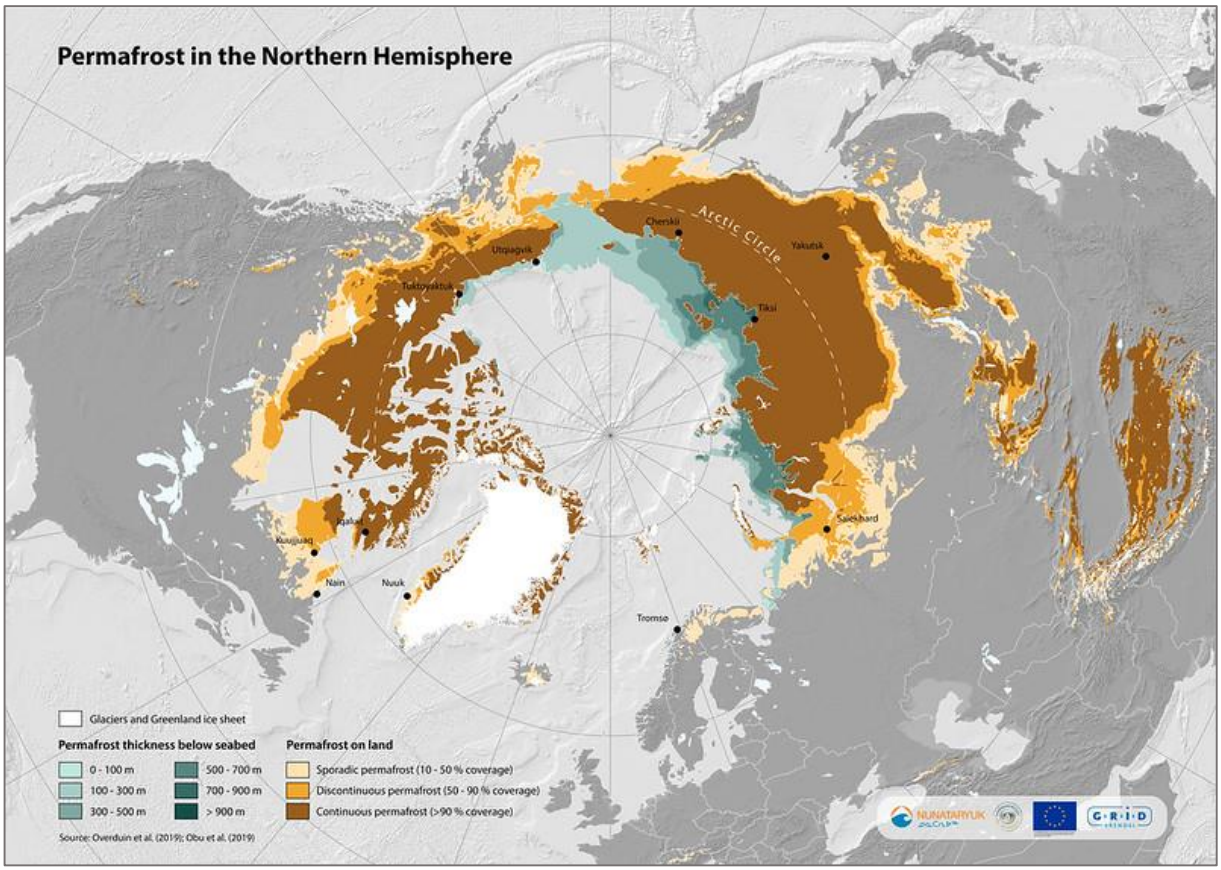

Figure 2. Distribution of terrestrial and subsea permafrost in the Northern Hemisphere (nunataryuk.org).

2.2 Coastal erosion along the Beaufort Sea Coast

The Beaufort Sea coastline is stretching from Point Barrow in Alaska to the Arctic archipelago situated in the Northwest Territories of Canada (Figure 3), with 65% of the coast being unconsolidated material and 35% being rocky or consolidated material (Lantuit et al., 2012; Obu et al., 2017).

Figure 3. Location map of the Beaufort Sea Coast

The nature of the coastal materials strongly influences the erodibility of the coastline. The Beaufort Sea Coast presents a wide diversity of coastal types, including ice-poor and ice-rich tundra cliffs, low tundra cliffs, barrier islands, spits and flat wetland complexes. The material composing the coast is deltaic and glacial. Most studies are concentrated along the Alaskan coast near Drew Point, the Yukon coast (especially Qikiqtaruk/Herschel Island), the Mackenzie delta and the Tuktoyaktuk Peninsula (Harper, 1990; Manson et al., 2005; Solomon, 2005; Jones et al., 2009; Lantuit et al., 2012; Obu et al., 2017; Irrgang et al., 2018). The analysis of aerial and satellite imagery allows to assess rapid coastal retreat and its spatial and intra-annual variability. The morphology and dynamics of the Canadian Beaufort Sea Coast have been studied by several authors (Harper, 1990; Lantuit et al., 2012; Couture, Fritz, Irrgang et al., 2017; Obu et al., 2017; Burn, 2019), which provide a description of the Beaufort Sea coastal processes with a special attention to coastal retreat. Harper (1990) reveals that the Canadian Beaufort Sea coast experiences widespread retreat rates with values of up to 18 m/yr. (Figure 4). More recent studies have shown that most of the Beaufort Sea Coast is subject to erosion and is retreating much faster in recent years (Lantuit et al., 2012, Couture et al., 2017; Cunliffe

et al., 2019). Rapid and extensive erosion is occurring in Qikiqtaruk/Hershel Island, which present average erosion rates of 2.2 m/yr. (Cunliffe et al., 2019), but also in the Mackenzie Delta region, presenting annual retreat rates between 2.1 and 6.1 m/yr., with 22.5 m/yr. reported in some sectors (Solomon, 2005). This high retreat rates are expressed under slump forms, or block collapsing and are governed by ground-ice thawing. The Yukon coast and Tuktoyaktuk Peninsula are present lower average erosion rates up to 0.7 m/yr. (Solomon et al., 2005; Irrgang et al., 2018). Figure 4 is showing the average erosion rates along the Arctic coastlines.

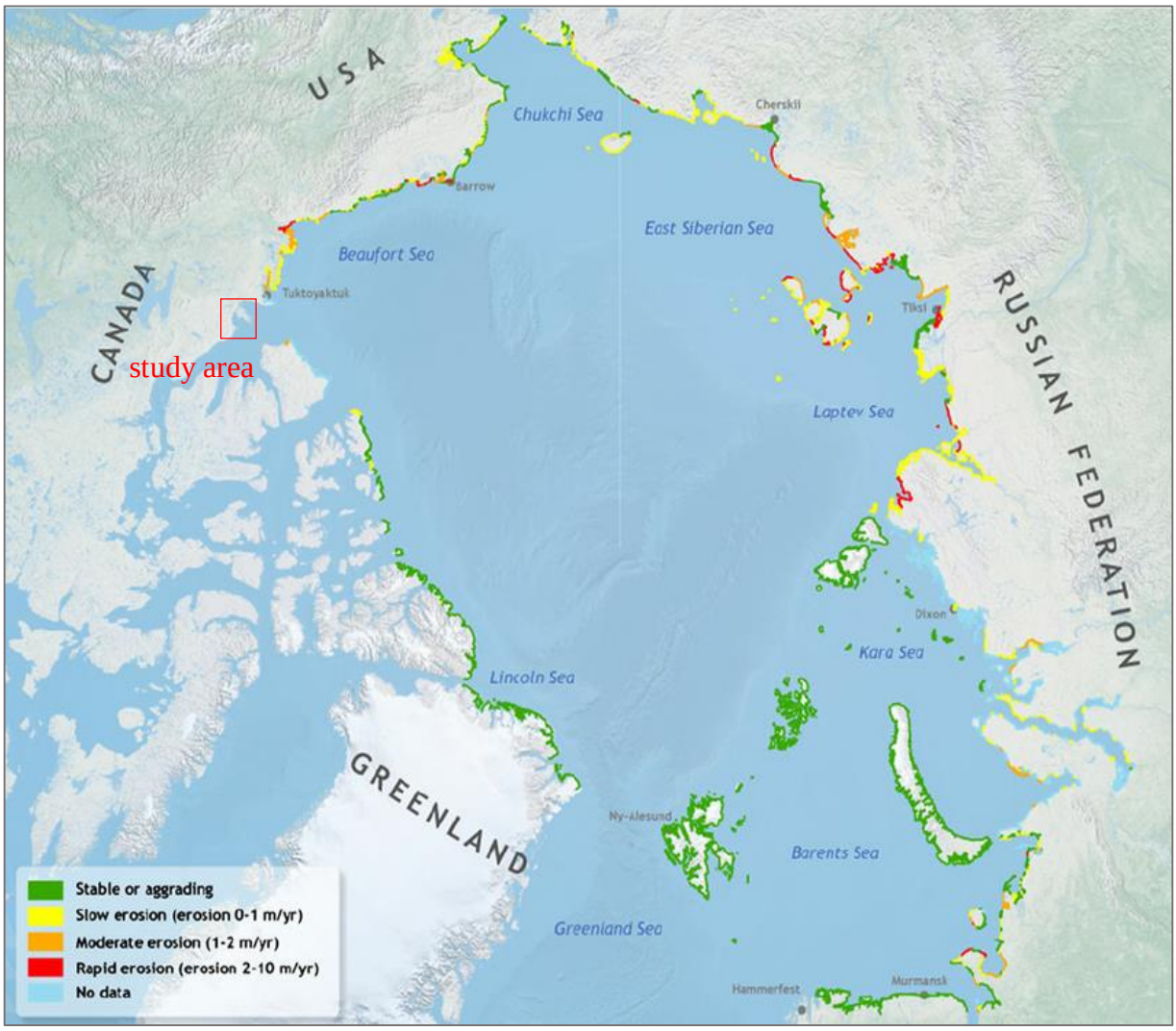

Figure 4. Average erosion rates along Arctic coastlines (from Lantuit et al. 2012)

Moreover, morphologic parameters and ground-ice concentration in cliffs and sediments have an influence on permafrost degradation. Ice-wedges and ice-wedge polygonal are typical features of permafrost landscapes. They form by the infiltration of melt water in surficial winter contraction cracks, which freezes and pushes the soil laterally, and grow by the succession of these cycles. Various studies have shown their formation and distribution (e.g. Harper, 1990;

Hequette & Barnes, 1990; Mackay, 1995; Burn & O'neill, Fritz et al., 2016; Burn, 2019). When exposed in the coast, ice-wedges define block collapses and retrogressive thaw slumps develop in ice-rich deposits and in massive ground ice sectors, which favour coastal erosion (Lantuit & Pollard, 2008).

Scarce studies on coastal changes have been done eastwards of the Tuktoyaktuk Peninsula. An early review of the physiography of Darnley Bay, resumes the orientation of glacial features as moraines and esker and postglacial channels and terraces (Mackay, 1952), but no research have been done on coastal changes at the scale of the bay. Mackay and Burn (2005) studied terrestrial wind-abrasion induced by katabatic winds over 50 years in Paulatuk, but report that little changes could be seen. The latest coastal change research in Paulatuk Peninsula was done by Sankar et al. (2019) and reveals an increase in erosion rates over the short-term (2006-2016) with mean rate of change of -0.24 m/yr. along the western coast and by -0.34 m/yr. along the eastern coast. However, their long-term study (1984-2016) reveal a mean change rate of 0.11 m/yr. (Sankar et al., 2019) .-0.24 m/yr. along the western coast and by 0.34 m/yr. along the eastern coast. However, their long-term study (1984-2016) reveal an accumulation rate of 0.11 m/yr. (Figure 5).

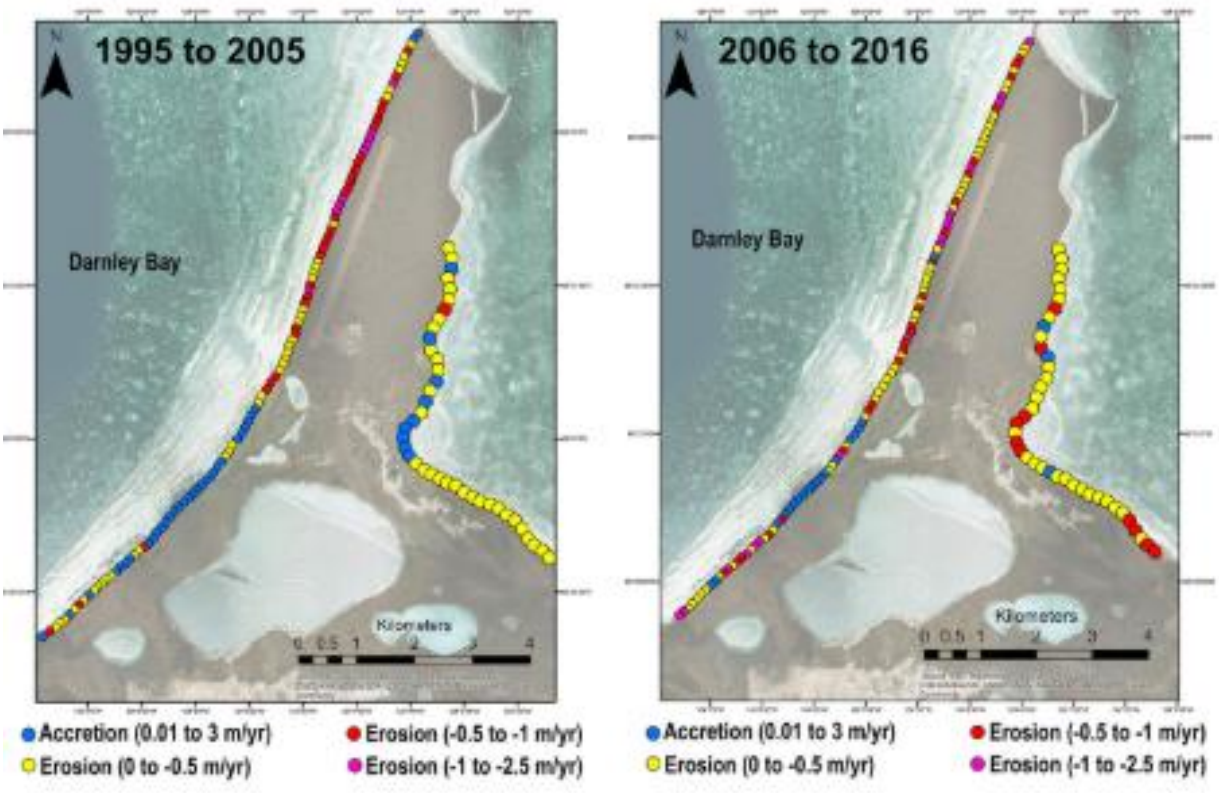

Figure 5. Increase of erosion rate in Paulatuk from 1995-2020 and 2006-2016 period. (from Sankar et al., 2019)

3. Study area

3.1 Geographical background

Darnley Bay is a large inlet situated in the northern Canadian territories, in the southern shore of the Amundsen Gulf. The bay is 45 km long and 32 km wide at its mouth. The bay is limited in the northeast by Cape Parry and by Cape Lyon at his northwest point. It is classed as a Marine Protected Area since 2009 in reason of its important ecological and biological values. It is the habitat of various mammals, such as the beluga or the bowhead, but also for Arctic Char, an important source of food for the Inuvialuit communities (Figure 6).

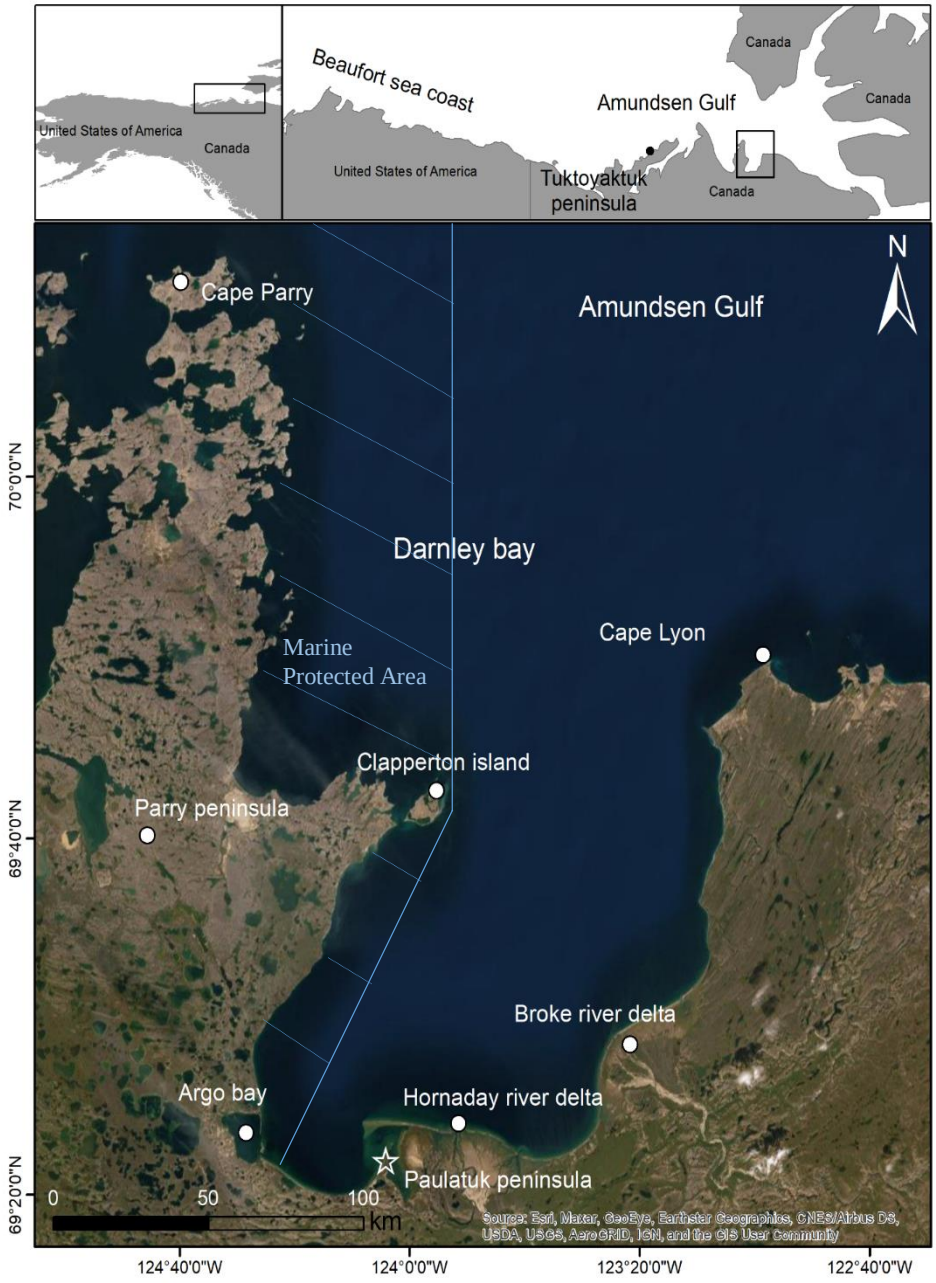

Figure 6. Regional setting of the study area.

The region is in the continuous permafrost zone and its surficial lithology is characterised by fluvio-glacial deposits composed by silty sand and clayed diamictons, formed by the direct action of glacier ice. The north of Parry Peninsula is constituted by thin and discontinuous till and outcrop areas with a till veneer (Figure 7). Cape Parry and Cape Lyon are composed by limestone outcrops, with 20 m high coastal cliffs (Environment Canada, 2014).

Two rivers flow to the southern coast of the bay forming large delta complexes constituted by fluvio-glacial deposits. Broke river end up on the eastern coast and Hornaday River on the south of the bay close to Paulatuk. The west coast of Darnley Bay shows a thermokarst topography landscape on which recent marine transgression flooded basins the forming numerous bays and inlets (Paulic et al., 2012). The coastline of Parry peninsula, northward of Clapperton Island is marked by rocky headlands of Proterozoic-age dolostone while the southern coast present a smoother profile made of mixed unlithified deposits. A deltaic formation built by the Brock River is present southwards. The coast is mainly composed by beaches of sand and gravel. Beach barriers and spit are formed by the remobilisation of glacio-fluvial sediments transported by the two major river systems.

The land-cover is mainly constituted by barren land vegetation characterised by short sparse vegetation, reflecting the extreme climatic conditions, such as the katabatic winds. The coastal erosion of the Darnley Bay is limited to the brief ice-free season (August to October). However, this coast tends to experience high erosion rates due to the combined effects of thawing permafrost, thawing ground-ice, wave action and rising sea-level (Arctic Report Card, 2020). Although, Darnley Bay is a low wave-energy environment, the northern part of Parry Peninsula is the most sensitive to erosion because of its larger exposition to dominant swells. Currents and wave are wind-driven and are only generated in the open-water season, coupled with alongshore drift, they are able the remobilise shelf sediments and built depositional coastal forms.

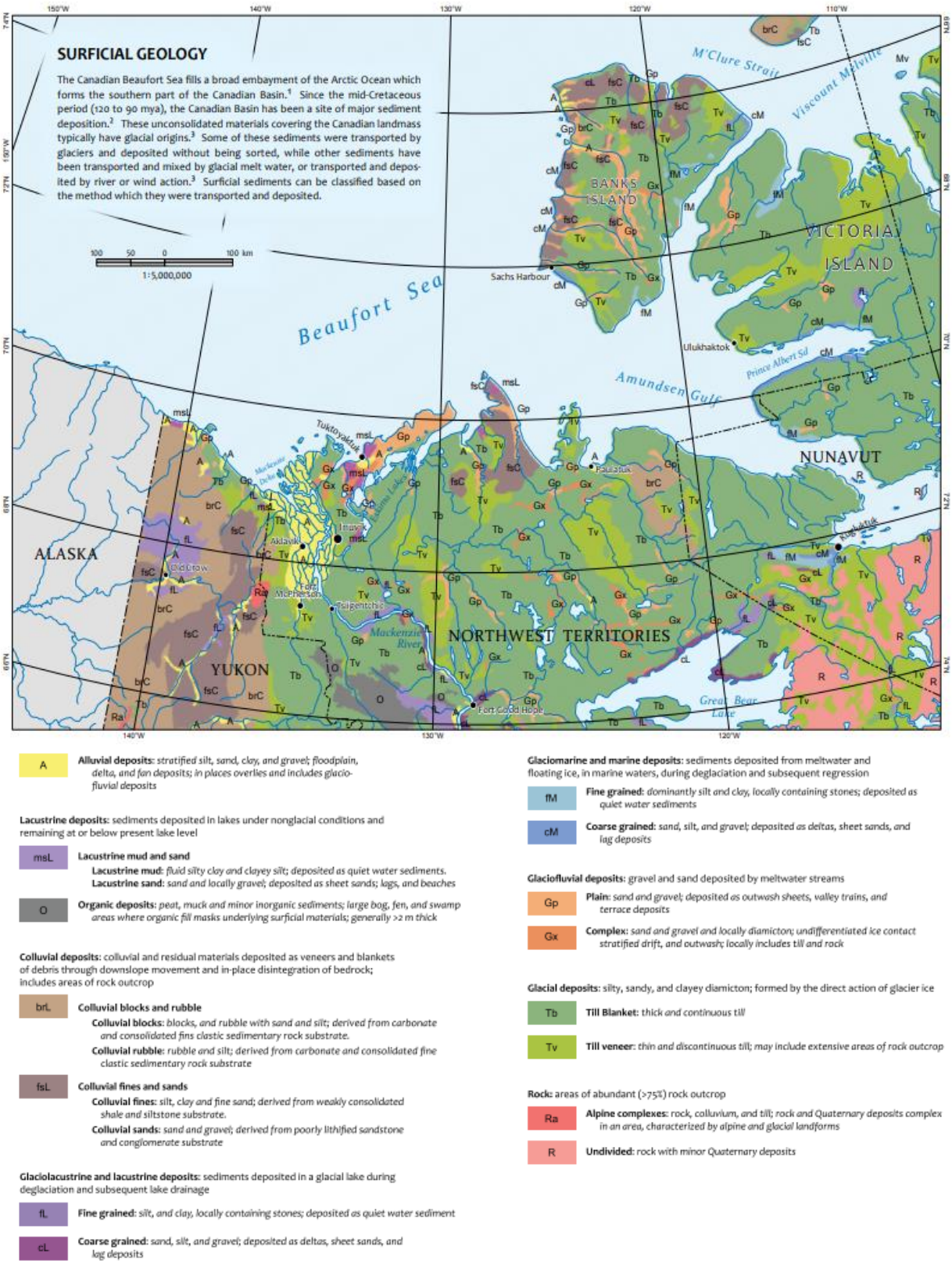

Figure 7: Surficial geology of Northern Yukon and the Northwest territories (Beaufort Regional Coastal Sensitivity Atlas 2012)

3.2 Climate

The Beaufort Sea coast region is characterised by a dry cold climate resulting in the formation of offshore sea-ice for 8 to 9 months. Darnley Bay is strongly affected by the maritime influence of the Amundsen Gulf. Situated just above the "line of Köppen", which define the isotherm +10 °C for the warmest month (July), the mean annual temperature is about -10 °C. The station located in Cape Parry provide data on climate normal and average temperatures per year. The hottest month (July) presents a mean air temperature of 11°C, while the coldest month (February) presents a mean temperature of -25 °C (Figure 6). Extreme temperatures vary from -47.2 °C (January) to +26.9 °C in July (Paulic et. al., 2012). Most precipitation are concentrated in summer between July and October and are brought by the maritime air masses. The mean annual precipitation is about 17 mm with the average maximum of 22.3 mm occurring in August (Figure 8). The average maximum snowfall is about 26.8 cm in October. The snow cover is about 25 cm depth in winter. The prevailing winds are influenced by the Amundsen Gulf and are blowing from the east, while katabatic winds are coming from the south. Cape Parry is exposed to north western storm swells and therefore shelters the interior of the bay where conditions are calmer. The ice-free season is relatively short in Darnley Bay. Freeze-up (sea ice formation) starts in October and cover the entire bay in November (Figure 9; Figure 10. The break-up is much longer, starting in July until October. Open water conditions are significant in August.

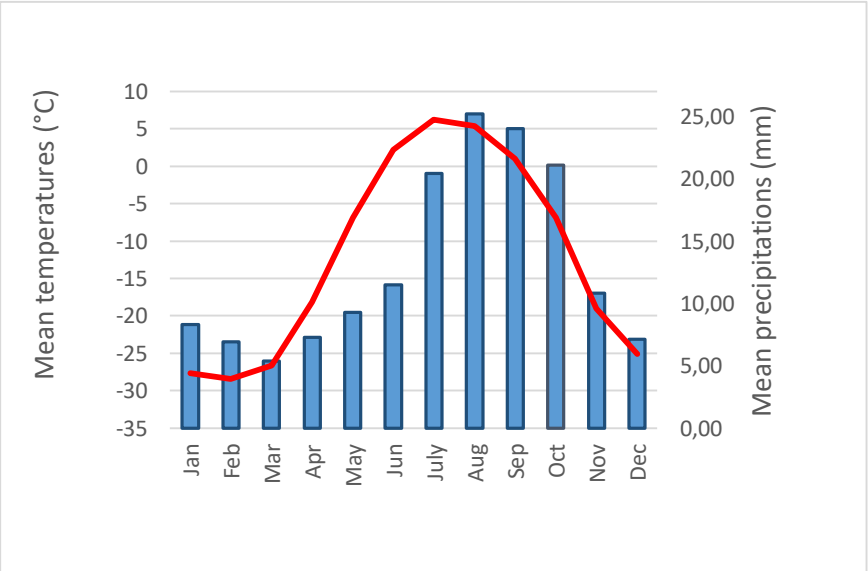

Figure 8. Average monthly temperatures (red) and precipitations (blue) at the Cape Parry station over 1971-2000 period. (Environment Canada)

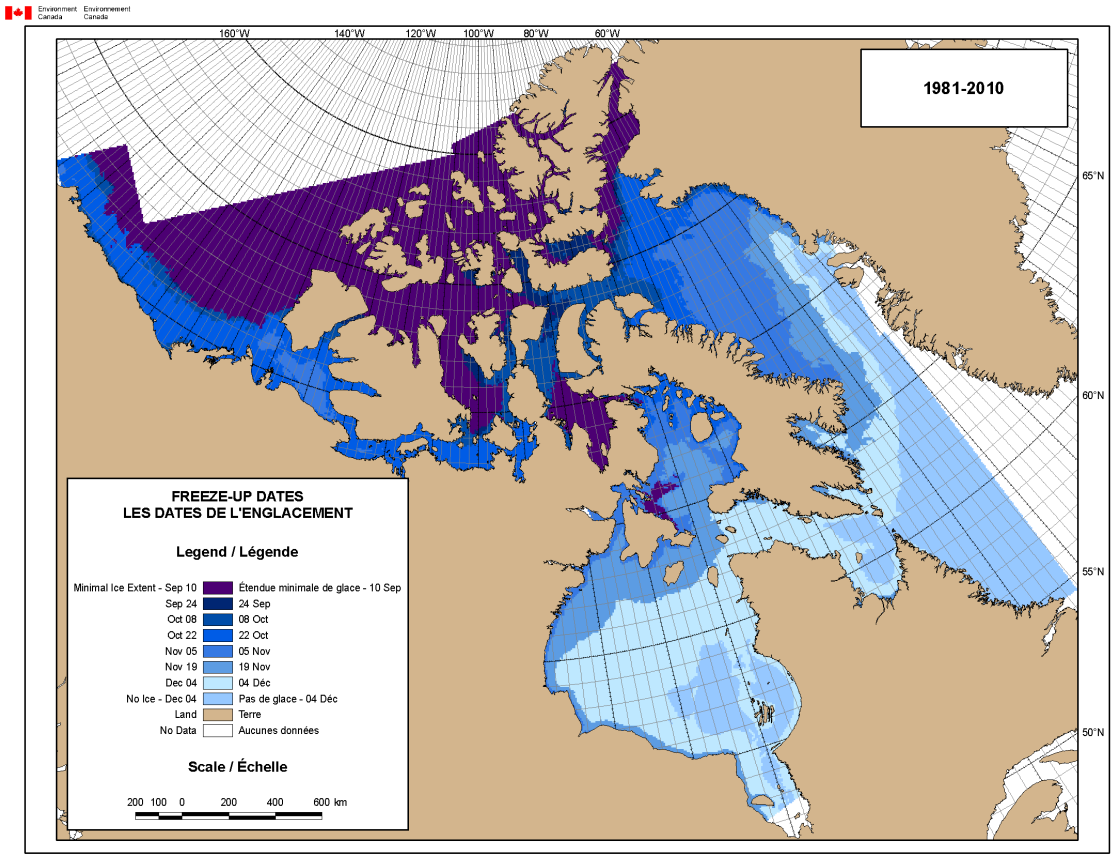

Figure 9. Northern Canada sea ice freeze-up dates from 1981 to 2020. (Canadian Sea Ice Service)

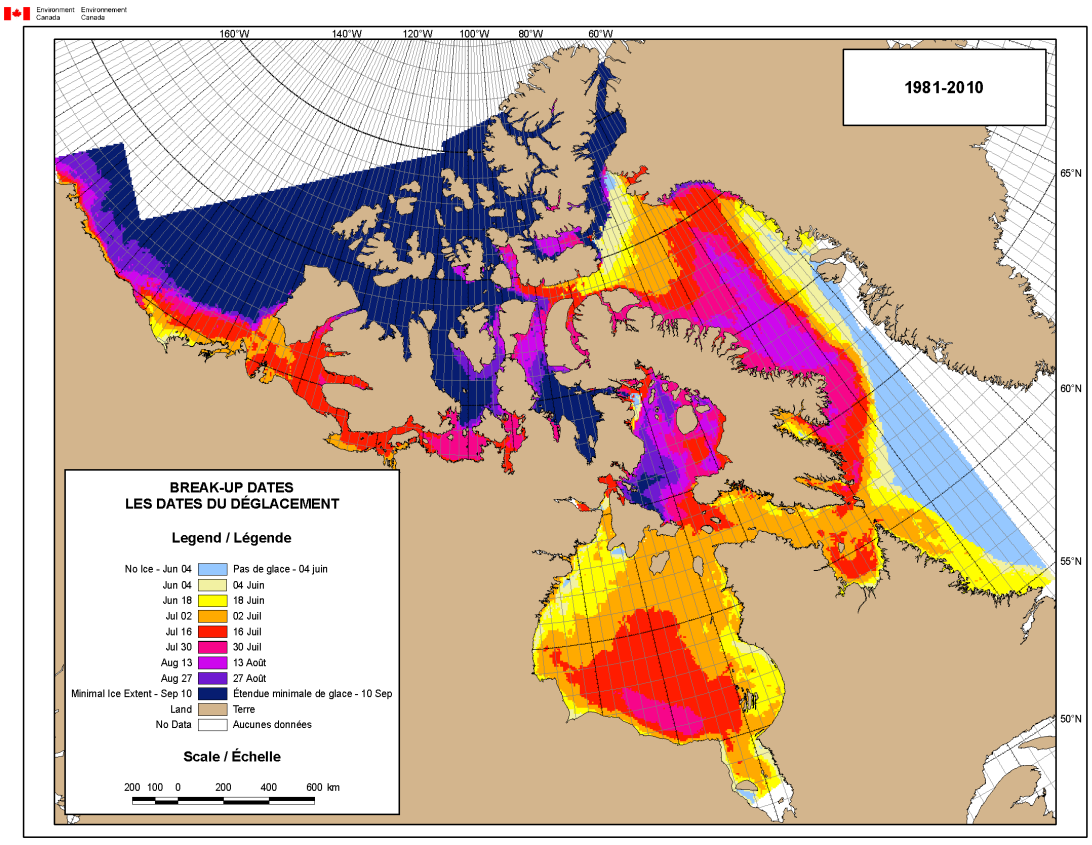

Figure 10. Northern Canada sea ice break-up dates from 1981 to 2020. (Canadian Sea Ice Service)

3.3 The Paulatuk peninsula

The Peninsula of Paulatuk is located in the southern coast of Darnley Bay (69º 21' N, 124º 04′ W) and is a low flat terrace with a mean altitude of 3.2 m, 3.5 km long and 0.9 km wide, constituted of fluvio-glacial deposits of silt and sand that form its coastline. The region is characterised by a micro-tidal regime with a range from 0.3 to 0.5 meters (Environment Canada, 2014). Inland landforms are dominated by ice-wedge polygonal networks with scarce ponds and an enclosed coastal lagoon. A mixed sediment spit is lying in the north-west resulting of the dominant alongshore drift. The inside coast is protected from the north-west wind swells whereas the western coast is subject to erosion and wave attack during ice-free season. The Inuvialuit hamlet of Paulatuk has 327 inhabitants and is located in the southeast part of the Paulatuk Peninsula (Figure 11). The first Inuit groups settled on the peninsula in 1920 to exploit the coal present on the territory, which they used as heating fuel (thecanadianencyclopedia.ca). The community lives from traditional hunting and fishing but also from local crafts. The exploration for oil and natural gas has opened new economic opportunities for the residents of the peninsula. Paulatuk is only accessible by air or sea. The previous airstrip that was built south of the hamlet was rebuilt along the west coast after a plane crash in December 1983 because of its poor orientation to the winds from NE and SSW (aviotionsafety.net).

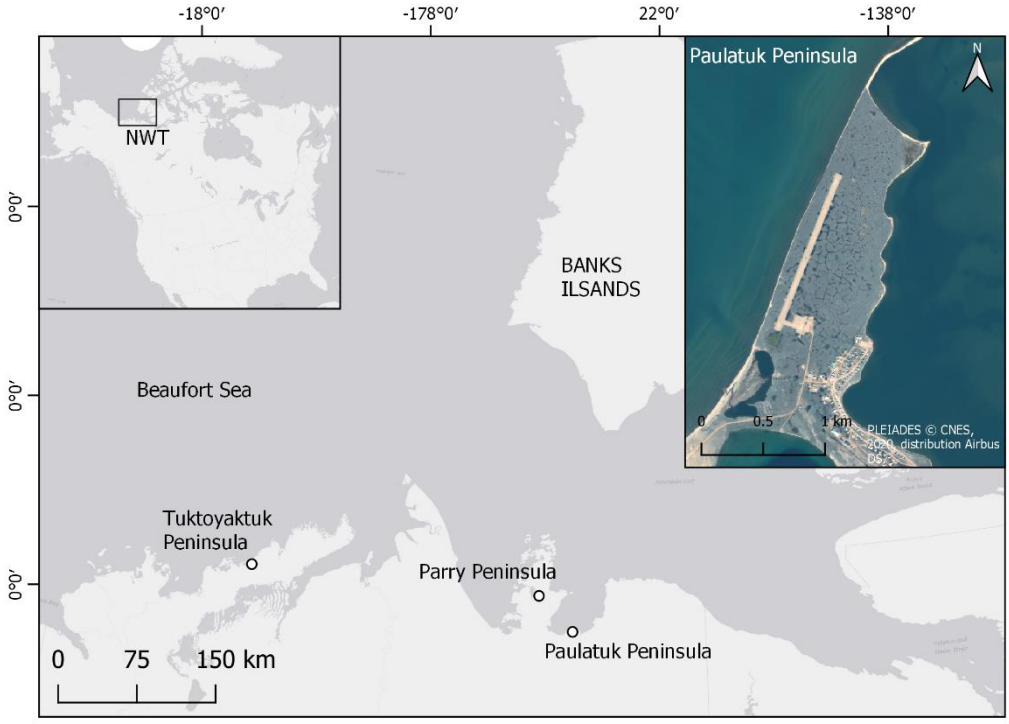

Figure 11. Location map of Paulatuk Peninsula

4. Materials and methods

4.1 Introduction

This work combines photogrammetric and remote sensing techniques for spatial analysis in order to assess coastal changes in Darnley Bay over 55 years. The analysis is performed on a regional and local scale with the geomorphological characterisation of the coast coupled with a coastal change analysis. (Figure 12).

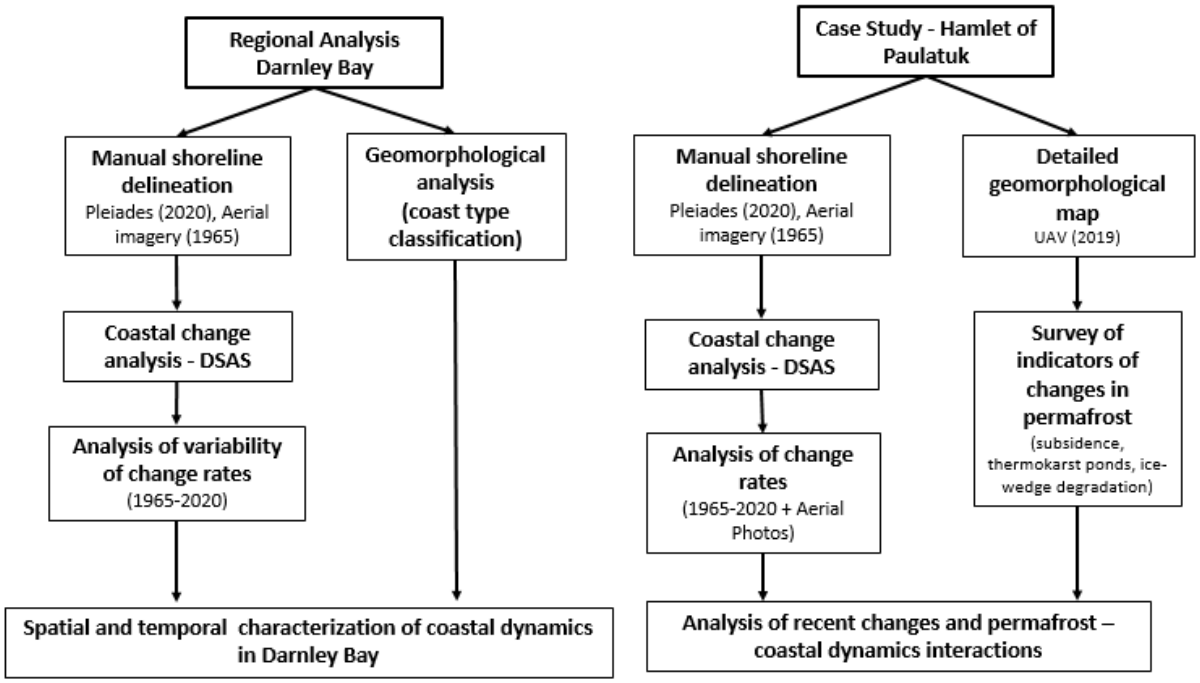

Figure 12. Regional and Local analysis workflow

The regional analysis is based on the processing of, aerial photography of 1965 from Energy, Mines and Resources of Canada distributed by NRCan and very high resolution satellite images from 2020 provided by CNES and Airbus, in order to establish a spatiotemporal characterization of coastal dynamics within Darnley Bay. The coastline was manually digitized for each year to perform the coastal change analysis with DSAS. Simultaneously, a geomorphological analysis for classifying the coast types was performed based on the interpretation of the Pleiades imagery.

Our case study focuses on the Paulatuk Peninsula located on the south of the Darnley Bay, following the same workflow of the regional analysis for the coastal change analysis (Figure 12). A detailed geomorphological map of the settlement was prepared using an ultra-high resolution UAV orthomosaic of 2019 coupled with a DSM. The material used is compiled in Table 1

Satellite Data	Bands	Acquisition date	Resolution [m x m]	Site	Image source	Scale of analysis
Pleiades	4	Aug 2020	0.5 x 0.5	Darnley bay	ISIS-Airbus	regional/local
UAV	4	Aug 2019	0.25 x 0.25	Paulatuk	IGOT-ULisboa	local
DSM	1	Aug 2019	0.5 x 0.5	Paulatuk	IGOT-ULisboa	local
Arctic DEM	1	June 2017	16 x 23	Darnley bay	Arctic DEM	regional
Aerial photography	1	Aug 1965/1975	0.6 x 0.6	Darnley bay	NRCan	regional/local

Table 1. Remote sensing and derived data used in this study

4.2 Remote sensing data.

4.2.1 Very high resolution Pleiades imagery

Multispectral high resolution satellite imagery from 2020 have been acquired within the ISIS - Pleiades Programme distributed by Airbus DS. The Pleiades imagery was acquired through the Polar Space Task Group (WMO), within an agreement between IGOT and CNES. Launched in December 2011, the Pleiades is a high-resolution optical observation system designed to provide a high acquisition capacity with a revisit time of less than 24 hours to meet both civilian and military requirements. The satellites capture images with a swath of 20 km, in panchromatic mode (1 band) with a very-high optical resolution of 50 cm as well as in multispectral mode (4 bands) with a resolution of 2 meters, which are then co-registered and merged. The 11 scenes acquired were pan-sharpened using ENVI 5.6 with a resolution of 50 cm and cover the western coast of Darnley Bay, from Cape Parry to the Hornaday river delta (Figure 13). Geometric and radiometric processing were performed on the images, including sub-swaths combination, Rational Polynomial Coefficients model (RPCs) and de-noising.

Because of their very high resolution and their alignment accuracy, Pleiades images are suitable for small scale analysis in various applications such as cartography, hydrology, marine environment, geophysic and defense purposes. In this study, these scenes are used for accurate manual digitizing of the complex shoreline of Darnley Bay and for geomorphological characterisation of the studied coast.

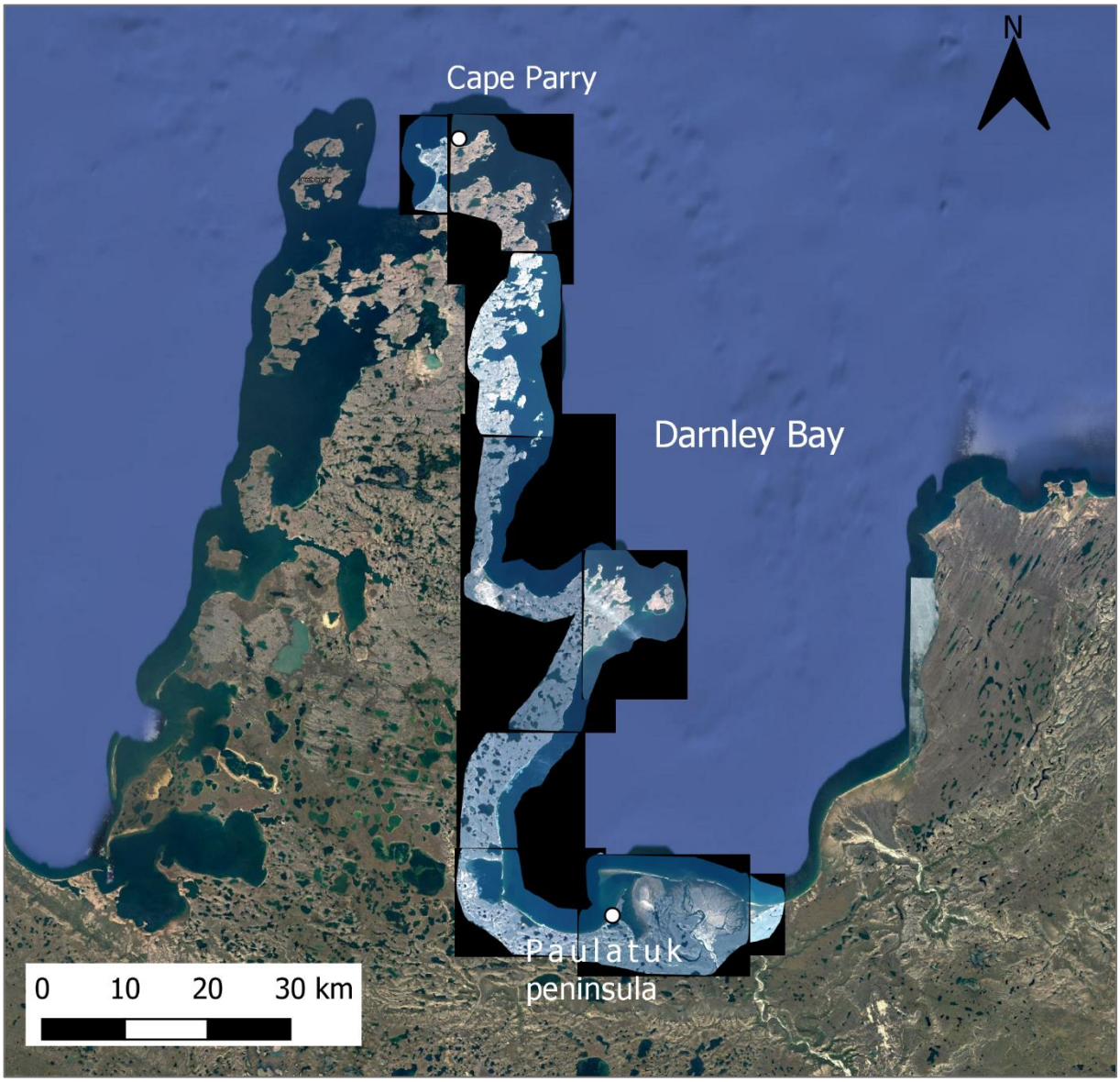

Figure 13. Coverage of the acquired Pleiades scenes over Google Earth imagery. PLEIADES © CNES, 2020, distribution Airbus DS. Background images: Landsat / Copernicus 2020 and IBCAO from Google Earth.

Figure 14. Example of image resolution. On the left the 1985 Landsat image at 30 m resolution, on the right the 2020 Pleiades image at 0.5 m, in the Cape Parry area.

4.2.2 Historical aerial photographs

Historical aerial imagery of 1965 provided by Natural Resources of Canada (NRCan) are used to assess shoreline changes along Darnley Bay over the period from 1965 to 2020. We used the data sets of the rolls 18909, 18919, 18922 accessible through the "*eodms-sgdot.nrcan*" website. The panchromatic images were captured in August 1965 at an altitude of 7 km by a vertical viewing angle to create a CRONAR film of 9.2 cm. The focal length is about 152 mm. These images have a high value as they provide historical informations about the landscape at a given time and are useful for the analysis of change through time. Photogrammetric operations were conducted to correct the optical distortions produced during their capture. A total of 17 monochrome air photos at 1: 50 000 scale have been georeferenced and orthorectified with the construction of RCPs using the 20 m Digital Elevation Model (ArcticDEM) in ENVI 5.6. Orthorectification processing was applied to remove internal and external distortions, relief effects and to assign correct geographical coordinates to the images. To do this, the internal orientation is constructed from the camera specs: camera model, focal length (mm) and fiducial marks coordinates. The construction of the external orientation was done by selecting common reference points (GCPs) between Pleiades image and the aerial photos, assigning the points their coordinates (X and Y) and the elevation from the DEM. This procedure allows the program to calculate the RCPs for the treated image. The last step consists of the refinement of the RCP model. ENVI takes into account the selected GCPs and estimates the errors (RMSE in meters)

for the X, Y, and Z axes to calculate the horizontal and vertical accuracy. The final product is an ortho-photography exported in TIFF format.

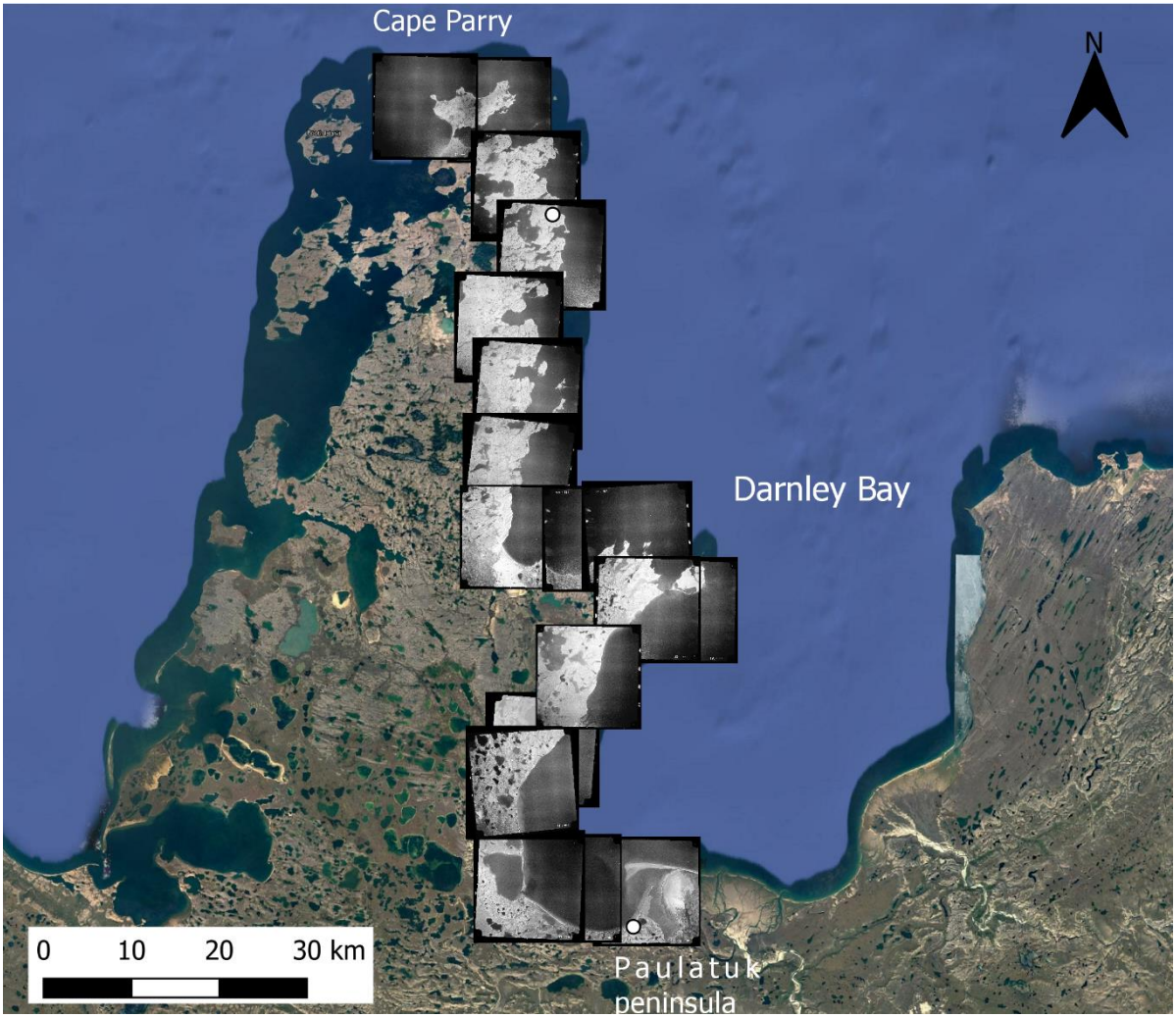

Figure 15. Coverage of the aerial ortho-photographies displayed over Google Earth imagery. NRCAN Aerial Photography 1965. Background images: Landsat / Copernicus 2020 and IBCAO from Google Earth.

Given in the very scare infrastructures in this area, placing common reference points between 1965 and 2020 needs to be done precisely to maintain accuracy, but is extremely challenging. To do so, proxies used must remain consistent over time. Natural proxies such as small islands, the center of small ponds, ground-crack intersections and vegetation patches were chosen (Figure 17). The good resolution of these aerial photographs allowed to digitize the shoreline using various proxies: bluff-top line, vegetation line and wet-dry line (see section 4.4). These images were also used for the delineation of ice-wedges situated below the foundations of the current infrastructures, such as the airstrip and buildings in the Paulatuk Peninsula detailed study area. The submetric resolution of the pansharpened Pleiades imagery and the aerial photographs, allow a precise analysis of the geomorphic processes and coastal processes

occurring. Their comparable resolution (0.5 m and 0.6 m) allows a precise analysis of shoreline change further discussed.

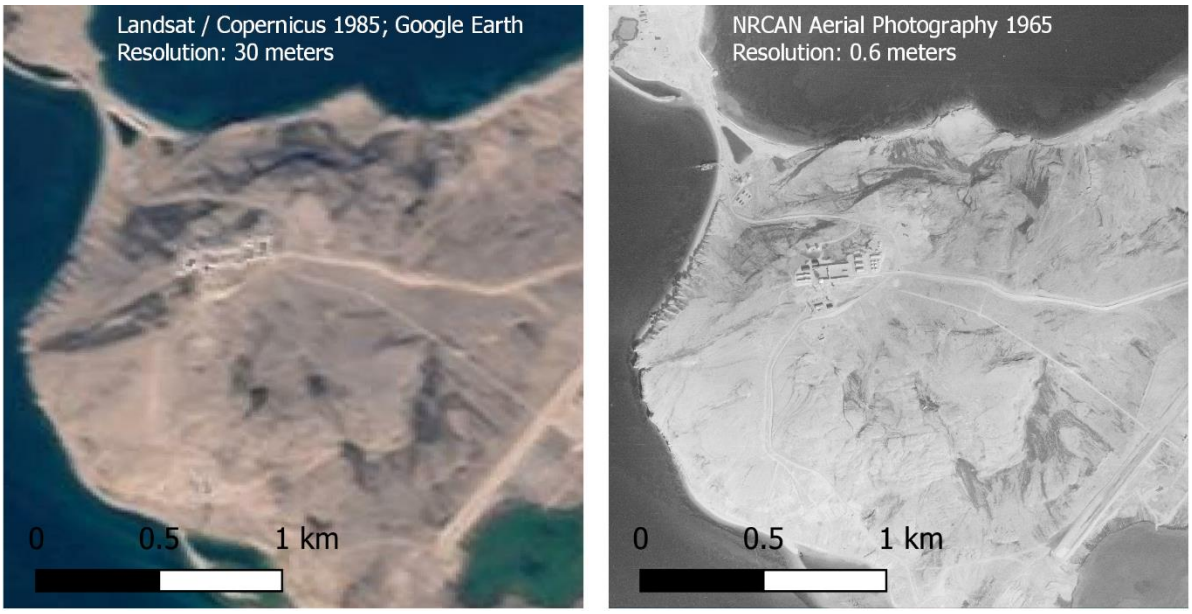

Figure 16. Example of image resolution. On the left the 1985 Landsat image at 30 m resolution, on the right the 1965 NRCAN aerial photography, in the Cape Parry area.

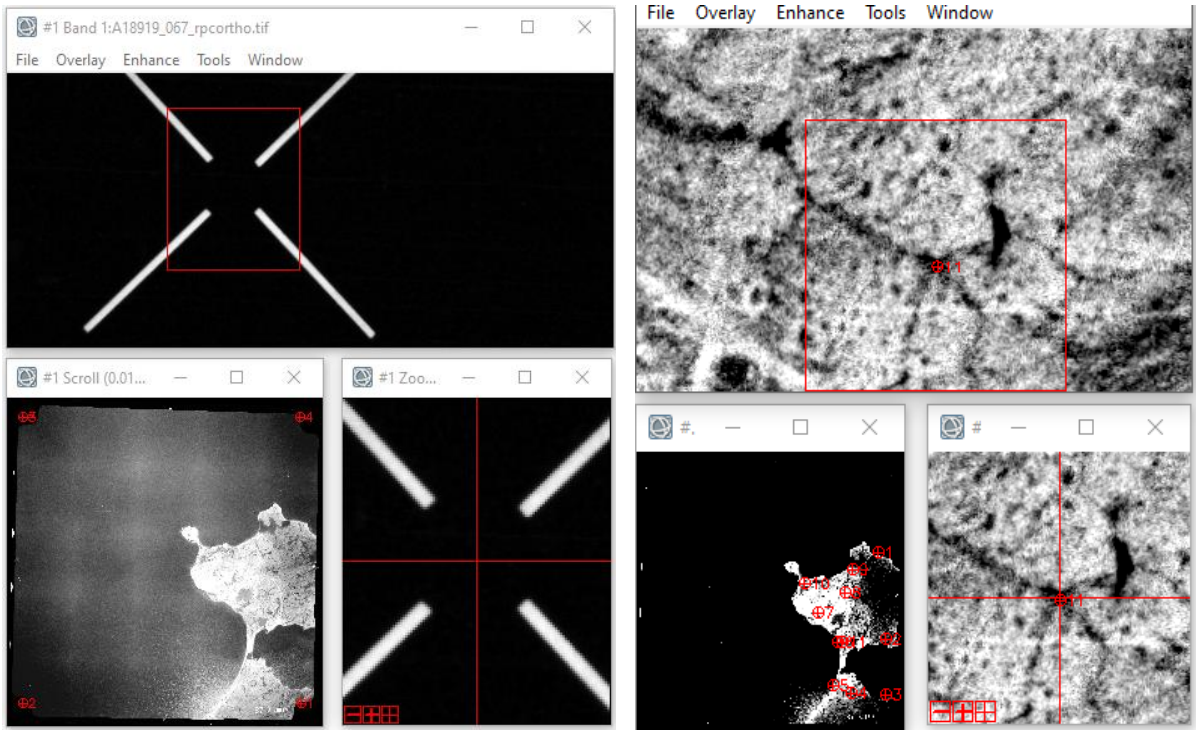

Figure 17. Fiducial marking (left) and GCPs marking (right) in ENVI 5.6 windows display. The left window shows that ice-wedges intersections can be used for reference point placing.

4.2.3 Ultra-high resolution UAV imagery

The Nunataryuk-ULisboa team conducted unmanned aerial vehicle (UAV) field data collection between June and August 2019 at several coastal sites around the Beaufort coast including Tuktoyaktuk, the Pingo Canadian Landmark Park and the Paulatuk Peninsula. The objective of the mission was to follow up on the 2018 survey and the accurate collection of field data, which provided a high quality 3D baseline survey and collecting ground truthing data for satellite imagery analysis. The whole Paulatuk settlement was surveyed with aerial photos with ultra-high resolution (2.5 cm). The imagery was collected using a SenseFly eBee Classic fixed-wing UAV with a Sensefly SODA 20 MP optical camera. Georeferencing was done using GNSS RTK DGPS and 58 Ground Control Points (GCPs) well distributed over the dataset area (3.4 km²), in order to obtain an optimal accuracy. The processing of the raw images was done using PIX4D photogrammetry software. The root mean square error of the point cloud calculated using 17 independent check points was 0.04 m (X), 0.03 m (Y) and 0.08 m (Z). An orthomosaic and Digital Surface Model (DSM) have been generated with 5 cm resolution (Figure 18 and Figure 19).

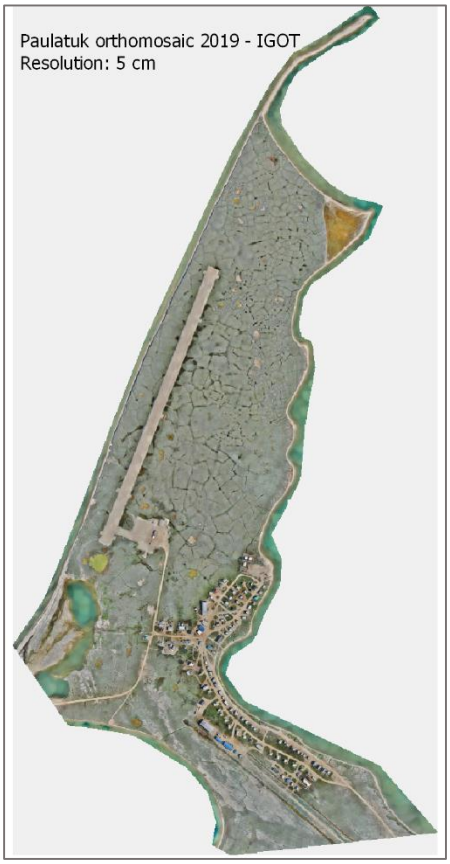

Figure 19. Orthomosaic of Paulatuk. IGOT 2019

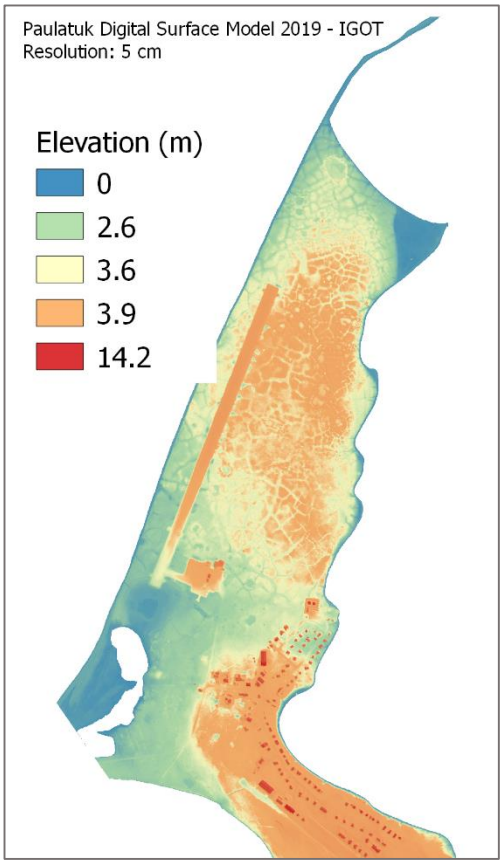

Figure 18. DSM of Paulatuk, displayed with color palette and hillshading. IGOT 2019

4.2.4 The Arctic Digital Elevation Model

In order to proceed the orthorectification workflow, we used the ArcticDEM of Darnley Bay, provided by the Polar Geospatial Center. The ArcticDEM is a National Geospatial-Intelligence Agency (NGA) and National Science Foundation (NSF) project which provides a high-quality Digital Surface Model (DEM) of the Arctic derived from DigitalGlobe satellite imagery. The ArtcicDEM covers the entire territory north of 60°N and offers a spatial resolution of 2 m to 1 km. Since 2016, 7 releases are available. The output DEM is available in "strip" files or mosaics in GeoTIFF format and projected WGS 1984 EPSG Alaska Polar Stereographic. We acquired the DEM of Darnley Bay with a resolution of 20 meters from the ArcticDEM explorer (Figure 20).

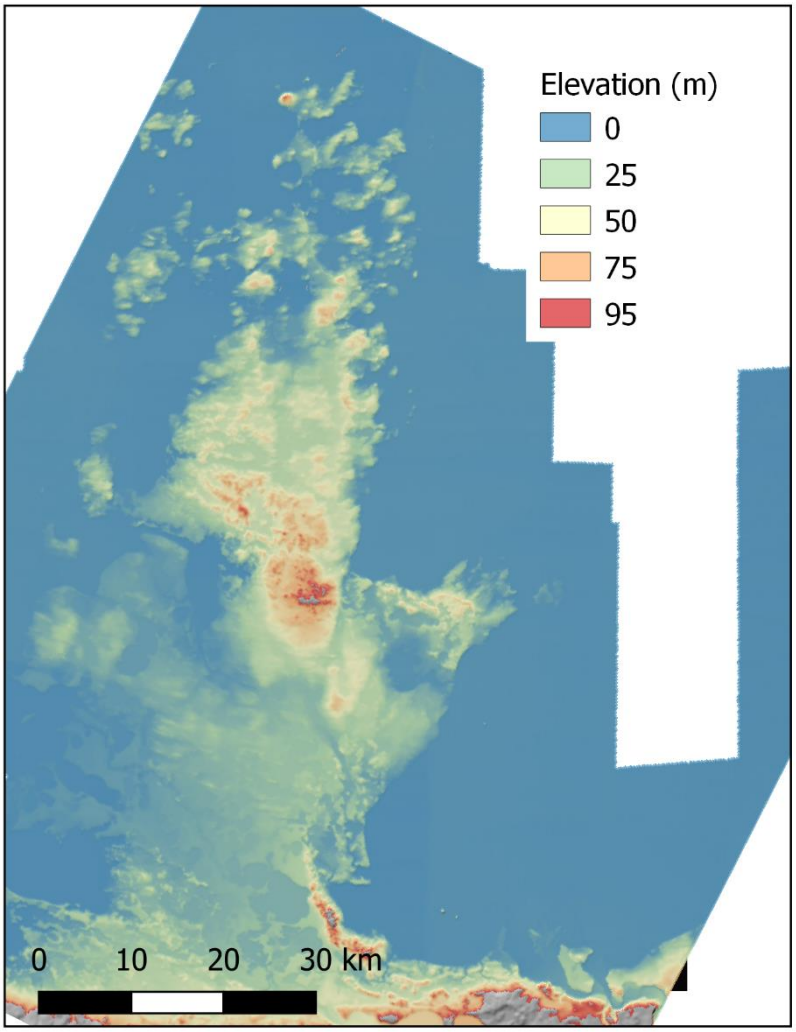

Figure 20. ArcticDEM 20 m of Darnley Bay area. Created by the Polar Geospatial Center from DigitalGlobe, Inc. imagery.

4.3 Regional scale coastal classification

4.3.1 Shoreline digitizing

The characterisation of the coast types was made by the analysis of the Pleiades satellite imagery. The coasts were classified according to the elevation and the type of exposed material. As several proxies for the coastline are possible to identify on the Pleiades images. In order to quantify the coastal erosion rather than the near-shore sediment dynamics we selected the vegetation limit and cliff-top, rather than the dry-wet lines or water level limits in order. Where the cliff-top of vegetation limit was absent, we have adapted the coastline digitisation with the available references.

4.3.2 Types of coasts

In order to arrive at a classification of coastline types, the identification was done by interpretation of Pleiades satellite images in addition to results collected by videography by Environment Canada along the Beaufort coast in their regional sensitivity atlas (Environment Canada, 2015). They classified the coastline of the Beaufort Sea coat in function of their sensitivy to oil spilling for prevention purposes. However, the only interpretation of satellite images does not allow to distinguish the observed sedimentary material. (organic material, sand, pebble, mud). The coastal forms determined in the Darnley Bay coast are exosed in the figures above. We identified 6 main coastal forms:

a. **Tundra bluff** : Unconsolidated cliffs composed of silty clays and organic material and are characterised by high ground-ice content. These shorelines are sensitive to thermal abrasion and wave action.
b. **Tundra slope** are ice-poor and present a sub horizontal to low slope face. These cliffs are generally lined by narrow beaches of gravel or sand. The principal processes of mass loss for ice-poor tundra cliffs are surficial washout and landslides.
c. **Rocky cliffs** are impermeable outcrops of consolidated rock. Erosion can create slots, caves and arches and slopes.
d. **Mixed sediment beaches** are sedimentary accumulation forms, mainly present along the coast. They are composed of mixed sediments ranging from pebbles to sand. These forms are subject to seasonal remobilisation by the action of sea ice, waves and alongshore currents.
e. **Tidal flats** are characterised by low slope foreshore commonly presents in sediment rich environment. They can be constituted of sand and mud and present a very dynamic.

Sandy tidal flats a very dynamic surface layer subjected to sediment remobilisation due to tide effect waves and surface run-off. They are ecologically valuable environments in reason of their high biomass production and the habitat they generates for bird populations. Tidal flats also act as a buffer against wave impact sea level rise for the backshore areas.

f. **Inundated low-lying tundra**: This type of shoreline is characterised by very low-lying coastal tundra that is inundated or submerged by marine waters during high spring tides or wind-driven surges. These areas are not located in the intertidal zone. They are marked by a pattern of regular geometric patterns of the ice-wedge polygons and shallow water ponds.

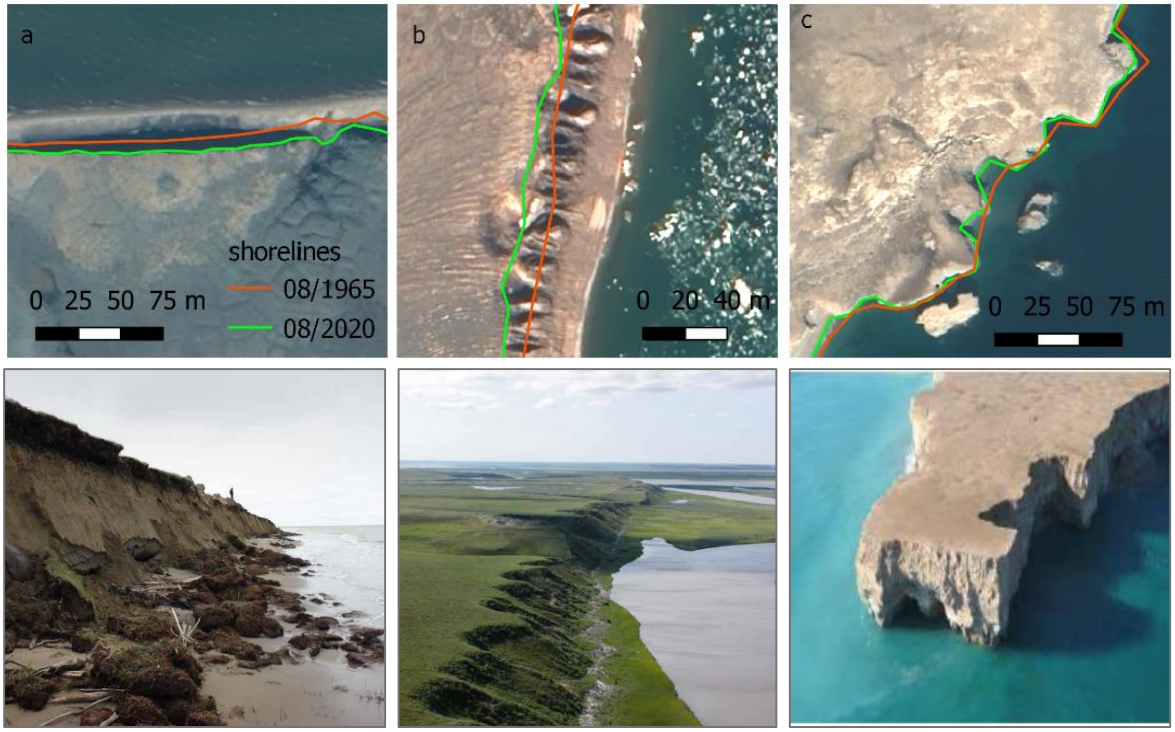

Figure 21. High coasts forms identified in Darnley Bay: (a) tundra bluff; (b) tundra slope; (c) rocky cliff. Images: PLEIADES © CNES, 2020, distribution Airbus DS ; Photos : Beaufort regional coastal sensitivity altas, 2015

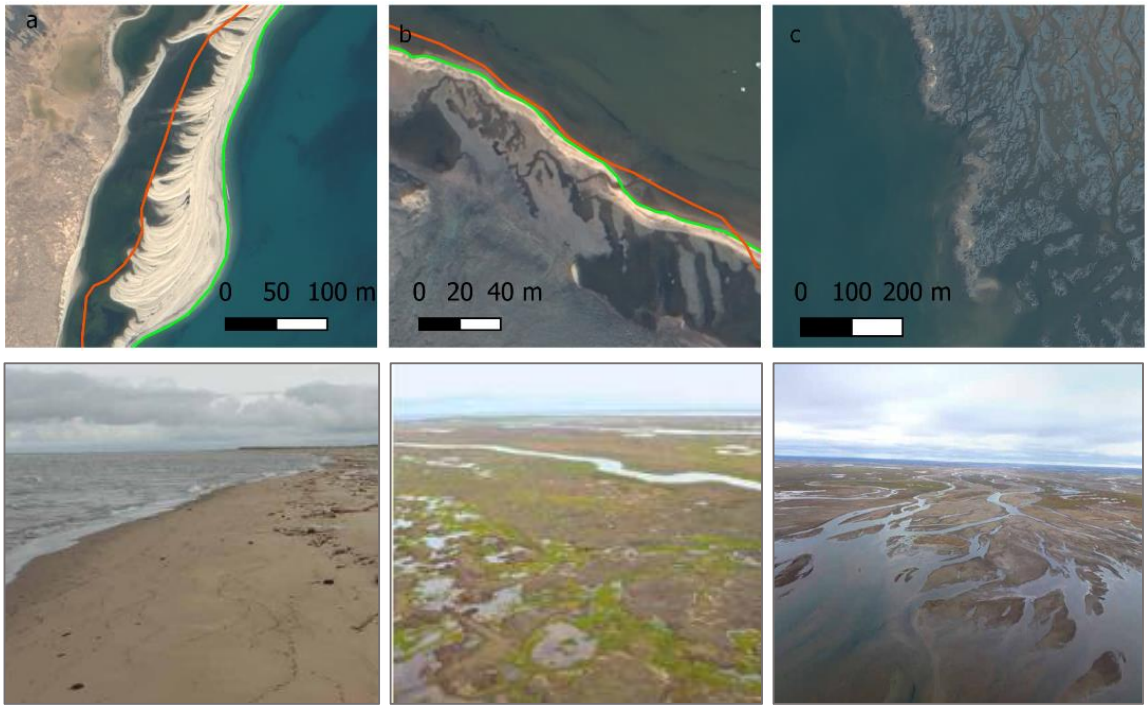

Figure 22. Low coast forms identified in Darnley Bay: (a) mixed sediments beach; (b) inundated low-lying tundra; (c) tidal flats. Images: PLEIADES © CNES, 2020; Photos: Beaufort regional coastal sensitivity Altas, 2015

4.4 High resolution geomorphological mapping at Paulatuk

A high resolution geomorphological map of Paulatuk was created using the ultra-high resolution UAV orthomosaic coupled with analysis of the DSM of 2019. The features digitization was performed in QGIS v3.4 photointerpretation.

A hill-shade layer was derived from the DSM to enhance the three-dimensional appearance of the terrain by using patterns of light and shadow. This representation of the surface made it easier to identify the landscape features. The high resolution of the orthomosaic coupled with the DSM allowed to map of very detailed terrain forms such as small thaw ponds and ice-wedges through. The 1965 aerial imagery covering the settlement was used for terrain comparison over the 55 years.

4.4.1 Coastal landforms

Coastal landforms are terrain morphology controlled by marine processes (e.g., tides, currents, longshore drift, wave action and storm surge). Coastal geomorphology strongly depends on lithology, meteo-marine forcings and erosional or depositional dynamics. In Paulatuk peninsula we identify 7 coastal landforms (Figure 23):

a. **Low tundra bluff / low active tundra bluff** are unlithified cliffs are composed of frozen poorly consolidated material such as organic matter, sand, silt and clay. These cliffs are fronted by sandy and gravel narrow beaches and are sensitive to temperature changes and wave action presenting various erosional features.
b. **Inundated tundra flat** refers to very shallow submerged areas stretching until the foreshore zone. They are usually under the influences of tides and present intertidal flats.
c. **Flooded lake basin** are here designated as a partially open body of water partially enclosed by a beach, they can be formed by the breaching of ancient coastal thaw lakes.
d. **Sandy beach** are narrow and stretches along the cliffs and are subject to current and wave reworking.
e. **Sandy spit** are accretional sedimentary forms anchored to headlands and are formed by waves and longshore drift forming ridges pattern.
f. **Dunes** are present on top of accretional sandy stretches and are formed by wind action coupled with sediment supply from currents and waves, their stability is characterised by their vegetation.
g. **Eroded ponds** are features resulting of the erosion of an old coastal thaw pond.

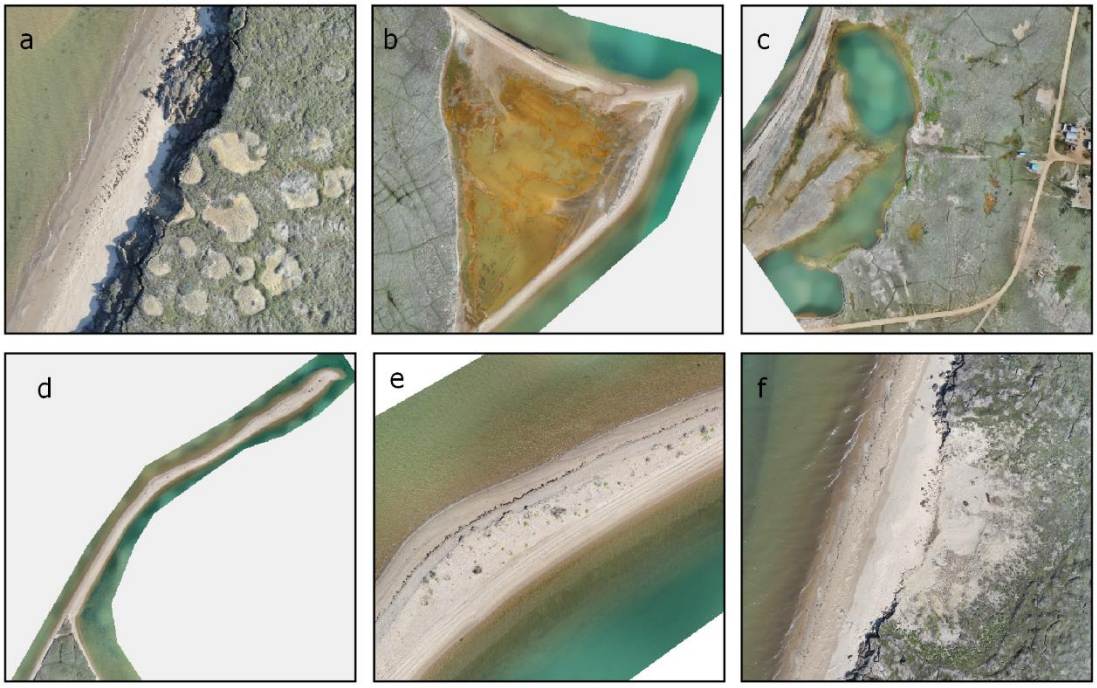

Figure 23. Coastal landforms identified in Paulatuk: (a) active tundra bluff and fronted beach; (b) inundated tundra flat; (c) lagoon; (d) sandy spit; (e) dunes); (f) eroded pond. Paulatuk orthomosaic – IGOT 2019

4.4.2 Periglacial landforms

Periglacial landforms are associated with permafrost and cryogenic and thermal processes. These landforms are related to climates subject to long and intense freezing conditions and are the result of the formation of melt of ground ice (Figure 24):

a. **Ice-wedge polygon troughs** are depressions associated to the presence of ice-wedges and formed by the successive freeze and thaw events of water and ice infiltrated within ground cracks. These process result in the formation of a polygonal network (Mackay, 1995).
b. **Center polygon thaw ponds / Interpolygonal thaw ponds** are water bodies formed by the melting of ground ice and snow in depressions formed by ice-wedges polygons. We made the distinction with the thaw ponds located in the depression formed in the center of the polygons (low center polygon ponds) and the interpolygonal thaw ponds, located in the troughs. Intepolygonal ponds present a darker water colour because they are deeper.
c. **Dry ponds** are drained thaw ponds due infiltration accompanying with thaw progression, by gullying inducing a draining of the water content or by evaporation.

d. **Ground-ice mound**s are small and convex cryostructures formed by the freezing of pore water under hydrostatic pressure.
e. **Peatlands** are poorly-drained wet soils composed of sediments and organic material.
f. **Wind-abraded area** are zones denuded of vegetation and can be the result of wind abrasion and desiccation.

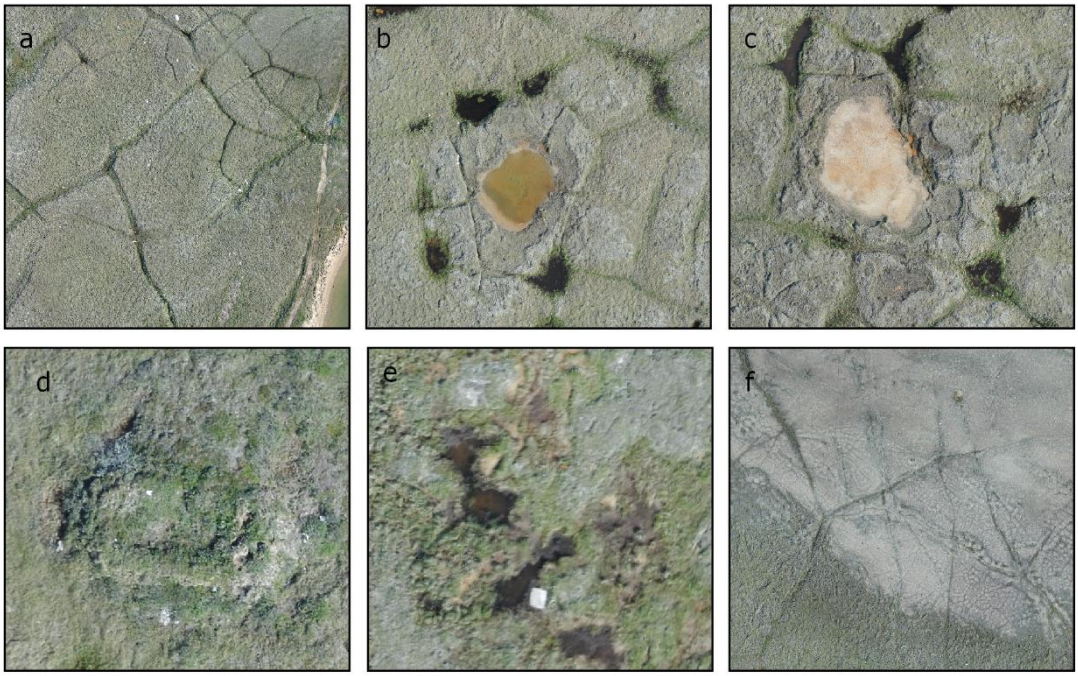

Figure 24. Periglacial features found in Paulatuk: (a) ice-wedges polygons; (b) center polygon thaw ponds pond and interpolygnal thaw ponds; (c) dry pond; (d) ground-ice mound; (e) peatland; (f) wind-abraded area. Paulatuk orthomosaic – IGOT 2019

4.4.3 Anthropogenic features

Established since 1920 in the peninsula, the Inuit community of Paulatuk has 327 habitants. From the comparison of imagery, we see that infrastructures surface have increased over the years. The present features include the airport runway and support infrastructure, various buildings and dirt roads. Bare-ground patches in the settlement have been identified as areas denuded of vegetation induced by human activity.

Figure 25. Infrastructures and human induced terrain alterations: (a) Airport runway; (b) habitations; (c) fuel tanks, (d) dirt roads; (e) water ponds; (f) bareground patch. Paulatuk orthomosaic – IGOT 2019

4.5 Coastal change analysis

4.5.1 DSAS transect creation

Once the digitizing of the coastline was done on the respective images, the analysis of coastal change was performed using Arcgis 10.4 software with the help of the DSAS v5.0 extension (Himmelstoss et al., 2018), which allows to perform statistical calculations of coastline evolution rates. The DSAS tool measures the differences between the different coastlines and automatically calculates the evolution rates (in m/year). To use this tool it is necessary to create a personal geodatabase that compiles the shorelines to be analysed and the baseline. Several parameters need to be set for the generation of the transects such as their spacing and smoothing distance, which will affect the distribution along the shoreline (Figure 26). For accurate results the transect needs to appear perpendicular to the shorelines (Figure 27). It is also important to estimate the uncertainty related to each coastline (Table 3). Finally, change statistics are calculated by the program for each transects. The results can be displayed in Arcmap and color ramps are applied in function to the change rates. The results are compiled in a table exportable in text format.

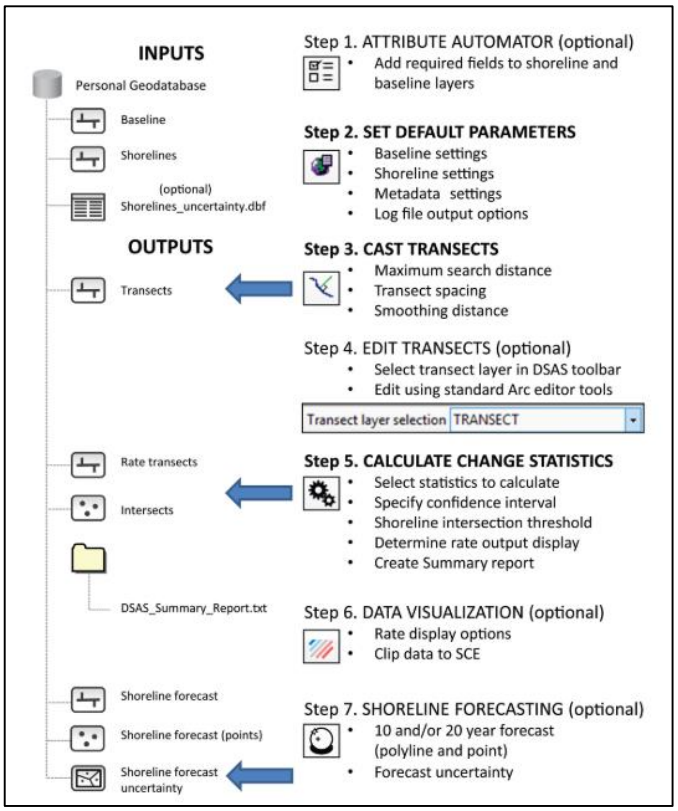

Figure 26. DSAS workflow (from Himmelstoss et al., 2018)

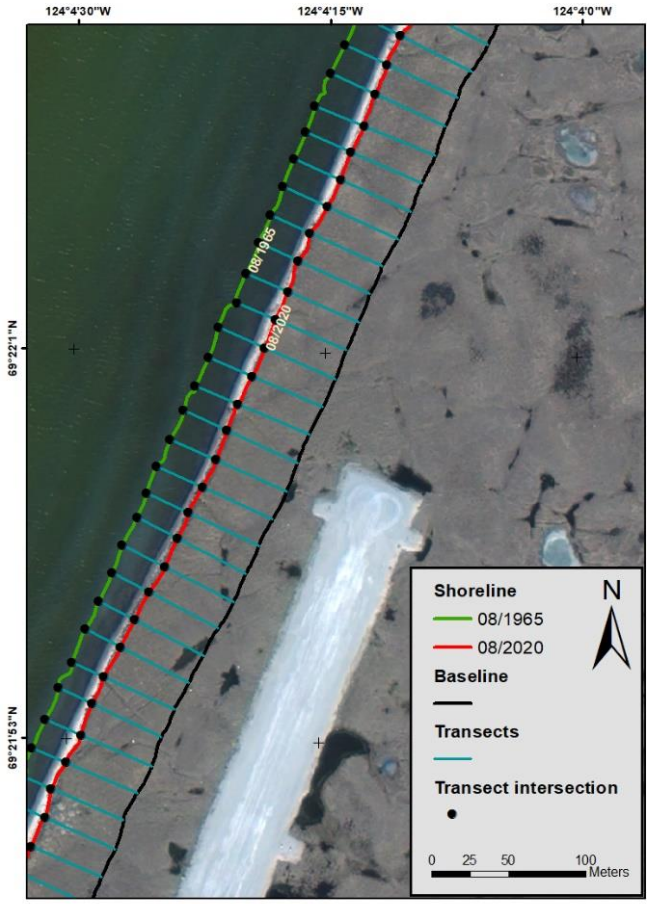

Figure 27. DSAS transects creation in Arcmap, west coast of Paulatuk peninsula.

4.5.2 Uncertainty estimation

The different imagery used for the shoreline extraction presents sources of errors, inherent to each images, which needs to be quantified to assess the significance of shoreline changes (Table 3). In this study, the uncertainty of shoreline position (Usp) was calculated for each shoreline as shown the following formula:

$$Usp = \sqrt{Urs^2 + Ura^2 + Ug^2 + Ud^2}$$

Equation 1. Shoreline position uncertainty.

Where Usp is Shoreline position uncertainty (m), Urs is the resolution uncertainty of the satellite imagery (pixel size, m), Ura is the resolution uncertainty of historical imagery (pixel size, m), Ug is the geroreferencing uncertainty (RSME, m) and Ud is the shoreline digitization uncertainty (1m).

The shoreline digitizing uncertainty an estimation the error generated during manual digitizing process. This value is chosen taking into account the pixel size (0.5 to 0.6 cm), doubled, giving a range of approximately 1 m error. Depending on the geographical region and the coastal morphology, the tide effect must be quantified as they can largely influence the position of the water-land interface depending on the tidal range and the slope of the foreshore. Here, we neglect this parameter since we are working on a regional scale and also because the effect of the tides is lesser knowing the micro-tidal range which extends from 0.3 to 0.5 m. As mentioned above, we prefer to digitise the vegetation line rather than wet-dry lines, which are not consistent over time. Furthermore the task is more complicated on monochrome aerial images where the colour contrast is not always clear (Cunliffe et al., 2019). The calculated uncertainties are compiled in Table 3.

capture date	ID of orthorectified images	GCPs	RMSE (m)	Pixel size	Usp 1965 (m)	Usp 2020 (m)
1965	A18909-068	10	3.6	0,7	±3.8	±1.3
	A18919-014	10	2.4	0,7	±2.7	±1.3
	A18919-032	14	2.3	0,7	±2.6	±1.3
	A18919-036	10	3.6	0,6	±3.8	±1.3
	A18919-052	14	3.2	0,6	±3.4	±1.3
	A18919-056	8	2.9	0,6	±3.2	±1.3
	A18919-067	10	4.2	0,6	±4.4	±1.3
	A18919-069	12	3.7	0,6	±3.9	±1.3
	A18922-038	9	8.4	0,6	±8.5	±1.3
	A18922-039	10	5.4	0,6	±5.5	±1.3
	A18922-041	14	4.0	0,6	±4.2	±1.3
	A19211-111	8	3.2	0,7	±3.4	±1.3
	A19211-144	9	2.8	0,6	±3.1	±1.3
	A19211-169	13	2.4	0,6	±2.7	±1.3
	A19211-174	11	3.4	0,7	±3.6	±1.3
	A19211-175	8	2.5	0,6	±2.8	±1.3
	A19211-177	11	3.9	0,6	±4.1	±1.3
Mean					**±3.9**	**±1.3**
2019	Paulatuk UAV	58	0.036	0,1	~	~
2020	Pléiades	~	0.35	0.5	~	~

Table 2. Compilation of errors related to processed images.

4.5.3 Coastal change indexes

We have chosen to calculate the End Point Rate (EPR) to measure variations between 1965 and 2020. The EPR is based on positional changes from the oldest to the youngest shoreline in a particular database. It is the the ratio between the time interval and the distance between two shoreline positions and gives the annual rate of change in meters. Thus, when only two coastlines are available, the EPR is still a good index for assessing kinematics (Thieler et al., 2005).

5. Coastal classification

5.1 Characteristics of the coast

Darnley Bay is situated in the Northwest Territories or Canada, at the entrance of the mouth of the Amundsen Gulf. We analysed the western coast of the bay which is the eastern coast of Parry peninsula, extending from Cape Parry, at its northern limit, to Paulatuk peninsula, its southern limit. The coast shows 16 rocky islands concentrated northern of Clapperton Island, which is the largest, measuring c. 4.7 x 2.7 km wide. Clapperton Island is situated in front of a large peninsula, dividing the coast in two distinct lithological units. The sector A is representing the lithified coast stretching from Clapperton Island to Cape Parry and the sector B represents the unlithified coast from Clapperton Island to Paulatuk (Figure 28). The statistics the coast types are represented in table 3.

	Class	Shoreline length (km)	%
Sector A	Fluvioglacial-sediments beach	121	24
	Tundra slope	60	12
	Tundra bluff	19	4
	Rocky cliff	180	36
	Rocky slope	114	22
	Inundated thermokarst lake	11	2
	Inundated low-lying tundra	0	0
	Sandy tidal flat	6	0
	Sandy delta	0	0
	Total	511	100
Sector B	Fluvioglacial-sediments beach	51	18
	Tundra slope	134	47
	Tundra bluff	33	12
	Rocky cliff	22	7
	Rocky slope	13	4
	Inundated thermokarst lake	3	1
	Inundated low-lying tundra	19	7
	Sandy tidal flat	3	1
	Sandy delta	4	1
	Total	282	100

Table 3. Coast type coverage in sector A and B.

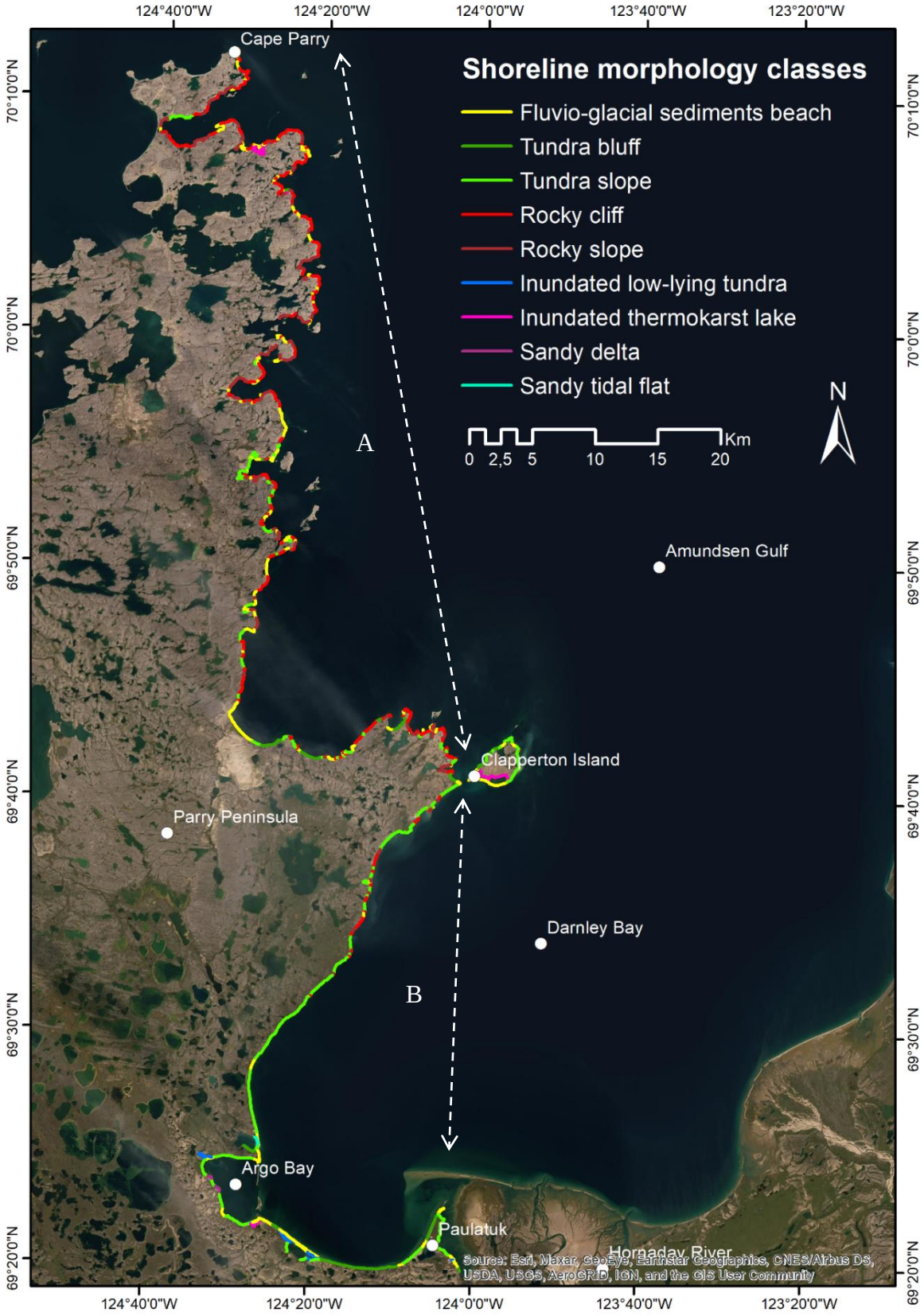

Figure 28. Shoreline classification map of the eastern coast of Parry peninsula.

5.1.1 Sector A

The northern coast, from Cape Parry to Clapperton Island is characterised by a very indented rocky coast, composed of Proterozoic-age dolostone forming numerous inlets and rocky headlands. The results show that the lithified coastlines are concentrated north of Clapperton Island (Figure 28). Rocky cliffs and rocky slopes accounts for 58 % of coastline of the sector A (Table 3). The high areas are composed of rocky cliffs up to 20 m where erosion has created notches arches and pinnacles. The rocky slopes are fronted by narrow beaches of mixed sediments, interrupted by numerous inlets formed by the opening of ancient coastal lakes. Locally, the rocky coast is intersected by low sections composed of unconsolidated material drained by rivers favouring the accumulation of sediment. These accumulation forms are reworked by waves and local currents deposited at the extremities of headlands and small islands forming barrier beaches tombolos and spits. At the same latitude as Clapperton Island a section of coast made of unlithified material and stretches on 12 km facing the northwest direction (Figure 29a). This portion is characterized by a long barrier beach to the west, set up by numerous coastal tributaries. The eastern part of this area composed of unconsolidated material exposing tundra bluffs and tundra slopes

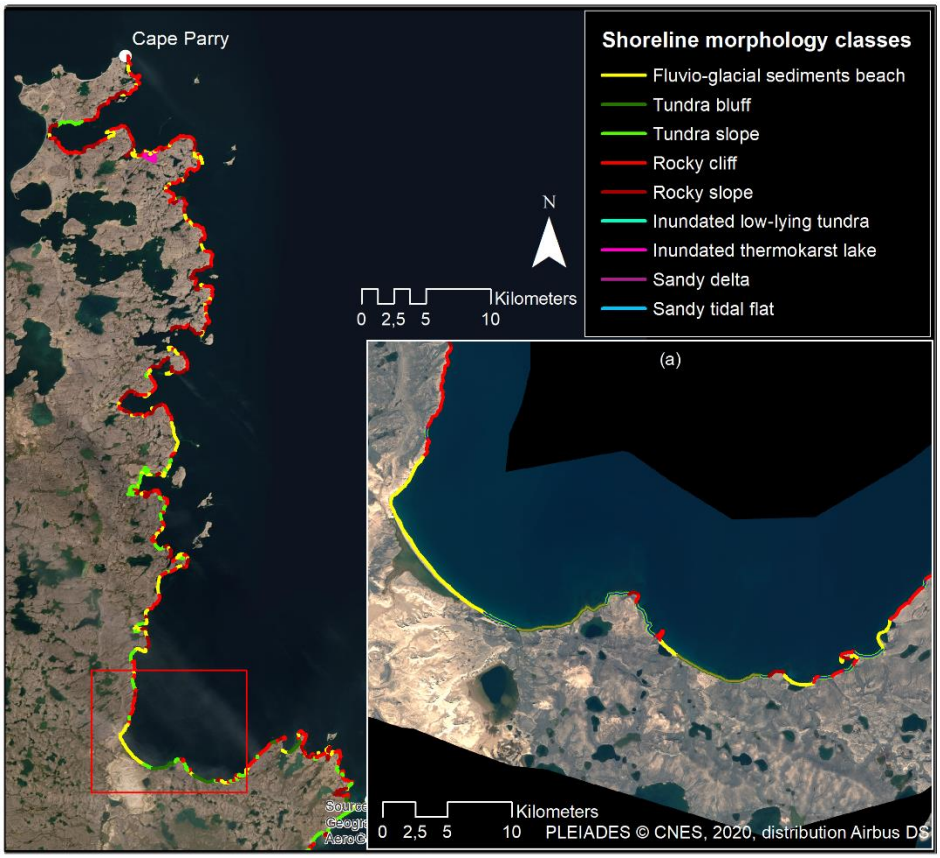

Figure 29. Coastline classification in sector A.

5.1.2 Sector B

The coastline between Clapperton Island and the Paulatuk Peninsula has a smooth, profile. From Clapperton Island to Argo Bay, the coastline is oriented in a south-southeast direction. The southern part of 130 km, from Clapperton Island to Paulatuk is composed of unlithified organic and silty materials (i.e. tundra soils). Tundra bluffs and slopes represent 59 % of this sector (Table 3) and are bounded by narrow sandy or a gravel beaches. This coast is cut by rivers coming from the thermokarst lakes of the hinterland which can form large mouths or deltaic formation, such as the two small deltas present at Argo Bay or the big delta formed by the Hornaday river. Argo Bay is the largest bay inserted in the south west and is the result of the breaching of a coastal lake flooded by the sea (Harper, 1990; Manson et al., 2004). Long strips of mixed sediments partially close off the coastal bays. The north-south orientation of these forms attest to the littoral drift direction in this area. Following to the southeast, the Paulatuk Peninsula is low fluvio-glacial terrace (Sankar et al., 2019) located at the head of the bay and has a north-south orientation. This peninsula is characterized by a low active tundra bluff, with a sandy spit embedded in the north, extending north-eastward. Paulatuk is partially protected from northern swells by a sandy flat spit connected to the Hornaday River delta (Figure 30).

Figure 30. Unlithified coast and associated coast types.

5.1.3 Mobile fluvio-glacial sediments features

22% of the digitized coast is constituted by accumulation landforms composed of remobilized fluvio-glacial sedimentary material. Sandy and gravel features are remobilized during summer by waves and alongshore drift currents to form spits, tombolo and barriers beaches and ridged beaches (Figure 31a) connected to the headlands and which show the orientation of the current (Figure 31c). However, due to the orientation of the study coast, the short open-water season, the very small tidal range and limited wave action, remobilization and transport of materials is very slow. Berms and regular ridges are visible along beaches and spits (Figure 31a) which can indicate that the sediment may have been be reworked by sea-ice, pushing sediments against the coast during strong katabatic winds events (Hequette & Barnes, 1990, French, 2018). The Figure 24 is showing accumulation landforms

Figure 31. Accretional features present along the coast. Ridged beaches (a); Tombolos (b); Spit (c), Barrier beach (d). Images: PLEIADES © CNES, 2020, distribution Airbus DS.

6. Long-term shoreline change rates

The quantification of coastal changes over 55 years has been done by calculating change statistics along transects intersecting the shoreline in the two reference dates: 1965 and 2020. The End Point Rate value provides the mean annual rate of change. The spatial distribution of shoreline change rates between 1965 and 2020 is shown on the map in Figure 32. The results reveal that the mean EPR value for the whole coast is -0.1 m/yr., with 70 % of the studied coastline being stable, 26 % is subject to erosion and 4% accreting (Table 4). Among the types of coast identified, unlithified coastlines are presenting the fastest retreat rates up to 3 m/yr. on mixed sediment beaches and 69 % of the tundra bluffs are eroding. By opposition, 84 % of the rocky cliffs are stable. These results suggests that change rates are not uniform in the space and a dependent of the type of coast.

Class	Coverage km (%)	Mean EPR (m/a)	Max. erosion rate (m/yr.)	Median EPR (m/yr.)	Erosion %	Stability %	Accretion %
Fluvioglacial sediments beach	172 (22)	-0.1	-3.0	0.0	25	65	9
Tundra slope	194 (25)	-0.1	-2.5	-0.1	35	61	5
Tundra bluff	52 (7)	-0.2	-1.4	0.0	69	31	0
Rocky slope	128 (16)	0.0	-0,8	-0.1	19	78	4
Rocky cliff	199 (25)	0.0	-0.7	0.0	16	84	0
Inundated thermokarst lake	15 (2)	-0.1	-0.5	-0.1	28	63	9
Inundated low-lying tundra	20 (3)	0.0	-0.2	0.0	19	78	3
Sandy tidal flat	4 (0)	-0.3	-0.7	-0.3	64	36	0
Sandy delta	4 (0)	-0.3	-1.0	-0.2	65	31	4
Total	788 (100)	-0.1	-3.0	0	26	70	4

Table 4. Summary statistics of shoreline change rates by coastal classification classes.

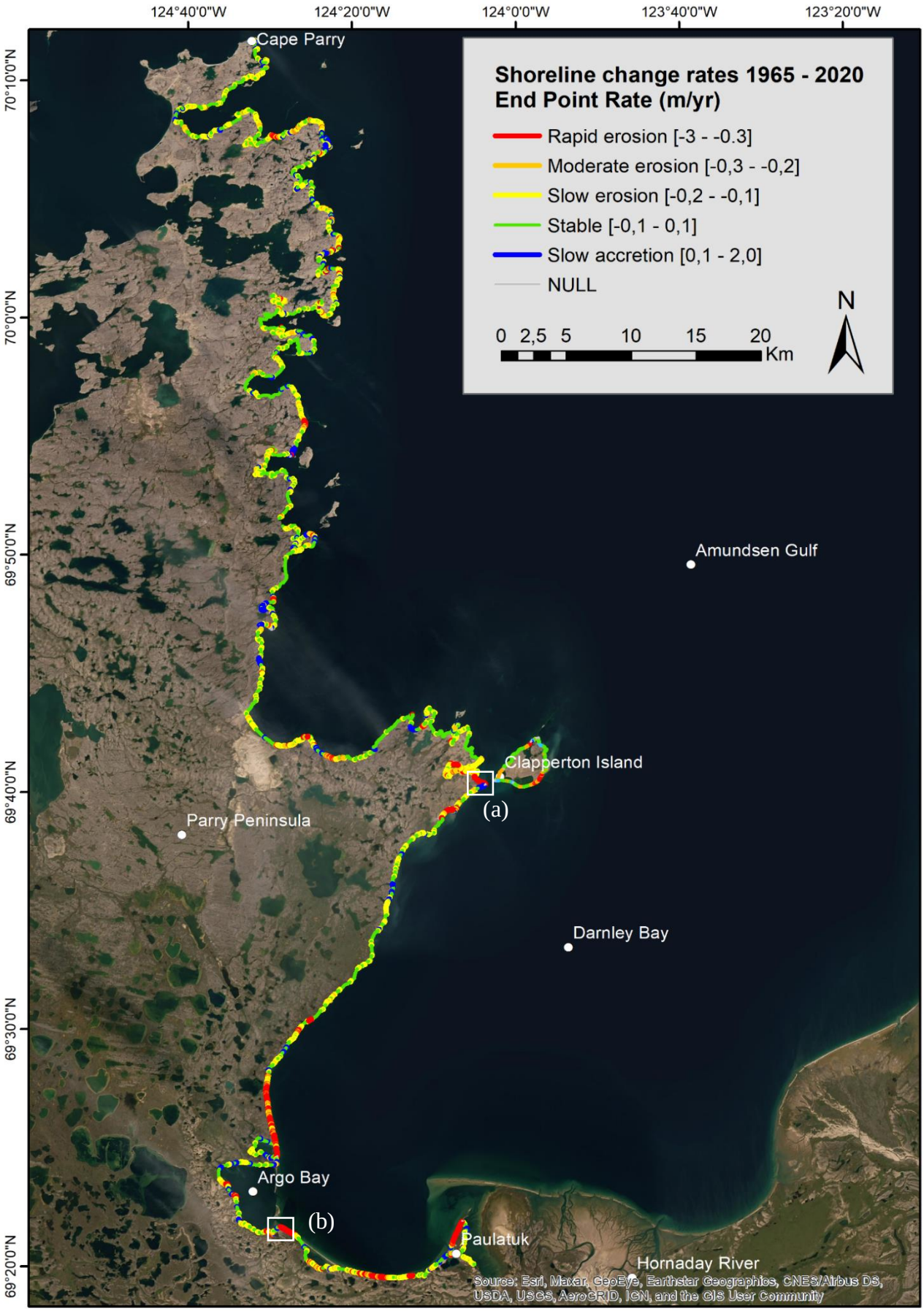

Figure 32. Shoreline change rates between 1965 and 2020 in the eastern coast of Parry Peninsula.

6.1 Spatial variability of shoreline change rates

This section is detailing the spatial variability of shoreline change rates in function of lithological units established previously. The results show that coasts made of unconsolidated materials represent the majority of eroding coasts. Indeed, tundra coasts account for 63 % of the retreating coastlines and present the second fastest retreat rate (2.5 m/yr.) measured along tundra slopes (Figure 27). These coasts are sensitive to thermal abrasion and wave action due to their high ice content and sedimentary composition. To a lesser degree, there is very little change along the rocky coastline between Clapperton Island and Cape Parry. Rocky cliffs and slopes are characterised by a significant stability. 84 % of rocky cliffs and 78 % of rocky slopes are not experiencng changes (Table 4). Overall, the rates of coastline change agrees with the type of material exposed.

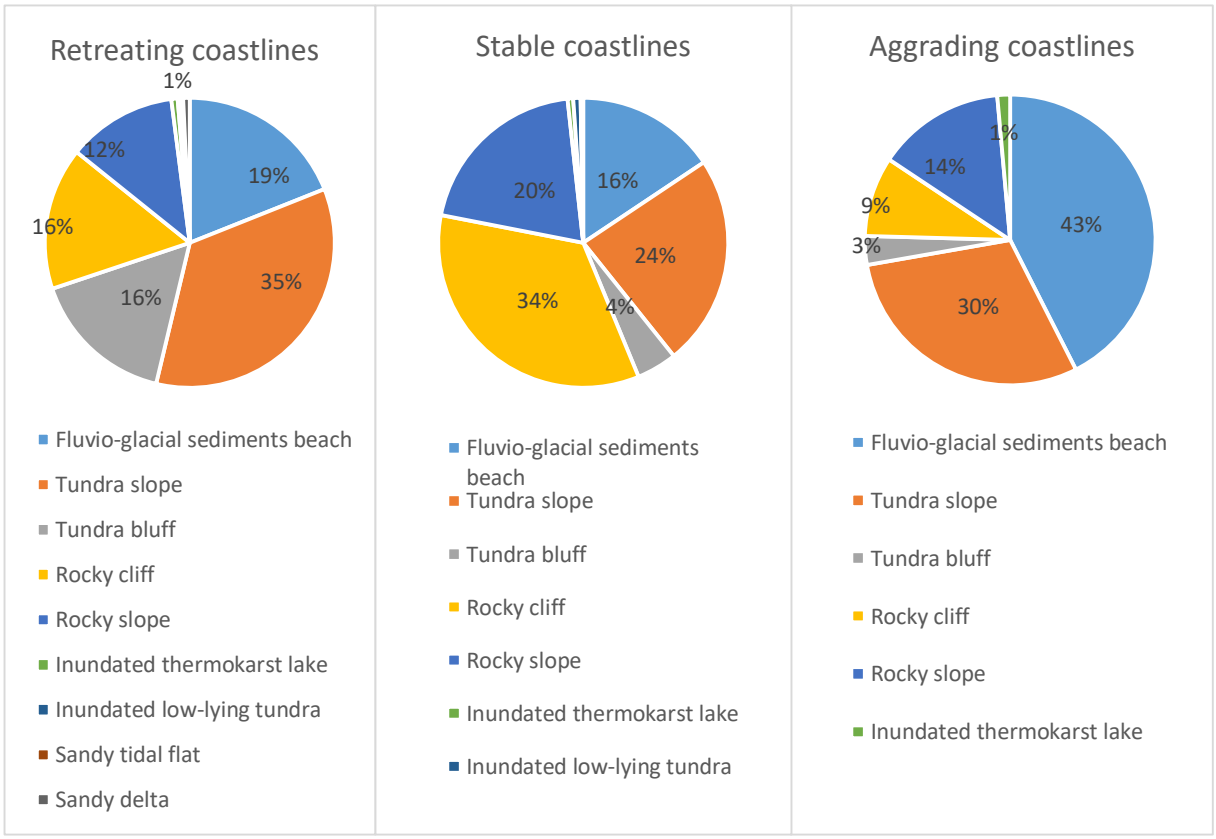

Figure 33. Coastal dynamics and the associated coast type.

6.1.1 Changes occurring along the sector A

The results are showing that the lithified coast shows 72 % stable. The high erosion and accretion rates are mostly occurring along mixed sediment stretches. The maximum retreat rate (-0.9 m/yr.) occurs is along tundra slopes present in inlets. However, this coast presents the highest accretion value (2 m/yr.) measured along a sandy spit (Figure 34b). Erosion occurring on rocky cliff remains very localized and might be the result of sudden mass movements creating notches (Figure 34a).

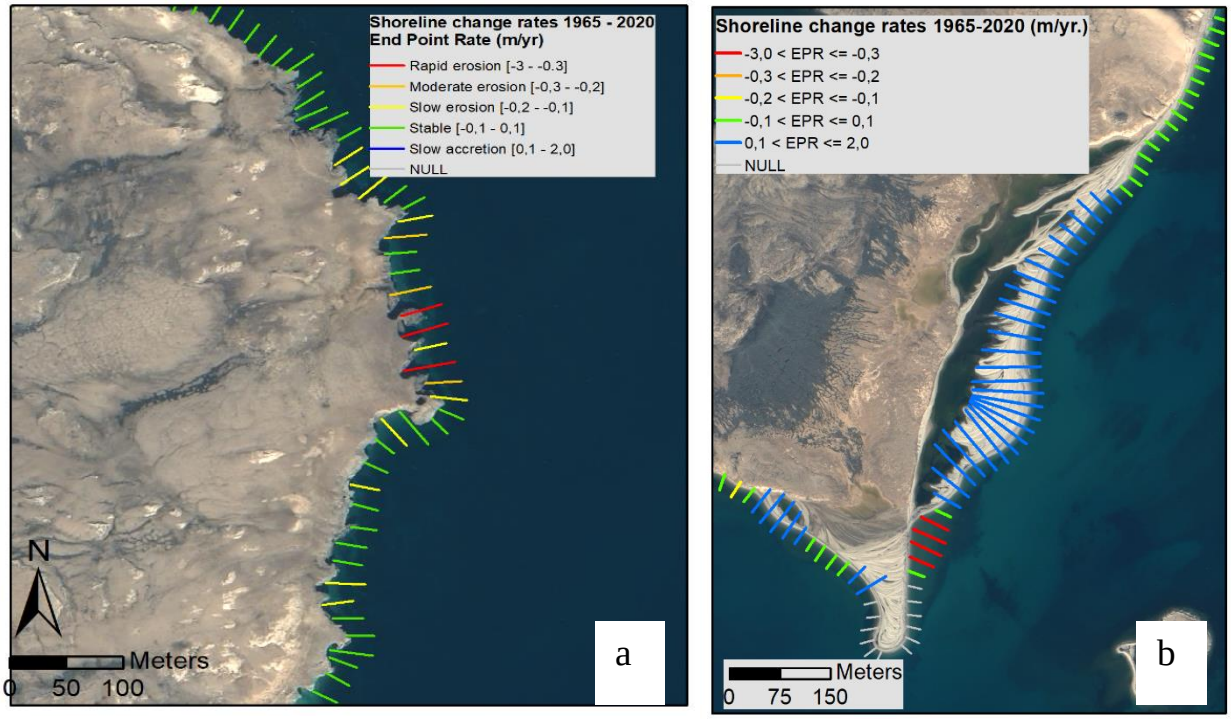

Figure 34. Changes rates measured along a rocky cliff (a) and a sandy spit (b). Images: PLEIADES © CNES, 2020, distribution Airbus DS

6.1.2 Changes occurring along the sector B

a. Depositional features.

The mean change rate of the unlithified coast -0.1 m/yr. Although this value is low, the lithified coast presents the fastest erosion rates. Erosion occurs mainly along bluffs/slopes and mixed sediment stretches. The results reveal that 70% of the coasts made of unconsolidated material are eroding (Table 4). Indeed, the highest retreat rate (3 m/yr.) was measured along the mixed sediment spit situated up-north of Argo bay (Figure 35). Although the mean retreat rate depositional features is 0.1 m/yr., 65 % of these forms remains stable and 25 % are experiencing erosion. Sandy spits and beaches are the most sensitive to change and to sediment reworking by marine processes. However changes measures along depositional features does not always reveal a loss of sediment. Depending on the coastal dynamics and storm event at a given time, changes measured can be the result of a shifting of the depositional features (Irrgang et. al, 2018)

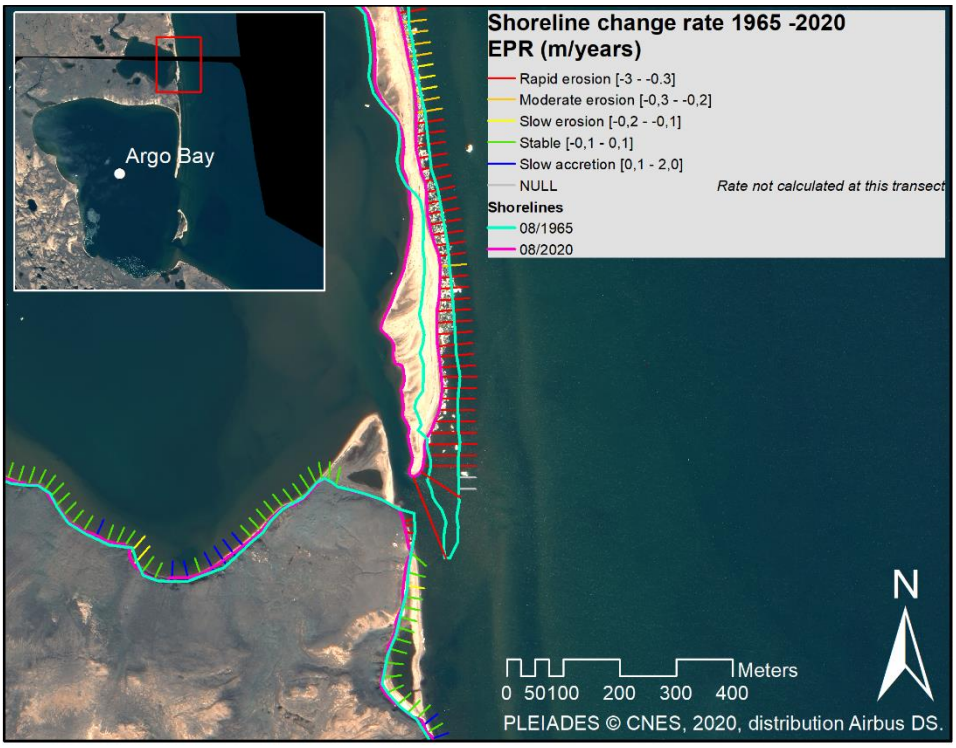

Figure 35. Changes occurring along a sandy spit north of Argo bay.

b. Tundra coasts

The site shown in the figure below is a typical case of coastline change along the Parry Peninsula coast. It is a tundra coast where erosion is active simultaneously on two opposite coast orientations (Figure 36). The sector shown in figure 36a is north exposed and shows a tundra bluff where coastal retreat reaches until 2.3 m/yr. The highest rates are situated at the northern tip of the spit. Note that the southeast facing coastline shows accreting rates up 0.8 m/yr., due to sheltered location and drift of the eroded sediments. Figure 35b, located further southwest in the same coastal area, and shows a tundra slope where rapid erosion rates occur in the south facing shoreline. This shows that the coast orientation does not seems to be a factor explaining the variability in the coastline changes in these factors.

The drift seems to be variable along the coast, the case Figure 36b seems to reveal the shoreline change variations that are not associated to exposure. A deeper analysis of the vicinity drift direction coupled with a geomorphological analysis could be done to explain the factors leading the variations occurring in this coastal area.

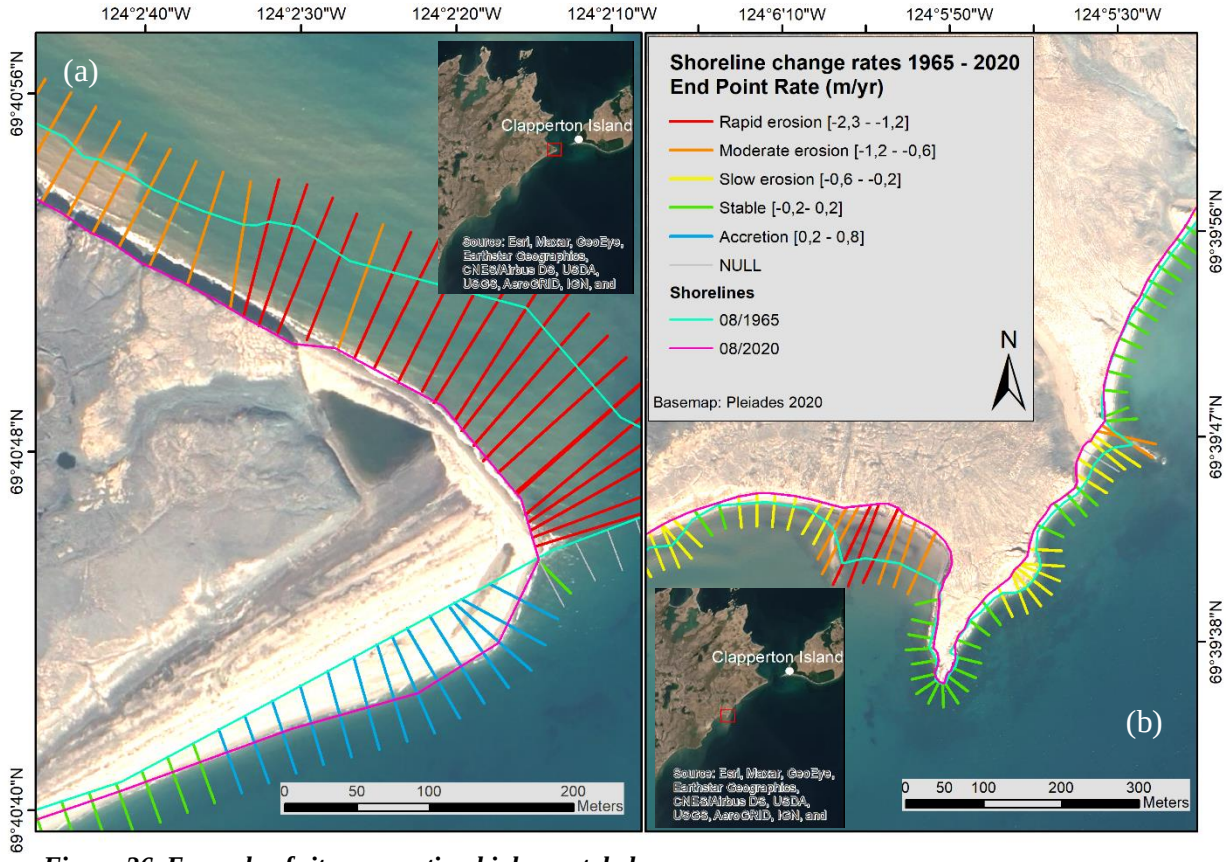

Figure 36. Example of sites presenting high coastal changes.
Images: PLEIADES © CNES, 2020, distribution Airbus DS

Long-term shoreline change rates

Figure 37 shows another example of the importance of backshore characteristics in coastal change. The eroding coast is an active tundra bluff having a north-east orientation. Note that coastline retreat is greatest along the polygonal soil bluff reaching 1 m/yr. By opposition, the shoreline of the ancient lake remains stable with some very slow aggrading portions gaining until 0.3 m/yr. The sandy spit up-north seems protecting that shore against wave action. This shore is protected by the sandy spit up-north. The inset as below shows that the southern part of the peninsula is mostly composed of tundra terrain dotted with thermokarst lakes which is a sign attesting of thermokarstic processes on unlithified soils.

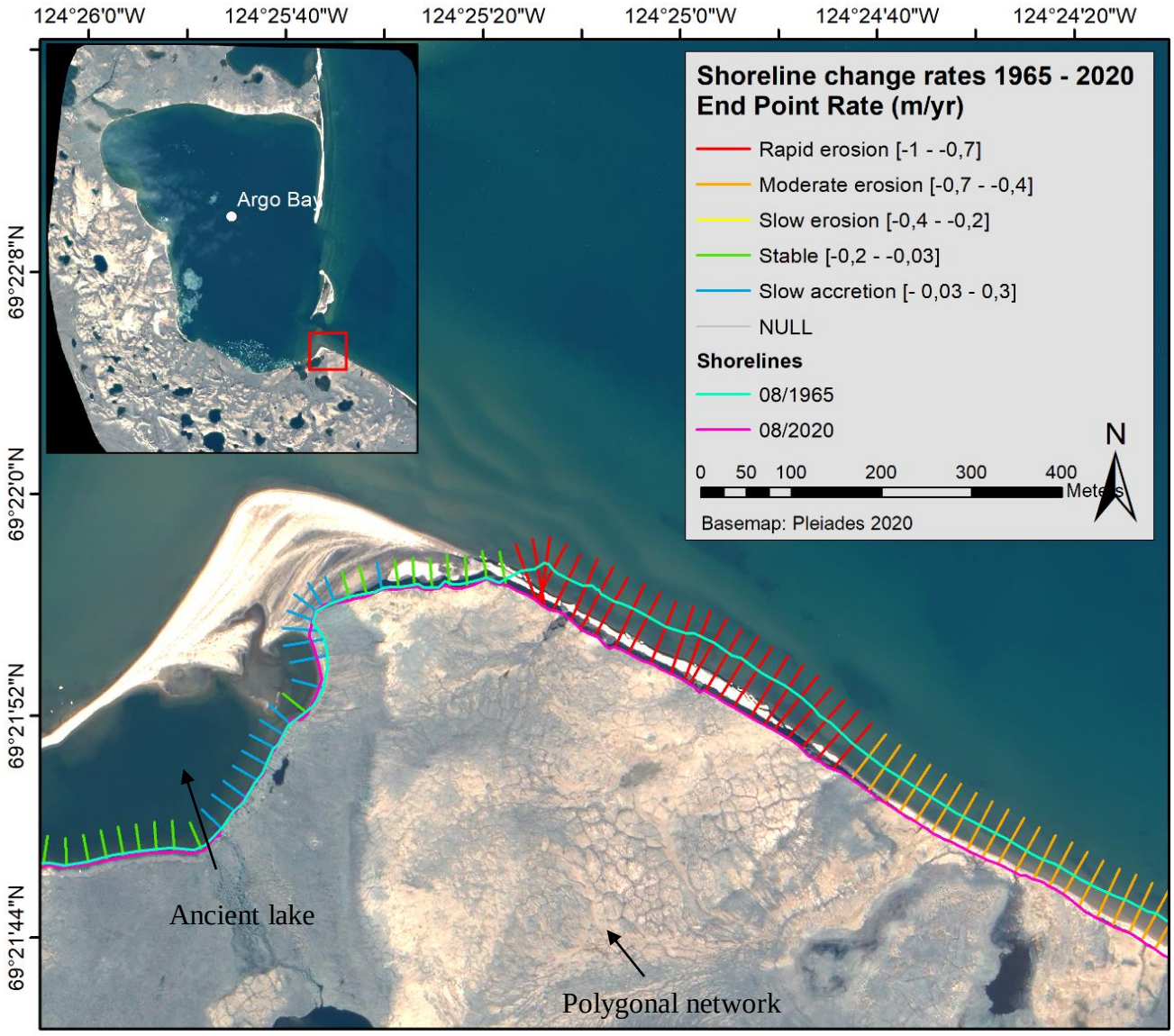

Figure 37. Tundra bluff presenting high erosion rates in the southern sector of Argo Bay. Note the polygonal network pattern situated on the backshore area. Images: PLEIADES © CNES, 2020, distribution Airbus DS

Coasts presenting a backshore with ice-wedge polygonal networks as shown in the figure above, represents only 30 km of the total coastline and are located within the southern part of the bay between Paulatuk and Clapperton Island. Figure 38 illustrates the rate of change of the coasts presenting a backshore with ice-wedges polygons. These forms are concentrated in the southern coast in low areas composed of unconsolidated sediments. 44 % of these shorelines are experiencing retreat between 2.5 and 0.1 m/yr. The mean annual retreat rate of these coasts is 0.2 m/yr. with a maximum retreat of 2.5 m/yr. These results signify that all coasts presenting ice-wedges backshore are absent of the consolidated coats zone. The regional scale analysis shows that polygonal, ice-rich soils are sensitive to erosion.

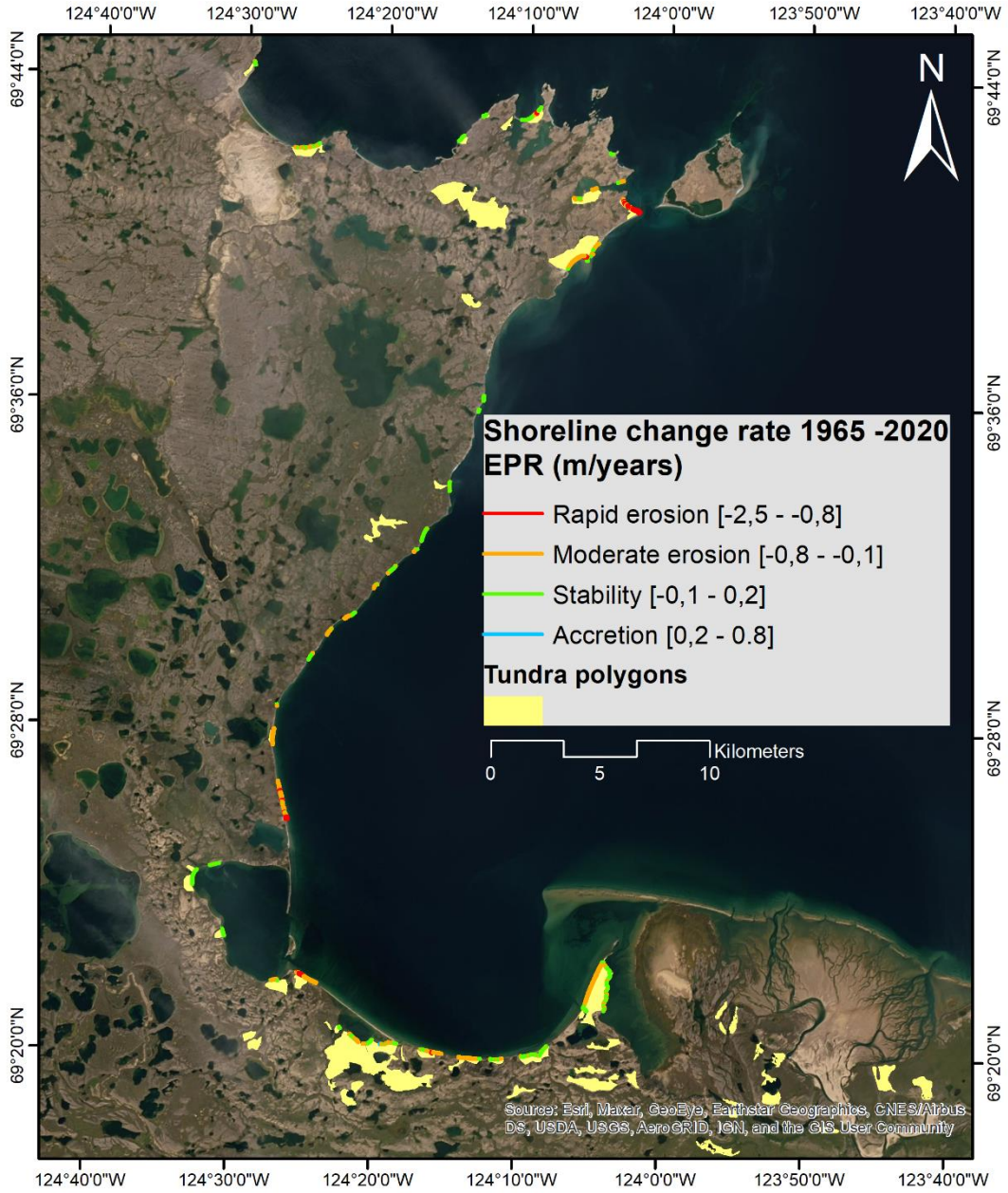

Figure 38. Shoreline change rate of the coastlines presenting ice-wedges polygon backshore.

6.2 High sediment transport from bluff to coastal water

Figure 39 shows the high turbidity of the coastal waters adjacent to the eroding coast. This plume of sediment indicates a transport of silt sediment 200 meters in the dynamic near shore zone. This may indicate the presence of current cells and direct material removing from the adjacent coast. Recent studies have shown that the origin of particulate organic carbon (POC) in Arctic coastal waters comes from the erosion of coastal permafrost and permafrost thaw (Jong et al. 2020). Which adds up relevance to the sediment transfer as depicted from this coastal sector

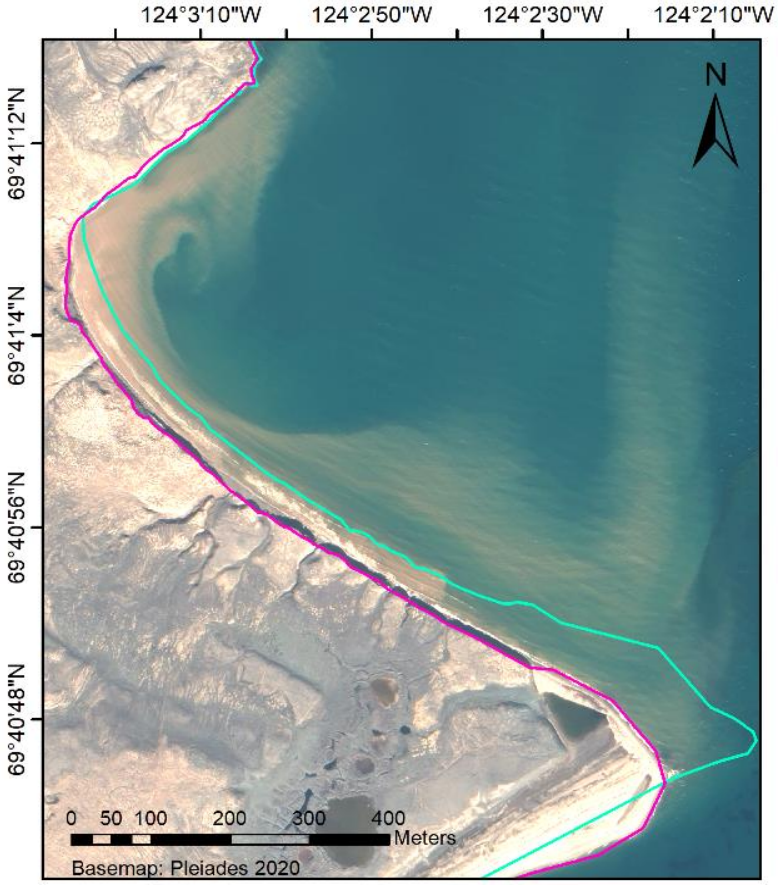

Figure 39. Sediment plume coming from the adjacent eroding and thawing bluff. It extend until 200 m offshore. PLEIADES © CNES, 2020, distribution Airbus DS

6.3 Discussion

6.3.1 Shoreline changer rates

The observed regional differences in coastal change rates can be explained by several environmental factors. As discussed above, the nature of the exposed substrate appears to govern the variability in measured rates of change. In addition, the general orientation of the coast, the duration of the sea ice season, the ground ice content and local climate affect the rates of coastal change. Along the Arctic coasts, average erosion dominates ranging from 0 to 1.1 m/yr. (Lantuit et al., 2012). The coasts of Canada and eastern Siberia have the highest erosion rates, while the rocky coasts of Greenland and the Canadian Arctic Archipelago have the lowest. The results of the coastal change analysis reveal a relatively stable coastline with an average erosion rate of -0.1 m/yr. along the west coast of the Parry Peninsula. This rate is very low when compared to previous long-term studies on unlithified coasts of the Beaufort Sea, where Irrgang et al. (2018) report an average rate of -0.7 m/yr. along the Yukon coastal plain or -2.2 m/yr. observed by Cunliffe et al. (2019) on Herschel Island. Indeed, changes occurring on these ice-rich unlithified coasts are governed by ice thawing resulting in rapid mass movements such as thaw slumps or block failure and where coastal progradation or retreat can exceeding 20 m/yr. at certain locations. (Lantuit & Pollard, 2008; Lim et al., 2020; Obu et al., 2017). Because of its morphology and its predominantly rocky composition with low ice content, the Darnley Bay coast does not show such a high rate and present a coastal dynamics specific to consolidated coasts. However, low erosion on high cliffs may generate large volumes of sediments further reworked. The analysis of DEMs based on cliff height and erosion rates is necessary in order to quantify volumetric changes over time.

6.3.2 Exposition to storm swells

Modelling of sediment transport along the Canadian Beaufort Sea coast have shown that westerly and northwesterly storm waves dominate longshore transports and that the Yukon coastline receive the most wave energy and longshore transit, followed by the Tuktoyaktuk peninsula. The protected orientation of the coastline studied together with its irregular configuration, seems to explain the small changes occurring due the effective dissipation and refraction of the dominant swell, in Darnley Bay through 55 years. However, easterly transport has increased in recent years (Hoque et al., 2009).

6.3.3 Open water season length

The length of the ice-free season is a major determinant of erosion. Indeed this ice acts as a buffer against storm waves. There are regional disparities in the formation of this sea ice between the Beaufort Sea and the Amundsen Gulf, which influences the length of the ice-free season and the vulnerability of the coastline to erosion.

The spatial and temporal variability of sea ice in the Canadian Arctic have shown an increase in the concentration of old sea ice around the mouth of the Amundsen Gulf during summer (Galley et al., 2005). The average, breakup begins in near shore areas along the Tuktoyaktuk Peninsula and Banks Island coasts and is followed by portions of Amundsen Gulf from west to east. The configuration of the Amundsen Gulf favors the presence of old ice during the summer, having an influence on the duration of the freeze-up period. This old ice may allow freeze-up to occur earlier each year and tends to reduce the open-water period and consequently the potential impact of the swell on the coasts (Galley et al., 2008). However this study has shown that the open water season in the Amundsen Gulf occurred on average 2 to 5 weeks earlier than the standard season, between 1980 and 2000. The episodes of premature sea ice melt were linked to El Nino events (Galley et al., 2005). In addition, studies by the Canadian Ice Service Digital Archive (CISDA) between 1968 and 2016, have revealed the significant decrease of summer sea ice surface over several regions of the Canadian Arctic. The Canadian Beaufort Sea region is experiencing decreases by up to 10% per decade while the Amundsen Gulf region is experiencing decreases up to 15% by decade (Derksen et al. 2019). This trend could play a major role in future Arctic coastline sensitivity to erosion processes.

6.3.4 Ground-ice content

Another factor which could may explain regional differences in coastal evolution is the ground ice content. Numerous studies on thermo-erosional processes demonstrated the influence of ground ice content on erosion rates along the Beaufort Sea Coast (Solomon, 2005, Galley et al., 2008; Obu et al., 2015; Lim et al., 2020). Ice-rich coast of the Beaufort Sea Coast presents coast the highest average erosion rate (1.1 m/yr.) but also the highest ground ice content of 28.5% (Overduin et al., 2014). Retrogressive thaw slumps and block failures are typical mass wasting processes, particularly present on ice-rich coasts such as the Yukon coastal plain, Richards and Herschel Islands. The coastline studied here does not show these typical marks of thermo-erosion suggesting that the ground-ice content is lower than the Beaufort Sea Coast.

Furthermore, the use of very long time-lapse such as the one used here, may not allow the identification of this short-lived features responsible by fast changes.

6.3.5 Terrestrial processes

Terrestrial hydrological processes may also contribute to erosion processes, mainly along unlithified coasts. Studies in Svalbard have demonstrated the removal of sediment from the cliff edge induced by snowdrift and precipitation (Sessford et al., 2015). The regional differences in mean precipitation between the southern Beaufort Sea Coast and Darnley Bay may also help to could explain the difference in retreat rates. For example, Tuktoyaktuk Peninsula receives the more precipitation (22 mm) in Cape Parry (17 mm)

6.4 Conclusion

This first quantitative study of coastal change on the west coast of Darnley Bay over 55 years indicates that:

1) The east coast of Parry Peninsula is shows a variability in the shoreline changes rates depending on the coast types. We identified two sectors significantly different in their erosion rates. The northern portion of consolidated material showing little erosional processes. The south sector is composed of unconsolidated material with higher rates of erosion due to its sensitivity to meteo-marine forcing.

2) The average shoreline change rate for the entire coast is -0.1 m/yr., which indicates that this coast shows a relative stability compared to coastal areas located further west. There is a significant difference in the average rate of change between the north coast (0 m/yr.) and the south coast (-0.2 m/yr.) suggesting that erosion is governed by the nature of the exposed substrate. Coasts composed of ice-rich unconsolidated sediments are significantly more sensitive to erosion than rocky coasts. Tundra bluffs and tundra slopes represent 3/4 of the eroded coastline. However, the average rate of change is counterbalanced by the abundant presence of mobile sedimentary forms, such as spits, barrier beaches, which present significant magnitude of change.

3) The elevation and composition of the backshore appears to govern the shape of the shoreline and its erosion rates, as demonstrated along the tundra cliffs with an ice wedge backshore.

4) Lithological composition and orientation of the coastline, as well as the short duration of the open water season are identified as factors explaining the relative stability of the studied coast.

7. Geomorphology and coastal changes of Paulatuk Peninsula

7.1 General geomorphological characteristics

With a southwest-northeast elongated shape the Paulatuk peninsula is a low-arctic tundra terrace with an average altitude of 3.2 m. It is composed by unconsolidated mixed fluvio-glacial material (Sankar et al., 2019), with frequent ice-wedge polygon networks and several thaw ponds in the surface (Figure 40). The coastline is characterised at the northwest by a low active tundra bluff of 3 m with a straight profile, with a narrow sandy beach, exposed to the northwest swells. A sandy spit anchored at its northern part is stretching north-eastward for about 680 m. The inside coast of the peninsula is characterised by a low tundra bluff also showing a narrow sandy beach with 4 concave small embayments favouring sediment accumulation.

On the southwest sector of the peninsula, a flooded lake basin is partially enclosed by a ridged beach. The northeast sector of the peninsula is an inundated tundra flat under tidal influence, partially enclosed by two narrow barrier beaches.

The sand accumulation patterns present along the coast such as the northern spit are attesting the longshore drift mobilising sediment from the southwest to the northeast. The eastern coast is subject to a longshore drift from the south to north as revealed by the accumulation forms fronting the concave sections. The peninsula is protected by a barrier island system 3.6 km to the north which plays an important role in the coastal dynamics. Also, the influence of the delta situated eastward may be significant (Figure 28).

The houses of the Paulatuk hamlet are situated along the south-eastern coast of the peninsula, protected from dominant swells and situated on a higher surface between 3 and 5 m of altitude (Figure 44a). It was indicated that katabatic wind action was not the cause of landscape change in Paulatuk (Mackay & Burn, 2011). However, it was noted that the high surfaces are denuded of vegetation. It is possible that this is due to desiccation of the wind at convex areas during katabatic wind events. Terrain convexity associated to ice segregation also promote bare patches such as in the areas where we observe a more intense division of the ice wedges (Figure 43b). The human activity on this territory contributes to its modification. In the case of the airport runway, water retention on its boundaries is evident, as well as associated to some houses where peat land soils are present (Figure 41). Infrastructures are built over ice-wedge and are potentially threatened by thaw through permafrost degradation as seen above with significant expansion of thaw ponds along infrastructures built over ice-wedges as seen along the airstrip (Figure 54).

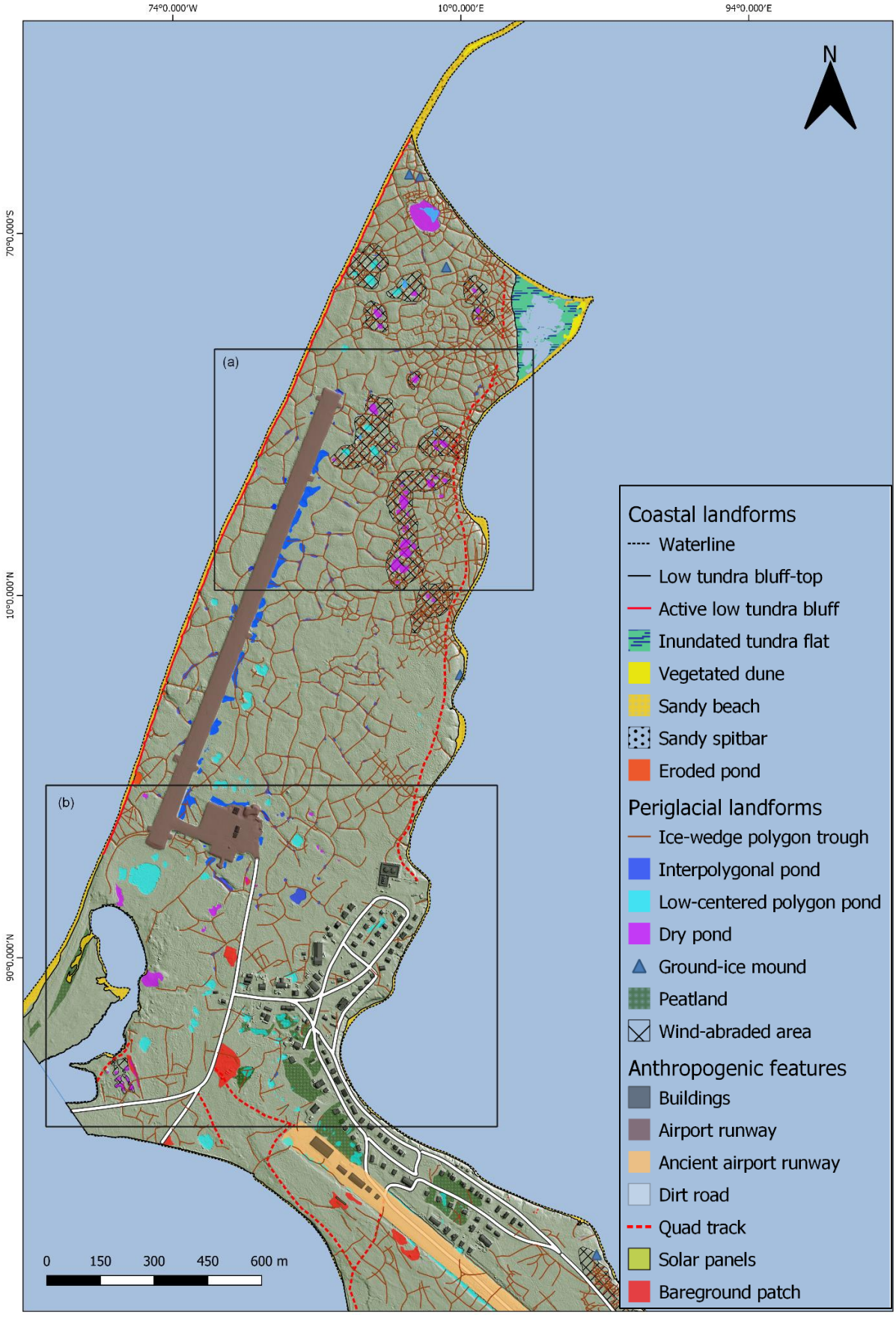

Figure 40. High resolution geomorphological map of Paulatuk peninsula. The base layer is the DEM from the 2019 drone survey.

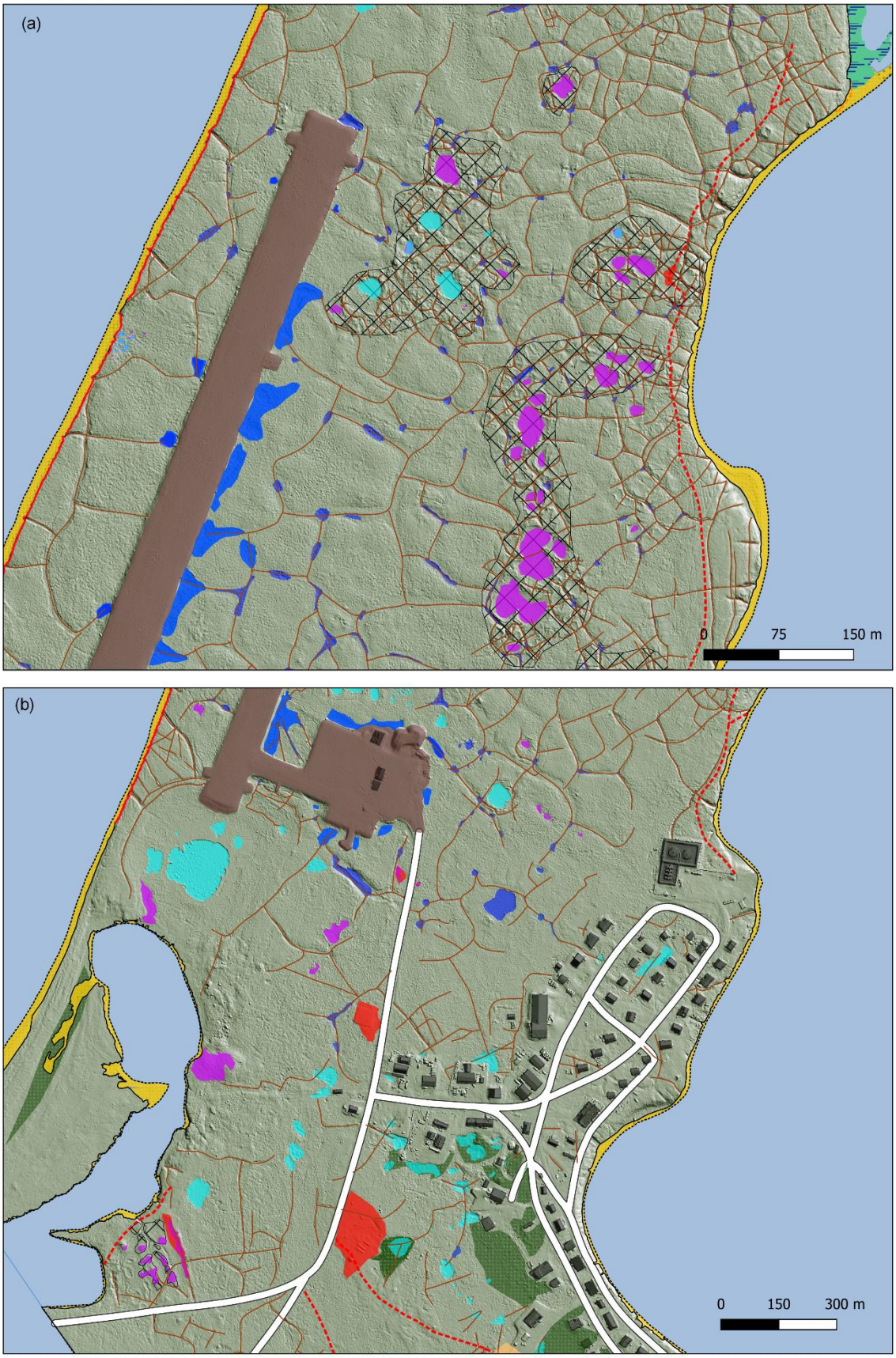

Figure 41. Insets (a) and (b) from Paulatuk geomorphological map.

7.2 Ice-wedge polygon networks

The Paulatuk Peninsula is a tundra landscape dominated by ice wedge polygonal networks. Ice-wedge troughs sum up to 6.2 km in length. The interpretation of the drone orthomosaic and DSM reveals differences among the distribution of ice-wedges. The density map shows that ice-wedge polygons are more concentrated in the north east of Paulatuk Peninsula (Figure 43b) Ice-wedge distribution can be explained by soil materials, by ground-ice concentration, as well as by age and genetical differences between material types (Bray & Shur, 2004). Subdivision of ice-wedges into secondary or tertiary wedges is related to material and age, as well as to winter climate variations (Burn & O'neill, 2015). The spatial variation of ice wedges, denser in the northeast, may suggest that the peninsula is composed of several lithological units. When viewed from above in an orthogonal perspective, polygons with depressed center present shallower ponds than those produced by ice-wedges degradation (Figure 42a). Deeper ponds are identifiable by their deep green color at their center (Figure 42).

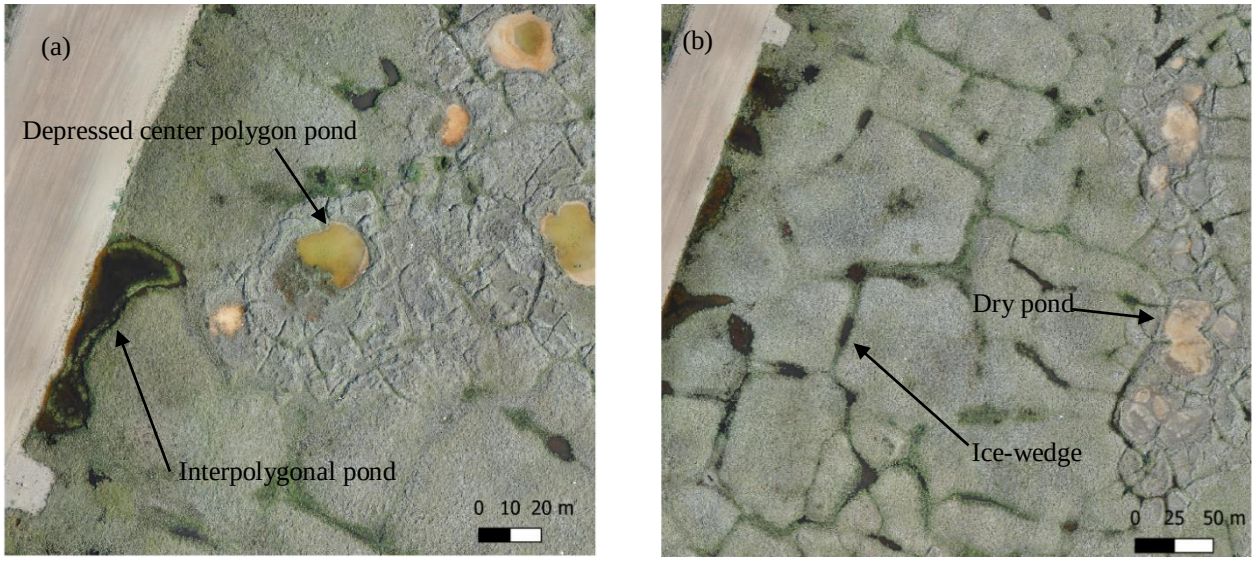

Figure 42. Aerial UAV orthoimages illustrating depth difference and vegetation filling between different thaw ponds (a) and ice-wedges trough and dry ponds (b)

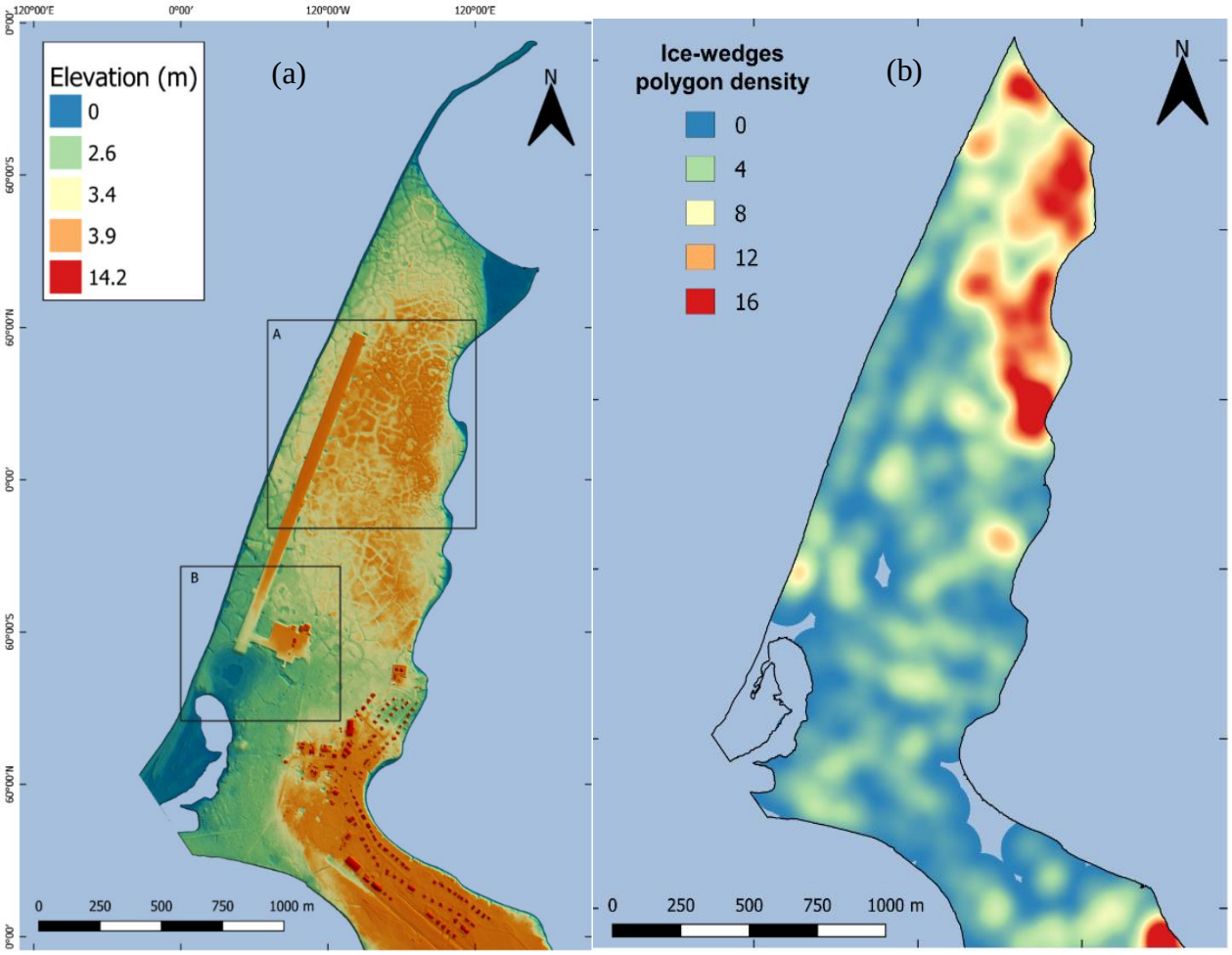

Figure 43. DSM of Paulatuk peninsula (a) and density map of ice-wedge polygons in Paulatuk. The legend represent the presence of ice-wedges in a radius of 100 m.

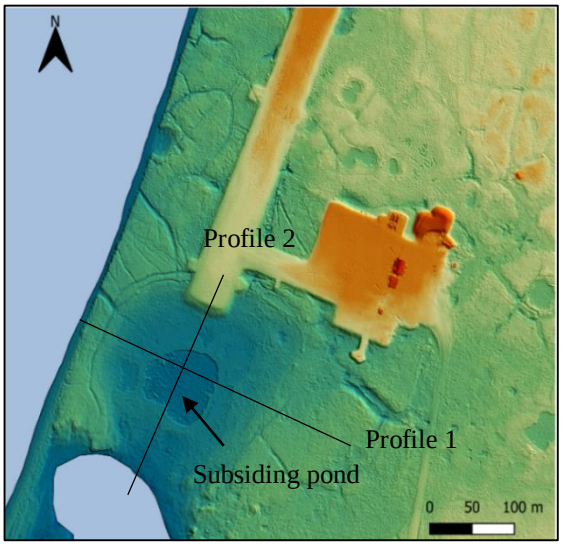

Figure 44. Topographic profiles position on subsidence zone.

7.3 Degrading permafrost

7.3.1 Subsidence

The analysis the Paulatuk Peninsula terrain with the DSM acquired in 2019 allows to identify signs of degrading permafrost. Recent research has shown that relief variations and in particular subsidence in ice-rich permafrost areas are important factors in the vulnerability of coastal permafrost to erosion (Lim et al., 2020). Terrain degradation is also affecting infrastructures established in permafrost areas. Since Paulatuk presents a surface dominated by ice-wedge networks, we can infer that the ground contains excess ice at least in the ice-wedges and that it might be sensitive to warming, resulting in subsidence. The Paulatuk DSM reveals two areas situated above 3.9 m. On one particular area (Figure 44), we notice a gradational decrease of the altitude towards the southwest. From the observation of the southern part of the airstrip, we can infer the hypothesis that the southwest area is subsiding (Figure 44). This subsidence zone is located towards the drained lake facing a flooded lake basin. It seems that the area is still losing mass and affects the neighbouring areas, such as the airport. As shown on the topographic profile 1 (Figure 45) the elevation of the center of the drained subsiding lake is equal to sea level. The profile 2 shows the presence of a berm of 0.8 m height separating the drained lake from the flooded basin. If subsidence becomes significant in this sector, the breaching of this berm will induce the flooding of the adjoining depression, threatening the southern part of the airstrip and could potentially induce erosion problems.

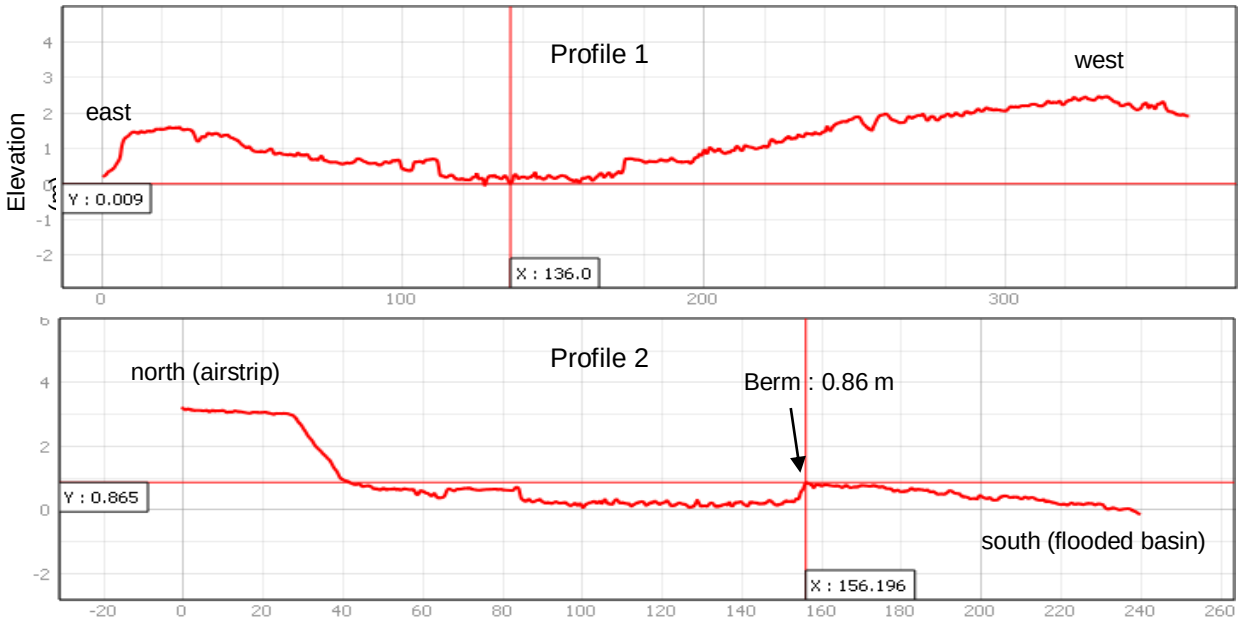

Figure 45. Topographic profiles from Paulatuk DSM (Figure 18), showing subsidence occurring south of the airstrip.

7.3.2 Thaw ponds surface evolution

As permafrost soils are sensitive thermal changes, their degradation is a result of their ice thawing. This degradation is expressed by surface instabilities and thaw related forms. In this section we used a historical aerial image of 1975 and the UAV orthoimage of 2019 to quantify the thaw pond surface evolution over 44 years in Paulatuk. Thaw ponds are present in the Paulatuk Peninsula and are due to the thawing of ground ice in the upper part of the permafrost leading to a subsidence of the land, generating depressions that become water filled (Andresen & Lougheed., 2015). Thaw ponds are also forming over thawing ice-wedges but also at the center of low-centered ice-wedge polygons (Figure 42). The presence of dry ponds suggests that some of these have disappeared due to the effect of various factors, including evaporation, vegetation or sediment infilling and/or drainage (Figure 46). Melt water can be evacuated from the ponds through active layer thickening processes due to permafrost degradation (Andresen & Lougheed, 2015) or by during the warm season by simple thaw progression. Inter-polygonal ponds are widening along constructions such as the airport strip situated in the western part of the peninsula. Thaw ponds also seems to be degrading in depressions and water accumulates along buildings and peat lands (Figure 47).

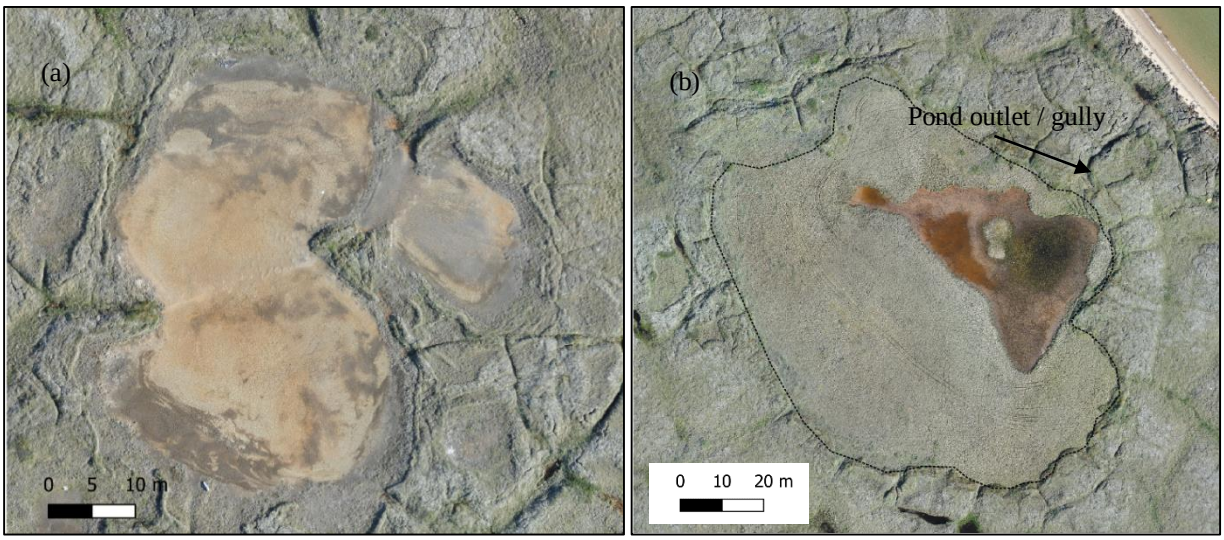

Figure 46. Dry ponds showing silty clayed bottoms (a) and partially drained in the process of vegetation colonization. (b). From 2019 UAV orthoimages.

Comparison of the total ponding area between a 1975 air photo and the 2019 UAV image shows an increase of 66%, or 33,814 m² in 44 years (Figure 47 and Figure 48). This number must be considered with care, since it may also reflect hydrological differences among the two years and not a trend. Furthermore, the difference in colour and resolution between the 1975 historical air photo and the 2019 drone image may have an influence in the definition of dry areas of very small water bodies. Disparities are observed among pond types. The greatest increase occurred in the inter-polygonal ponds. Ponds induced by the presence of construction show a net increase of 186 %, while we observe a decrease in the surface area of low-centre polygon ponds. We hypothesise that the degradation of the permafrost is visible by the increase of the surface of the thaw features, but also by their drainage due to the degradation of the active layer or by gullying (Figure 46b). However, for this to be properly tested, we would need a larger number of images and a shorter time-interval. The interpretation of the thaw pond distribution maps (Figure 47) allows to identify infrastructures as a major driver for the enlargement of thaw ponds.

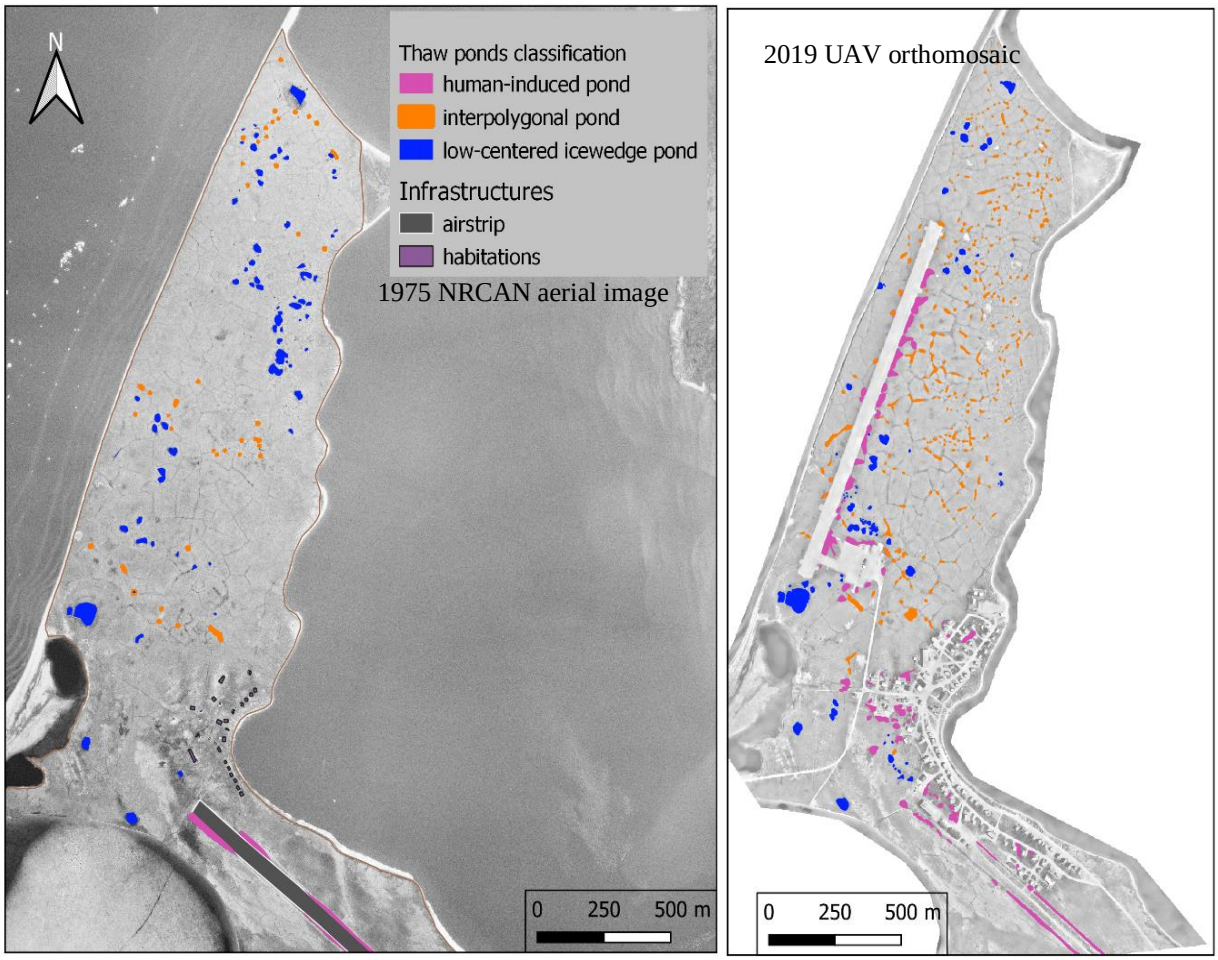

Figure 47. Thaw pond surface evolution between 1975 and 2019

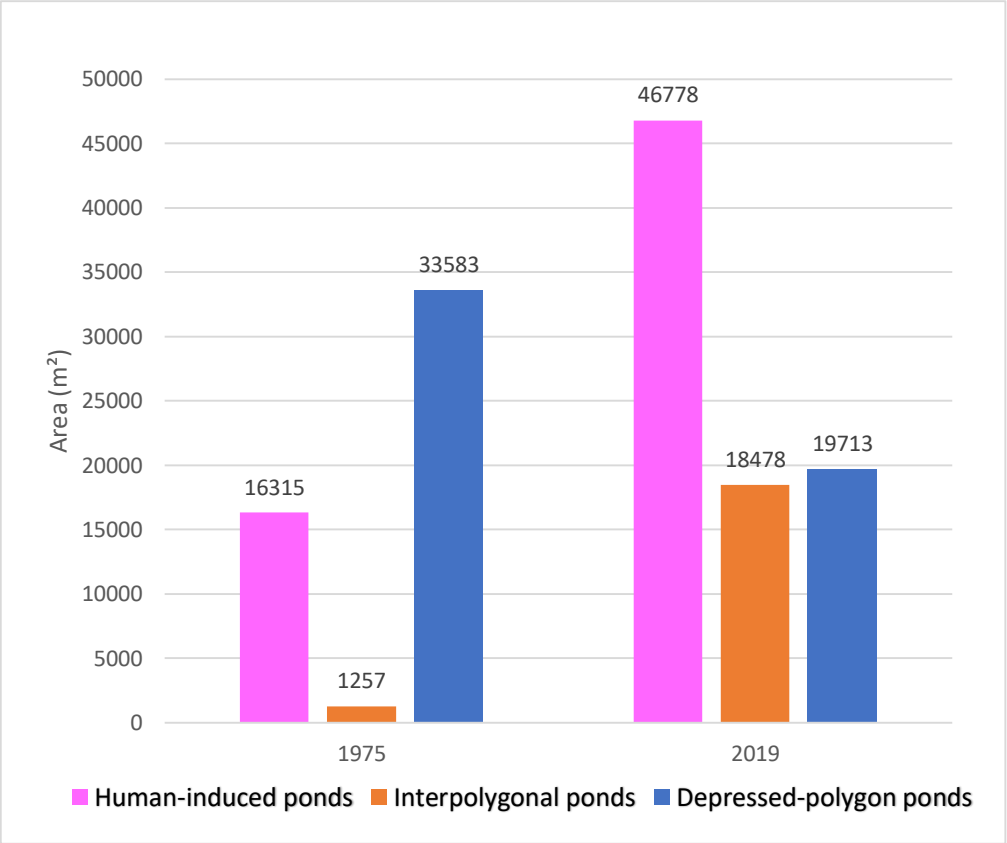

Figure 49. Thaw pond surface evolution between 1977 and 2019

Figure 48. Interpolygon thaw ponds near the Paulatuk hamlet in the summer of 2019. Photo: Gonçalo Vieira

7.4 Coastal change in Paulatuk

The delineation of the shorelines for the years of 1965 and 2020 allowed quantifying coastal change along the Paulatuk Peninsula over a 55-year period. The mean shoreline change rate was -0.14 m/y (Figure 50). Erosion occurred on 52 % of the coast, while 40 % was stable and 8% accreted. The results reveal a significant difference in change rates between the western and the eastern shorelines. The annual mean retreat rate of the western coast is 0.2 m/yr., with a maximum value of 0.7 m/yr. Erosion dominates most of the west coast exposed to northwest storm swells during the ice-free period. The east coast is relatively stable due to its protecting orientation by the peninsula and also by the barrier island systems and presents a maximum retreat value of 0.2 m/yr. Coastal erosion in the western coast is marked by the collapsing of the loose parts of the cliff-edge due to wave action avec thawing effect of the surficial layer (Figure 52).

A portion of the concave shoreline of the southern flooded basin is also showing rapid erosion rates up to 0.5 m/yr. (Figure 51). The erosion in this sector is directed landward and may affect the gravel road situated between the two water bodies.

Accretion occurs in areas where the bluff top could not be identified and may be a bias because vegetation line is used as a reference. The maximum accretion rate is up 0.5 m/yr. and occur in the sector north of the flooded basin. This accumulation form is not the result a sediment deposition due to coastal dynamics since it occurs in a shallow closed water system where dynamics are very low. These sediments could come from the fronted beach an accumulate submersion events. However, it seems that a discharge zone was previously located backward of this area and could indicate that this accumulation form is most likely a backfill than a natural deposition form.

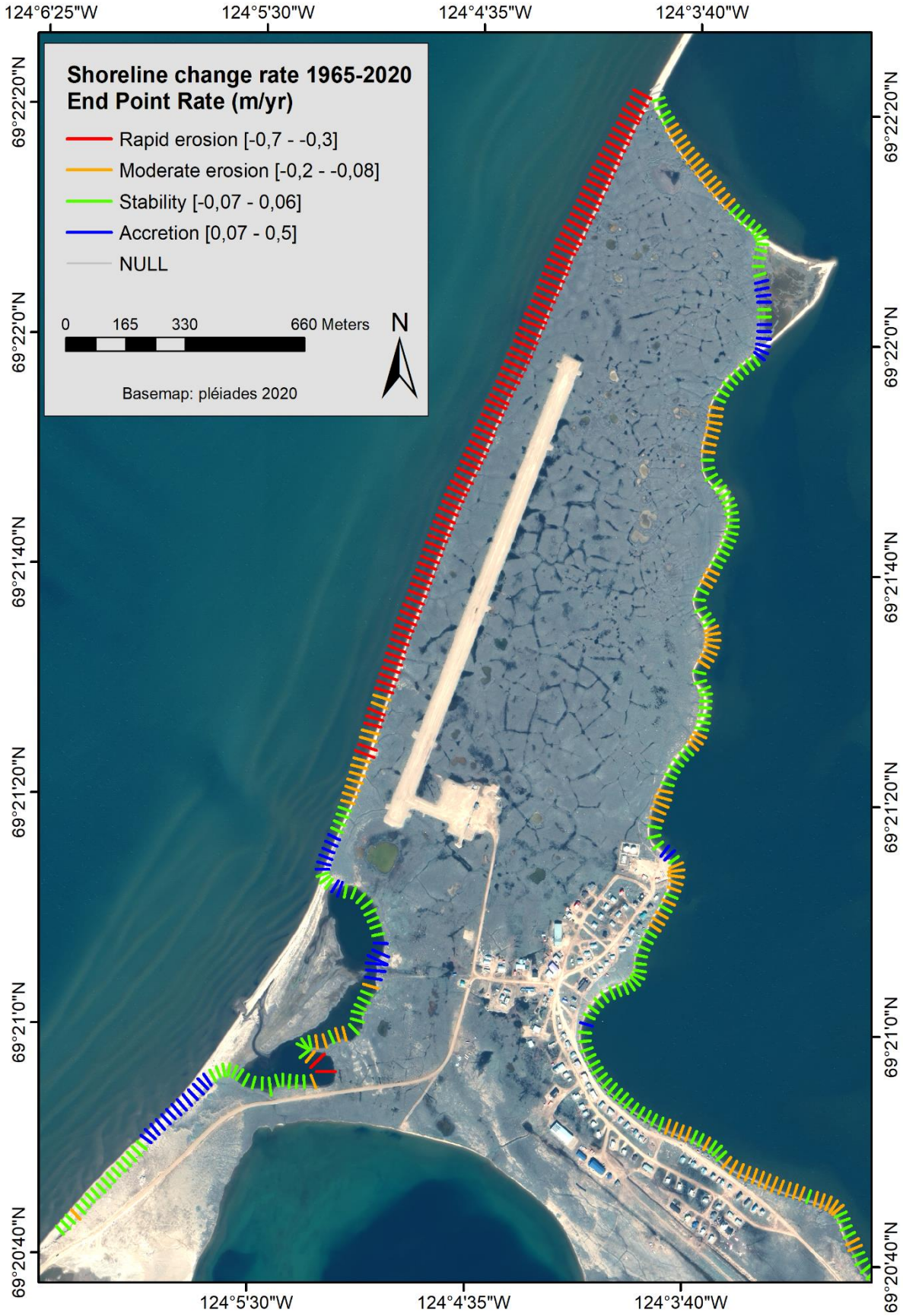

Figure 50. Shoreline change rates in Paulatuk Peninsula. PLEIADES © CNES, 2020, distribution Airbus DS

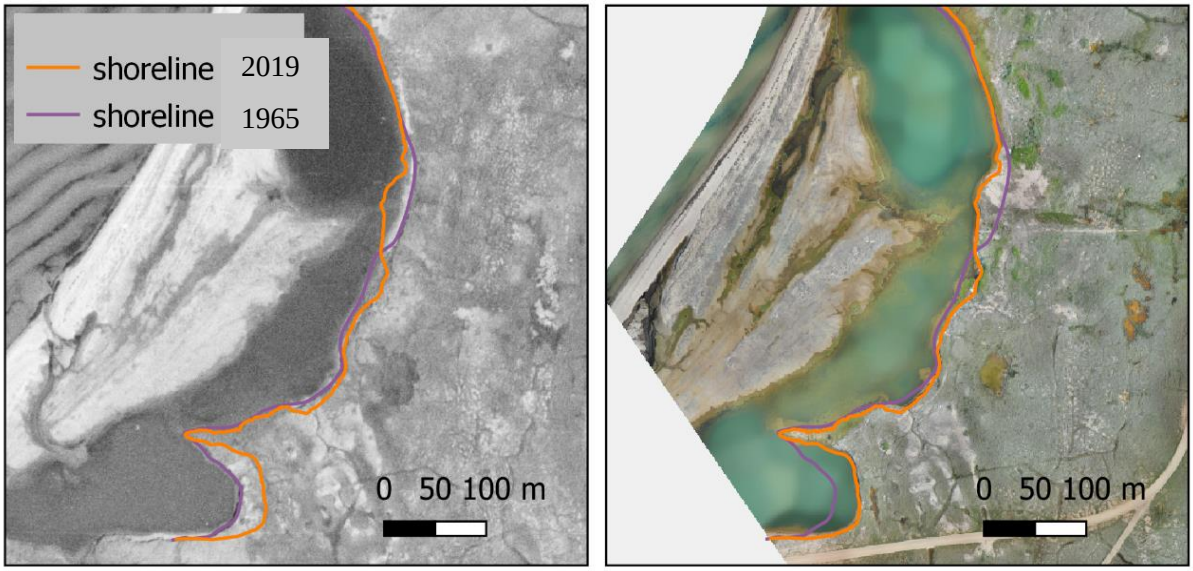

Figure 51. Flooded basin where accretion and erosion dynamics are occurring.

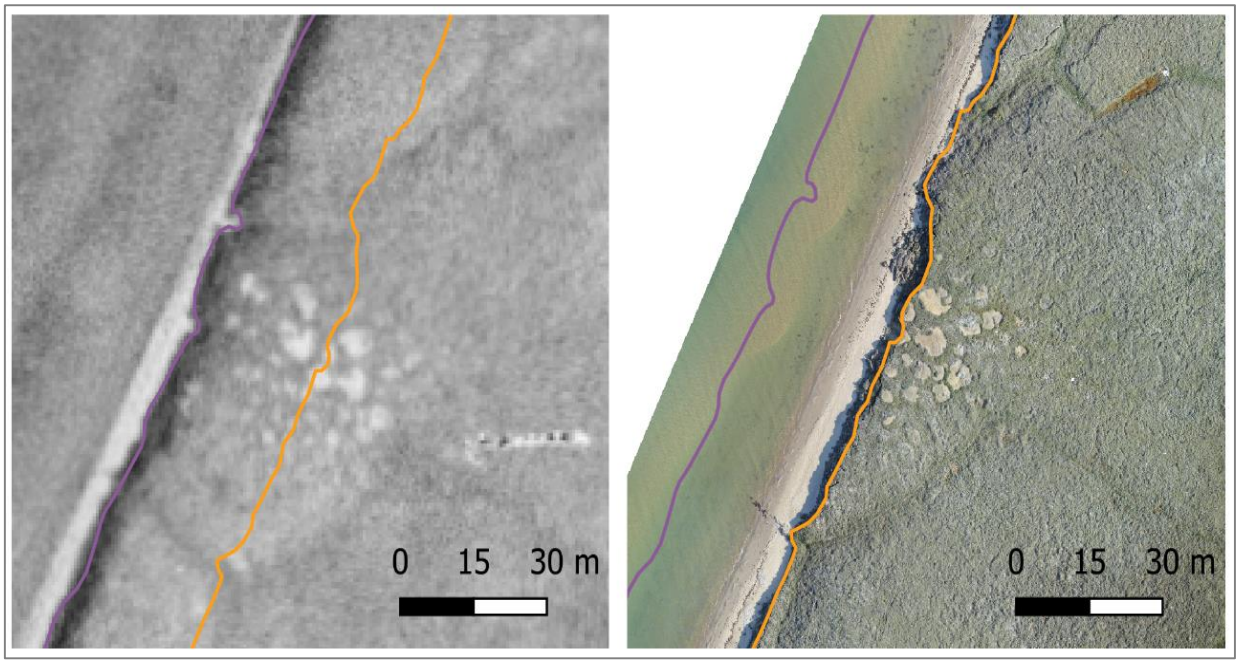

Figure 52. Thermal abrasion process on tundra bluff with differential erosion on old thaw ponds in Paulatuk. Left image: 1965 NRCAN air photo. Right image: UAV 2019 orthoimage.

7.5 Discussion

7.5.1 Shoreline change rates

Analysis of coastal changes in Paulatuk reveals that erosion dominates over 52% of the coastline, notably on the west coast, while the east coast is more stable. These trends are consistent with the results of Sankar et al. (2019) that analysed changes over the 1984-2016 period and estimated that 69% of the coastline was subject to an average erosion of -0.43 m/yr. Our analysis reveals that the average erosion value was -0.14 m/yr. over a much longer period. However, the differences in values between these two studies may be related to a possible increase in the erosion rate over the short term as shown by Sankar et al. (2019), but also by the different coastline references sectors and resolution of the processed images. Sankar et al. (2019) used the land-sea interface with a reflectance analysis method on satellite images with a resolution of 15 to 30 meters. Since our goal was to link erosion to permafrost degradation and the presence of ice-wedges along the coast, we used the vegetation boundary to delineate the coastline manually on high resolution images. Spatio-temporal analysis by Sankar et al. (2019) indicates an increase and acceleration of erosion rates in (2006 - 2016) due to the shorter sea-ice period and the increase of storm events.

Various studies on Herschel Island and along the Yukon coast showed that ice-rich permafrost coasts are subject to high rates of erosion governed by slumping mass-wasting processes activity (Couture & Pollard, 2000; Couture et al., 2017; Obu et al., 2017; Irrgang et al., 2018). High retreat rates up to 22 m were measured along high bluffs (>10 m) but also along low bluffs of 5 m. The retreat rates also depends on sediment removal capacity of the nearshore currents (Obu et al., 2017, Irrgang et al., 2018). The low elevation of the Paulatuk shoreline does not allow such extreme erosion events to occur. In Paulatuk, the erosion process is much slower and is a result of the limited wave action on the western coast coupled with thermal abrasion. Indeed, wave action is relatively moderate due to the small fetch, the barrier islands protection role and long sea-ice season.

7.5.2 Permafrost degradation in Paulatuk

The degradation of permafrost has social, economic and ecological impacts. Ground instability poses major geotechnical challenges for permafrost pipeline systems. Civil engineering will also have to adapt to ground deformation resulting in deformation of roads and railways and cracks in buildings. Soil instability is also an issue for foundations and infrastructure. In May 2020, 20,000 tons of diesel oil were spilled into the soil and rivers in the city of Norilsk in northern Russia. This pollution was found to be caused by thawing permafrost, which led to the collapse of the city's power plant fuel tank basement (Rajendran et al., 2021). In the same way as the southern part of the Paulatuk airstrip, a study made in the discontinuous permafrost zone, attests to the subsidence and cracks affecting the airstrip of several airports in northern Quebec (Fortier & Savard, 2010). Although techniques to stabilize structures on unstable ground exist, their economic cost is consequent.

Several geomorphological features result from the degradation of the permafrost, such as thaw ponds. Note that our results on thaw pond degradation were made by the analysis of only two scenes. Since the variability in the dynamics of thaw pond surfaces may be important from one year to another and along the thaw season, it is important to carry more analysis in the short-term temporal scale. However, surface water drainage processes are driven by the degradation of the active layer and by gullying. In Paulatuk, gullies are present along the coast and are formed by the degradation of ice-wedges and are a factor explaining driving the pond drainage. Higher erosion at coastal ice-wedges is not significant at a local scale.

The snow depth is also an important factor explaining permafrost degradation driven by the active layer thickening. Snow acts as an insulator and influences the soil thermal regime and permafrost degradation. Studies have shown permafrost degradation through active layer thickening was linked to snow cover depth and duration. In northeast Siberia, snow depth is responsive of 50 % of the soil temperature regime (Kumar et al., 2016). It thus, will be important to know the thickness, duration and spatial distribution of the snow cover over Paulatuk to understand the degradation of permafrost. It is possible that the airstrip embankment has a thermal effect on the ground, leading to its subsidence in the south, and that snow accumulation is increased in the airstrip embankment contact, leading to increased thaw an enlargement of the ponds and the formation of peaty zones.

7.5.3 Vulnerability of Arctic coastal communities and infrastructures

The impact of thawing permafrost on Inuit communities and infrastructure has been studied in several regions. Some Arctic regions have experienced an increase in air temperature of more than 4 °C since 1975, such as Utqiaġvik, Alaska (Borough et al., 2017). This increase in air and ocean temperatures has led to a melting of the ice caps and of the ground, and has an impact on the lives of Inuit communities who are dependent on their territory and seasonal patterns for food access through hunting and fishing. Climatic migration is already happening, with an example being the village of Shishmaref, in Alaska, threatened by erosion and marine submersion, relocated in 2016. Tuktoyaktuk is also subject to frequent flooding events (Radosavljevic et al., 2016) with relocation works going on and a new settlement location in place (Figure 53).

Figure 53. Coastal risks in the Arctic. Waves breaking on Tuktokaktuk hamlet during 2019 storm. Photo: Weronika Murray (a); Coastal erosion threatening the village of Shishmaref, in Alaska, after a storm event. Photo: Gabriel Bouys (b)

Yet, due to its geographical situation, the settlement of Paulatuk is not very exposed to severe storm events. Coastal risk at Paulatuk is thus smaller than in the previously mentioned areas. A reason is that the hamlet is located along the eastern coast of the peninsula, which is stable, and facing relatively calm waters. The elevated situation of the hamlet, above 4 m prevents the hamlet from flooding events.

However, thermokarst activity can be a threat for human welfare and infrastructures as climate warms in the Arctic. As shown in Figure 52, in Paulatuk, the airport runway was built over ice-wedges. It can be seen that thaw water from inter-polygonal ponds tends to flow along the ice-wedges following the frozen ground boundary and accumulate in depressions in the runway limit. The northern part of the village is over ice-wedges, as well as peaty soils. As climate warms, these ice-wedges may thaw and threaten the stability of the overlaid constructions (Figure 52).

As seen in Figure 54, in summer, water accumulates in ice-wedge troughs. These shallow stagnant ponds have been found to increase thawing activity during the summer and freeze-up during the winter. The active layer is thicker under ponds and promotes thawing processes (French, 2018).

The accelerated degradation of permafrost may also promote health problems for Inuit communities. Recent models indicate that under a high greenhouse gas emission scenario (RPC8.5), thawing permafrost will result in the transfer of natural terrestrial mercury (Hg) to aquatic environments. On a global scale, melting permafrost could lead to increased mercury concentrations in fish, which is a major nutrition source for coastal communities (Schaefer et al., 2020).

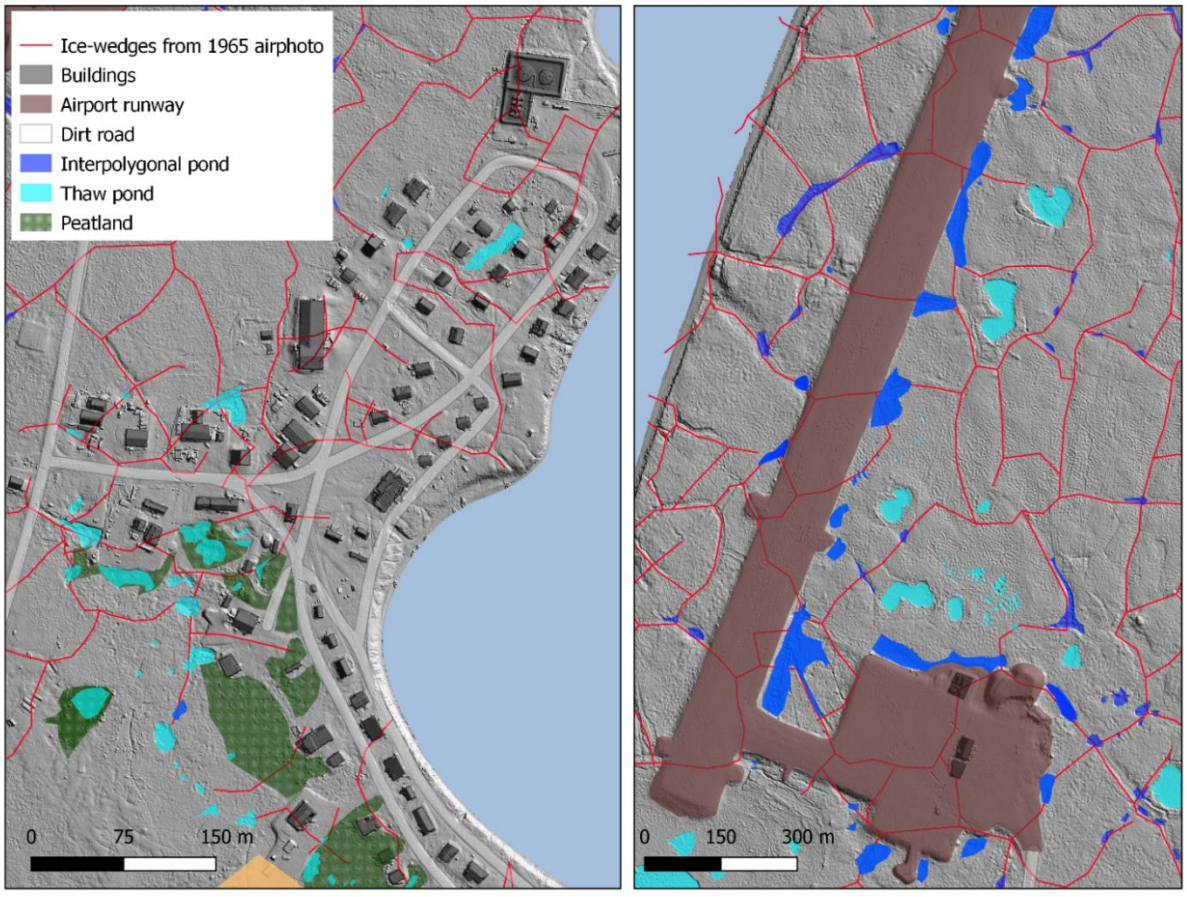

Figure 54. Ice wedges underlying the infrastructure in Paulatuk. A – Hamlet sector, B – Airfield.

7.6 Conclusion

In this study, a geomorphological description of the Paulatuk Peninsula associated with a quantification of coastal changes over 55 years (1965 and 2020) was made. The main conclusions are:

The detailed geomorphological map produced with the 2019 UAV orthoimage and DSM allowed the better understanding of the terrestrial and coastal processes affecting the peninsula and associated landforms. Ice-wedges are a predominant feature associated with thawing processes inducing pond development. The presence of infrastructures is leading to an alteration of the ponding surface. The interpretation of the DSM allows raising the hypothesis of a subsidence phenomenon occurring in the southwest area of the airstrip, which could potentially be a threat for the neighboring infrastructures such as the airport runway. In addition, the mapping of historical ice-wedges with the aerial photography of 1965 provides relevant spatial information to the local community about the presence of ice-wedges beneath infrastructures such as the fuel reservoirs and airstrip.

The analysis of the thaw ponds surface evolution between 1975 and 2019 coupled with the subsidence effect suggests an ongoing degradation of this permafrost terrain through active layer thickening. However, temporal variability analyses of ponding surface and in-situ data are needed to evaluate this hypothesis.

The analysis of coastal rate of change over 55 years indicates that the peninsula has relatively low mean rate of shoreline retreat (0.14 m/yr.). The results show the significance of wave exposure in the retreat of the coastline. The highest erosion rates (0.7 m/yr.) are present along the western coast and in a sector of the southwest flooded lake basin, whereas the eastern coast remains relatively stable.

The factors determining the changes in the peninsula are the association of wave action with the thermo-abrasion process leading to slumping along the tundra bluff. The regional situation within Darnley Bay, as well as the local protection of the barrier island system of the Hornaday delta, are found to be factors explaining the stability of Paulatuk Peninsula.

Inuit communities are on the front line of the consequences of Arctic warming, which are inducing modifications of the ways of life of the Inuit and their ancestral traditions. The coastal erosion and the degradation of the soils of the Arctic zone is also a challenge in terms of engineering. Arctic communities will have to adapt to ensure food access, a healthy living and a sustainable economy.

8. Conclusions

The Polar regions play a major role in regulating the global climate. However, the rapid warming of these regions and in particular the Arctic due to human activities is causing fast environmental changes and inducing accelerated melting of land and sea ice. In this study, we highlighted the coastal erosion dynamics along the different types of permafrost coasts of Darnley Bay. We used remote sensing techniques in order to characterize the coastal geomorphology and quantify shoreline changes over 55 years at regional and locale scales.

The study of the coastal dynamics in Darnley Bay provides a quantification of the shoreline change rate at a regional scale, indicating the relative stability of the eastern coast of Parry Peninsula (-0.1 m/yr.). The coastal dynamics analysis over a 55 year period confirms the significant difference of changes rates between the different lithological units constituting the study area. The results reveals that 74 % of the southern sector is eroding since 1965 and present a mean annual retreat rate of 0.1 m/yr. Highest rates are located along tundra coasts having ice-wedge networks in the backshore, with -2.5 m/yr. The mean retreat rate of coasts having a polygonal backshore (0.2 m/yr.) allow to infer that polygonal soils are significantly more sensitive to erosion than other material exposed along the coast. By opposition, only 28 % of the northern and consolidated coast is eroding. Mobile sediment features present a large amplitude in their change rates change (-3 m/yr. – 2 m/yr.) along the whole coast.

The local scale analysis carried in the Inuvialuit settlement of Paulatuk confirms that the peninsula eroded at a mean rate of 0.14 m/yr. between 1965 and 2020. However significant disparities in the change rates are observed between the western coast and the eastern coast. Highest erosion rates (0.7 m/yr.) are occurring along the western coast and along a sector the flooding basin in the southwest. The stability of the eastern coast can explained by its sheltered orientation from the dominant northwest swells. The erosional processes active along the peninsula are identified to be the association of wave action and thermal abrasion processes inducing a slumping of the low tundra bluffs. The permafrost degradation of this territory has been assessed through the analysis of the evolution of thaw ponds surface over 44 years (1975 – 2019), as well as of potential subsidence phenomena occurring in the southwest sector of the peninsula. The detailed geomorphological mapping allowed to identify the infrastructure as a major factor driving the thaw pond enlargement. In addition, the ice-wedge mapping provides relevant information for the local community about their spatial distribution and potential threat for infrastructures stability. However, further topographic surveys or DEM acquisition

Conclusions

Campaigns are necessary to estimate permafrost degradation through volumetric changes analysis over time. Among the factors identified which could explain the regional variability of change rates, we highlight the fact that the study coast is presenting a sheltered orientation to the northwest storm swell. The composition and ice content of the coasts plays a major role in their sensitivity to erosion. The longer sea-ice season of the Amundsen Gulf the low precipitations on Parry peninsula are can also explain why regional disparities. However, although the rates of change differ according to the type of coastline, erosion seems to be accelerating over the last decades in relation to longer ice-free season and increasing storm events (Couture et al., 2017; Cunliffe et al., 2019; Sankar et al., 2019).

The knowledge of geocryological characteristics of the soils remains a challenge to assess the vulnerability of the coasts. Quantification of coastal change and permafrost degradation is essential to estimate terrestrial carbon transfer and the release of toxic elements such as mercury into aquatic environments, but also to enable adaptation by Inuit communities and civil engineering. In order to improve the analysis, further data acquisition by UAV surveys of key sites such as Paulatuk can be useful to study coastal erosion and permafrost degradation at a short-time scale of analysis. However, topographic surveys or DEM acquisition campaigns are necessary to estimate permafrost degradation through volumetric changes analysis over time.

References

Abram, N., Gattuso, J.-P., Prakash, A., Cheng, L., Chidichimo, M. P., Crate, S., … Schuckmann, K. von. (2019). *The Ocean and Cryosphere in a Changing Climate* (H.-O. Pörtne, D. C. Roberts, V. Masson-Delmotte, P. Zhai, M. Tignor, E. Poloczanska, … N. M. Weyer, Eds.). In Press.

Andresen, C. G., & Lougheed, V. L. (2015). *Disappearing Arctic tundra ponds: Fine-scale analysis of surface hydrology in drained thaw lake basins over a 65 year period (1948–2013)*. 466–479. https://doi.org/10.1002/2014JG002778.Received

Bray, M., & Shur, Y. L. (2004). Geomorphology of the northeast planning area, National Petroleum Reserve Alaska.

Burn, C.R., & O'neill, B. (2015). Subdivision of ice-wedge polygons , western Arctic coast. *Geoquébéc*, (September).

Burn, Christopher R. (2019). Permafrost Landscape Features. In *Encyclopedia of the World's Biomes* (Vol. 2). https://doi.org/10.1016/B978-0-12-409548-9.12423-6

Couture, N. J., Fritz, M., Irrgang, A., Pollard, W., & Lantuit, H. (2017). Coastal Erosion of Permafrost Soils Along the Yukon Coastal Plain and Fluxes of Organic Carbon to the Canadian Beaufort Sea. *Journal of Geophysical Research: Biogeosciences*, *123*, 406 422. https://doi.org/10.1002/2017JG004166

Couture, N. J., & Pollard, W. H. (2000). *The sensitivity of Canada ' s Yukon Coastal Plain to a warming climate*. (Harper 1990), 2890.

Cox, C. J., Stone, R. S., & Douglas, D. C. (2017). Driver and environmental responses to the changing annual snow cycle. (December), 259–2578. https://doi.org/10.1175/BAMS-D-16-0201.1

Cunliffe, A. M., Tanski, G., Radosavljevic, B., Palmer, W. F., Sachs, T., Lantuit, H., … Myers-smith, I. H. (2019). Rapid retreat of permafrost coastline observed with aerial drone photogrammetry. *The Cryosphere*, *13*, 1513–1528.

Fortier, R., & Savard, C. (2010). Engineering geophysical investigation of permafrost conditions underneath airfield embankments in Northern Quebec. *63rd Canadian Geotechnical Conference*, 1307–1316.

French, H. M. (2018). *The periglacial environment* (Fourth).

Fritz, M., Wolter, J., Rudaya, N., Palagushkina, O., Nazarova, L., Obu, J., … Wetterich, S. (2016). Holocene ice-wedge polygon development in northern Yukon permafrost peatlands (Canada). *Quaternary Science Reviews*, *147*, 279–297. https://doi.org/10.1016/j.quascirev.2016.02.008

Galley, R. J., Key, E., Barber, D. G., Hwang, B. J., & Ehn, J. K. (2008). *Spatial and temporal variability of sea ice in the southern Beaufort Sea and Amundsen Gulf : 1980 – 2004*. *113*(May), 1–18. https://doi.org/10.1029/2007JC004553

References

Gatineau, Q. (2015). *Beaufort regional coastal sensitivity atlas.*

Godard, A., & André, M.-F. (2013). *Les milieux polaires* (Second). Paris: Armand Colin.

Godin, E. (2015). *Le processus de thermo-érosion du pergélisol dans la zone de pergélisol continu*. Université de Montréal.

Harper, J. R. (1990). Morphology of the Canadian Beaufort Sea Coast. *Marine Geology*, *91*, 75–91.

Hequette, A., & Barnes, P. W. (1990). Coastal retreat and shoreface profile variations in the Canadian Beaufort Sea. *Marine Geology*, *91*(1–2), 113–1332.

Himmelstoss, E. A., Henderson, R. E., Kratzmann, M. G., & Farris, A. S. (2018). *Digital Shoreline Analysis System (DSAS) version 5.0 user guide: U.S. Geological Survey Open-File Report 2018–1179*. https://doi.org/10.3133/ ofr20181179.

Hoque, A., Solomon, S. M., & Perrie, W. (2009). Modeling nearshore sediment transport along the Canadian Beaufort Sea coast. *Geological Survey of Canada*, 954–961.

Irrgang, A. M., Lantuit, H., Manson, G. K., & Günther, F. (2018). *Journal of Geophysical Research : Earth Surface Variability in Rates of Coastal Change Along the Yukon Coast , 1951 to 2015 Journal of Geophysical Research : Earth Surface*. *2005*, 779–800. https://doi.org/10.1002/2017JF004326

Jong, D., Bröder, L., Tanski, G., Fritz, M., & Lantuit, H. (2020). *Nearshore Zone Dynamics Determine Pathway of Organic Carbon From Eroding Permafrost Coasts Geophysical Research Letters*. https://doi.org/10.1029/2020GL088561

Kumar, J., Collier, N., Bisht, G., Mills, R. T., Thornton, P. E., Iversen, C. M., and Romanovsky, V. (2016. *Modeling the spatiotemporal variability in subsurface thermal regimes across a low-relief polygonal tundra landscape*, *The Cryosphere*, 10, 2241–2274, https://doi.org/10.5194/tc-10-2241-2016, 2016

Lantuit, H, & Pollard, W. H. (2008). Fifty years of coastal erosion and retrogressive thaw slump activity on Herschel Island , southern Beaufort Sea , Yukon Territory , Canada. *Geomorphology*, *95*, 84–102. https://doi.org/10.1016/j.geomorph.2006.07.040

Lantuit, Hugues, Overduin, P. P., Couture, N., Wetterich, S., Aré, F., Atkinson, D., … Vasiliev, A. (2012). The Arctic Coastal Dynamics Database : A New Classification Scheme and Statistics on Arctic Permafrost Coastlines. *Estuaries and Coasts*, *35*, 383–400. https://doi.org/10.1007/s12237-010-9362-6

Lim, M., Whalen, D., Martin, J., & Mann, P. J. (2020). Massive Ice Control on Permafrost Coast Erosion and Sensitivity Geophysical Research Letters. *Geophysical Research Letters*, *47*, 9. https://doi.org/10.1029/2020GL087917

Mackay, J. R. (1952). Physiography of the Darnley bay area, N.W.T. *Association of Pacific Coast Geographers*, *15*, 5.

Mackay, J. R. (1995). Ice wedges on hillslopes and landform evolution in the late Quaternary, Arctic coast, Canada. *Canadian Journal of Earth Sciences*, *1105*, 1093–1105.

References

Manson, G. K., Solomon, S. M., Forbes, D. L., Atkinson, D. E., & Craymer, M. (2005). Spatial variability of factors influencing coastal change in the Western Canadian Arctic. *Geo-Mar Lett*, 138–145. https://doi.org/10.1007/s00367-004-0195-9

Obu, J., Lantuit, H., Grosse, G., Günther, F., Sachs, T., Helm, V., & Fritz, M. (2017). Geomorphology Coastal erosion and mass wasting along the Canadian Beaufort Sea based on annual airborne LiDAR elevation data. *Geomorphology*, *293*, 331–346. https://doi.org/10.1016/j.geomorph.2016.02.014

Overduin, P. P., Strzelecki, M. C., Grigoriev, M. N., Couture, N., Günther, F., & Wetterich, S. (2014). *Geological Society , London , Special Publications Online First Coastal changes in the Arctic*. https://doi.org/10.1144/SP388.13

Paulic, J. E., Bennett, R., Harwood, L. A., & Howland, K. L. (2012). *Ecosystem Overview Report for the Darnley Bay Area of Interest*.

Pollard, W. (2018). Chapter 15. Periglacial Processes in Glacial Environments. In *Past Glacial Environments* (pp. 537–564). https://doi.org/10.1016/B978-0-08-100524-8.00016-6

Radosavljevic, B., Lantuit, H., Pollard, W., Overduin, P., Couture, N., Sachs, T., … Fritz, M. (2016). Erosion and Flooding — Threats to Coastal Infrastructure in the Arctic : A Case Study from Herschel Island , Yukon Territory , Canada. *Estuaries and Coasts*, *39*, 900–915. https://doi.org/10.1007/s12237-015-0046-0

Sankar, R. D., Murray, M. S., & Wells, P. (2019). Decadal scale patterns of shoreline variability in. *Polar Geography*, *0*(0), 1–18. https://doi.org/10.1080/1088937X.2019.1597395

Schaefer, K., Elshorbany, Y., Jafarov, E., Schuster, P. F., Wickland, K. P., Sunderland, E. M., & Striegl, R. G. (2020). thawing permafrost. *Nature Communications*, (2020), 1–6. https://doi.org/10.1038/s41467-020-18398-5

Solomon, S. M. (2005). Spatial and temporal variability of shoreline change in the Beaufort-Mackenzie region , northwest territories , Canada. *Geo-Mar Lett*, 127–137. https://doi.org/10.1007/s00367-004-0194-x

Thoman, R. L., Richter-Menge, J., & Druckenmiller, M. L. (2020). *Arctic Report Card 2020*. https://doi.org/10.25923/MN5P-T549X

Wegner, C., Bennett, K. E., Vernal, A. De, Forwick, M., Fritz, M., Heikkila, M., … Promin, A. (2015). Variability in transport of terrigenous material on the shelves and the deep Arctic Ocean during the Holocene. *Polar Research*, *1*, 1–19.

Wiley, J., Chichester, S., & French, B. H. M. (2020). The periglacial environment, fourth edition.. *By Hugh M. French*. The periglacial environment. Fourth edition (July 2019) https://doi.org/10.1002/ppp.2009